

**STUDIES ON RABBIT INTESTINAL  
GLUCOAMYLASE MALTASE COMPLEX**  
(SIZE, SHAPE, STRUCTURE AND MECHANISM OF ACTION)

**A THESIS SUBMITTED TO THE  
UNIVERSITY OF HYDERABAD  
FOR THE DEGREE OF  
DOCTOR OF PHILOSOPHY**

**BY**  
**K. SHANKARAN, *M.Sc.***

**SCHOOL OF LIFE SCIENCES  
UNIVERSITY OF HYDERABAD  
HYDERABAD-500 134  
INDIA**

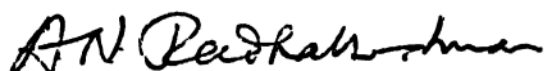
**August 1984**

DEDICATED TO MY FATHER  
WHO IS NO MORE



## DECLARATION

The candidate declares that this work has been carried out by him under the supervision of Professor A.N. Radhakrishnan, School of Life Sciences, University of Hyderabad, Hyderabad-500 134, India, and that this work has not been submitted for any degree or diploma of any other University.



PROF. A.N. RADHAKRISHNAN  
School of Life Sciences  
University of Hyderabad  
Hyderabad-500 134, India



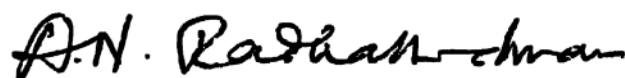
(K.SANKARAN)

August 24, 1984

## CERTIFICATE

This is to certify that the Thesis entitled "STUDIES ON RABBIT  
INTESTINAL GLUCOAMYLASE-MALTASE COMPLEX (size, shape,  
structure and mechanism of action)" is based on the results of the  
work carried out by Mr. K. SANKARAN, M.Sc., for the degree of DOCTOR  
OF PHILOSOPHY under my supervision. This work has not been submitted  
to any degree or diploma of any other University.

August 24, 1984



PROF. A.N. RADHAKRISHNAN  
(SUPERVISOR)  
School of Life Sciences  
University of Hyderabad  
Hyderabad-500 134, India



DEAN,  
SCHOOL OF LIFE SCIENCES

Prof. P.S. RAMAMURTY,  
Dean, School of Life Sciences  
University of Hyderabad,  
HYDERABAD-500 134. (India)

## ACKNOWLEDGEMENTS

I am very grateful and indebted to Prof.A.N.Radhakrishnan, M.Sc., Ph.D., D.I.I.Sc., F.A.Sc., F.N.A. for his excellent support, guidance and invaluable suggestions at every phase of this work. Looking back over the years and reminiscing the course of this work I could see that Prof. Radhakrishnan quietly rode like a colossus, but at no time gave me the impression that my originality suffered from lack of his recognition. He always suggested simple experiments whenever I was looking for an essential link, and very soon I would realise that I got my link. My hasty conclusions never perturbed him and he never criticised me for that - but he would point out to the flaw in an elegant manner which would only increase my regard for his vast knowledge.

In these five years I have learned the meaning of science, especially, the advantages of being open-minded in drawing conclusions. The umpteen casual discussions, which would contain examples from great scientists he knew personally or from the literature drove home the above points. This is an experience only a few are privileged to cherish and it is an art of turning a novice into a thinking researcher. A valuable lesson I learned from him was the meaning of ethics as in personal life, irrespective of temptation of an easier or a shorter route. During this

work I had occasions to interact with a variety of scientists from other institutions and this task was made easier by the high respect and love in which he is regarded among fellow scientists of India. He was not only a mentor in academics but extremely human in his kindness to his pupils. The understanding and consideration he shows towards a pupil during a personal crisis is remarkable. I myself have had this nice experience a few times. As an humble tribute through this thesis, I salute my mentor for what I am now and for what I will be in the future but the debt I will never be able to repay.

I am most indebted to Dr. S. Sivakami, now at University of Bombay, Bombay with whom I was associated during the early phase of this work. I always benefitted from her suggestions, criticisms and discussions. She was undoubtedly a motivating force and her participation and help in this investigation is gratefully acknowledged.

I thank the Vice-Chancellor of the University of Hyderabad, Hyderabad and the Dean, School of Life Sciences for their keen interest in this work. I thank the teaching staff who had taught me at this University and those who showed interest in my career. I should thank the office staff and other non-academic staff for their help. I particularly wish to thank Dr. N.C. Subramaniam and Dr. Maya Sundari for their keen interest in these studies.

I thank the Directors of the following institutions: Centre for Cellular and Molecular Biology (CCMB); International Crops Research Institute for Semi Arid Tropics (ICRISAT), Hyderabad; National Institute of Nutrition (NIN), Hyderabad; Indian Institute of Sciences (IISc), Bangalore and Central Food Technological and Research Institute (CFTRI), Mysore, for their kind permission to make use of various facilities of their institutions.

I like to particularly thank the following for their collaboration and for discussions on various aspects of this work: Dr. M.W. Pandit, Dr. K. Kannan (CCMB), Dr. D.V.R.Reddy, Mr. S.K. Manohar and Mr. Y. Bhaskar (ICRISAT) and Dr. K.Muralidhar now at University of Delhi, Delhi. I have had, in the course of these investigations several opportunities to take part in stimulating discussions with Dr. D. Raja Gopal Rao (CFTRI) (who also trained me in the technique of peptide mapping), Prof. M.A. Viswamitra, Prof. V.S.R. Rao (IISc), Dr. D. Balasubramanian, Dr. A.S. Kolaskar and Dr.D.Chatterji (CCMB) and Dr. V. Seetharamam (NIN).

I like to thank Mr. Pramod, CCMB (Ultracentrifugation Studies), Mr. M.V. Jagannadham, CCMB (Amino acid analysis), Mr. Murthy, NIN, (Amino acid analysis) and Mr. Douglas Kershaw, University of Leeds, Leeds, U.K., for some of the electron microscopic studies.

I personally thank my colleagues Sambasiva Rao (NIN), Guru Rajan, Ch. Mohan Rao, Mitra (CCMB), Shivakumar (CFTRI),

Rajendrakumar, University of Delhi, Delhi, Papa Rao, Athreya, D.T. Singh, Muralikrishna, Shivaram, Subba Ramiah, Sambasiva Rao, Vaman Rao, Venu of University of Hyderabad. I thank Vaitheeswaran, Raghunath and Jayanthan who helped me in the preparation of this thesis. I have derived help from many other friends not listed here. I acknowledge all of them personally.

I am most thankful to my seniors Dr. V. Ganapathy, Dr. K. Srikumar, Mrs. Premalatha Srikumar and Mr. Ramachandra Murthy for their kind help and cooperation at different phases of this investigation.

I thank Dr. R.P. Sharma (University of Hyderabad) and Prof. L.K. Ramachandran (Osmania University) for their kind gift of some chemicals.

My thanks are due to Mr. T.V. Gopal and Mr. A. Neelakantam for typing the thesis and to Sajjad Ali for photocopying.

This work was supported by a generous fellowship grant from the Council of Scientific and Industrial Research and I thank these authorities for their help.

## PREFACE

This thesis embodies the work on rabbit intestinal glucoamylase-maltase complex with respect to its size, shape, quaternary structure, its mechanism of action and a design of the active site. The subject matter has been covered under the following major headings:

Introduction: In this section we have reviewed the major aspects of brush border enzymes and have highlighted the potential of the present day hydrodynamic models to predict the shape and geometry of an oligomeric proteins. A small write up on the negative-staining technique has also been included.

Materials, Analytical and Theoretical Methods: The diverse methods used in this study have been grouped together to avoid repetition. The theoretical methods used in the study have also been given.

Results and Discussion: All the results including a relevant discussion are given in this section under appropriate headings. It includes information available and conclusions drawn regarding the quaternary structure of the enzyme, a possible mechanism of action and a possible design of the

active site. Towards the end of this section a speculative exercise has been attempted regarding the structure-function relationships of the enzyme, especially in view of the supra-quaternary structure of the enzyme. At the end of this section a brief summary of the work and concluding remarks are given.

The figures, tables and references have been numbered consecutively throughout the thesis and a consolidated bibliography is given at the end of the thesis. For a quick glance of the contents an index is given separately with page numbers.

Part of the work, especially on the size and shape of the enzyme has been published.\*

In spite of my mentor's great help in the use of the English language, of this Thesis, there may still be some inadequacies. A few complex sentences which I have tried to avoid may still be there, and I haven't yet mastered the art of simple elegance.

\*Studies on the size and shape of rabbit intestinal glucoamylase-maltase complex.'

Sankaran, K., Sivakami, S. and Radhakrishnan, A.N. and Pandit, M.W. Biochem. J. (1983) 213, 719-725.



## INDEX

<u>Introduction</u>	1-51
Studies on Microvillus glycosidases	1
Hydrodynamics and Quaternary Structure	27
Electron microscopy and quaternary structure	47
<u>Materials, Analytical and Theoretical Methods</u>	52-89
<u>Results and Discussion</u>	90-159
Purification of the two forms of the enzyme	90
Quaternary structure of the enzyme	92
Mode of membrane association	110
Mechanism of action, design of active site and immunochemistry	123
Structure-Function Relationships (A speculative exercise)	152-159
General Summary and Concluding Remarks	
Bibliography	

# INTRODUCTION

## STUDIES ON MICROVILLUS AND ITS GLYCOSIDASES

Digestion and absorption of food is most fundamental for all living beings. The food of higher organisms contains chiefly carbohydrates mainly in the form of polymers of glucose (starch and glycogen), proteins, which are polymers of amino acids and fat composed mainly of long chain fatty acids and their glyceryl esters. Mammalian gut, lined with specialised columnar epithelium is well adapted for digestion (conversion of polymers to monomers) and absorption (uptake of digested matter) of their food. The adaptation, at morphological level, involves tremendous increase (about 600 times) in the surface area, by formation of villi and microvilli, which are fingerlike projections respectively of the epithelium and the epithelial cells called enterocytes. Due to the thick array (about thousand per cell) of these microvilli, in the intestinal cells, they appear as a band under light microscope, known as 'brush border'. The digestion of food i.e. breakdown of polymers to monomers takes place at three levels, viz. cavital digestion, catalysed by secretory enzymes (mostly endoenzymes) in the lumen (cavity), the products being oligomers/monomers; contact digestion, catalysed by enzymes (mostly exoenzymes) attached to the enterocyte cell walls especially on the microvilli,

the products being essentially monomers; intracellular, catalysed by enzymes in enterocytes cytoplasm, the products being monomers formed from absorbed oligomers [1]. The conditions and the environment in which these events take place vary widely. In the mouth it is almost neutral pH, in the stomach it is acidic (pH 2) and in the intestine it is nearly alkaline (pH 8). The appropriate enzymes secreted or present on the membrane are optimally active under these conditions. The contact digestion and transport processes present on the microvilli seem to be closely associated but, the nature of their interactions still remains vague.

The variations in ~~these~~ adaptive organisation are induced by nutrient and hormonal factors. The essentiality of this organisation is appreciated in a diseased state including genetic disorders, where one or ~~the other~~ <sup>another</sup> element of this complex system is found missing or malfunctioning.

Digestion and absorption, vital functions of the body, are carried out effectively by complex and specialised structures. Since most of this intricate mechanism and machinery are housed in the brush border, isolation of brush border elements and their study at molecular level, wherever possible, have become both a necessity and fashion to correlate the structure with its function. These studies have

thrown considerable light on our understanding of this terminal digestion and transport, wherein a trans-membrane anchor peptide, which has been shown to anchor the catalytic portion of the molecule to the membrane (membrane bound condition), has been implicated in transport of product into the cytoplasm [2]. This is an attractive possibility yet to be proven conclusively. The intestinal glycosidases which are large proteins with their ability to catalyse more than one reaction and probably also involved in the transport of the products must possess a very interesting quaternary structure and unfortunately this is an area which has not been probed adequately.

### Ultrastructure of Microvillus

Microvilli are minute projections of about  $0.1\ \mu\text{m}$  in diameter and  $1\ \mu\text{m}$  to  $2\ \mu\text{m}$  in length from the luminal surface of enterocytes and are visible only under electron-microscope [3]. The plasma membrane of the microvillus, is continuous with the plasma membrane of the enterocyte and the central core consists of microtubules (about 20 of them) in the form of a bundle appearing as an hexagonal array in cross-section [4]. These are actually actin filaments [5,6] extending to the terminal web, located in the apical portion of enterocytes, immediately below microvilli. There are cross bridges between these filaments and between

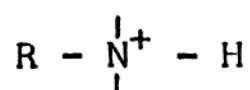
the filaments and membrane seen under electron microscope, providing additional strength. These cross bridges have been identified as  $\alpha$ -actinin [7]. The function of this core assembly is expected to aid some movement which may be important in stirring the contents in the lumen for better digestion or even to aid pinocytosis [4]. The plasma membrane of the microvillus is somewhat thicker than a typical plasma membrane and is covered on the luminal end (apex) by a fuzzy layer called glycocalyx which is rich in acid mucopolysaccharides (glycosamino glycans) which are poor in sulfate and rich in sialic acid [3]. This portion could be negatively stained and viewed under electron microscope where upon 60 Å particles are made visible, and they have been attributed enzyme functions (see below for details).

#### Location of hydrolytic activity on Brush Border membrane

##### Isolation of membranes and demonstration of activities:

Intracellular digestion was envisaged by Cajori [8] as early as in 1933. Dahlqvist and Borgstrom [9] demonstrated clearly that the disaccharidase activity is too weak to account for the total disaccharide digested and absorbed and hence suggested that the activity must reside on the cell walls of enterocytes, challenging the popular belief held for a long time on luminal digestion. They also showed clearly that  $\alpha$ -amylase activity, on the contrary, is mostly luminal. Miller and Crane [10] for the first time isolated brush border membranes

of hamster intestine and demonstrated high yields of disaccharidases activity in them [11]. Since then, with improved methods to prepare purer brush border preparations [12], the isolation of brush border and demonstration of various particle bound activities in them became one of the two popular techniques for location of enzyme activity on the brush border. The other method involves the use of fluorescent substrate analogues or reacting fluorescent antibodies with the enzyme systems in the intact intestinal epithelium. It was shown that in the presence of 1M Tris, in<sup>th</sup> cold the brush border preparations gave five bands separated on a glycerol density gradient centrifugation. While one fraction contained rod shaped molecules with rounded ends and of diameter of 60 Å, another fraction, associated with maltase and alkaline phosphatase activities, was membranous containing 60 Å particles, which were thought to house the enzyme activities [13]. The basic structure of the reagent required to rupture the brush border was found out to be



With improved preparations it was also possible to see the cross bridges between the rods in the core structure [14]. One remarkable feature, however, is the persistence of glycocalyx around the vesicles which was resistant to removal by the disruptive forces operative during the careful processing.

Histochemical procedures: By histochemical procedures an amino-peptidase was demonstrated by reacting it with its chromogenic substrate L-Leucyl-4-methoxy-2-naphthyl amide and simultaneously depositing an electron dense material at the reaction site [15]. Histochemical method using substrate analogues initially misled Dahlqvist and Brun [16] to postulate cytoplasmic distribution of disaccharidases which was proved later by Lejder [17] to be <sup>due</sup> ~~owing~~ to a procedural artefact wherein the labels were actually the ingested substrate or product molecules. The latter author devised an improved technique and demonstrated their external localisation on the membrane [17]. Doell et al [18] used fluorescent antibodies against lactase and sucrase and showed that they are located on the brush border. Though there was <sup>some</sup> ~~a slight~~ criticism <sup>about</sup> the purity of the preparations used, the use of pure enzyme preparations did not alter their conclusions [19]. Localisation of phosphatases can be achieved by reacting with lead which leads to a deposition of lead at the reaction site [20]. Splitting of 6-bromo-2-naphthyl- $\alpha$ -glucoside and simultaneous azo-coupling with hexazonium para-rosanilin helped unequivocal localisation of maltases (sucrase-isomaltase and glucoamylase) in the brush border. This reaction was shown to be inhibited by maltose and sucrose but not by other disaccharides [21].



Analysis of cryostat sections of 10 $\mu$  thick parallel to the surface showed that alkaline phosphatase, disaccharidases and dipeptidases have much higher activities in the tip portion of the villi than in the crypts and their strong association with the membrane was evident from the fact that they could be identified even in unfixed sections [22]. It is noteworthy that a weak fluorescence or positive staining is observed, depending on the technique used, even in the terminal web portion [23].

Mosaic pattern of activities: When brush border membrane fraction was digested with papain for 5 min almost all of the maltase, lactase and isomaltase activities were released and when chromatographed on Sephadex G 200, they appeared as a single peak near the void volume. Digestion up to 40 min released leucine-aminopeptidase but not alkaline phosphatase [24,25]. This difference in solubilisation led to the notion that these activities are distributed on the brush border in a mosaic pattern. Recently, immunological studies by Tsubou et al [26] indicate that sucrase-isomaltase, maltase and lactase on the rat intestinal microvillus membrane are probably arranged independently with a high degree of molecular freedom.

Glycocalyx and enzyme activities: Negative staining of the brush border preparations [15] revealed 60 Å diameter

particles in the glycocalyx [27,28]. When removed using papain and subjected to differential centrifugation the activities were associated with the <sup>intracellular</sup> particular fraction rather than membrane fractions. In undigested material the activities were associated with the membrane fraction. So the activities were thought to be associated with the glycocalyx part, residing in the 60 Å particles [28,29]. Nishi et al [30] observed ring shaped particles (outer diameter 100 Å and inner diameter 35 Å) on the glycocalyx and attributed them to sucrase molecules present at high concentration. However, a later study by Gitzelmann et al [31] using ferritin labelled sucrase antibodies showed that the sucrase is located on the membrane-proper and removal of glycocalyx gave rise to pronounced labelling. Benson et al [32] observed no correlation between the removal of 60 Å particles and release of hydrolases activity on papain digestion. Recently, Nishi and Takasue [33] localised intestinal sucrase-isomaltase on the membrane by specifically reacting it with its unlabelled antibodies and directly viewing the antigen-antibody complex under electron microscope, taking advantage of large concentration of sucrase-isomaltase on the membrane to give adequate electron opacity on complexing. In patients with celiac disease, glycocalyx is normal, but sucrase and other disaccharidase activities are low and also there seems to be no correlation between the evolution of surface coat and the activities, in different

animal species [23]. So at present it is not clear if the glycocalyx is devoid of activity or not.

### Distribution of glycosidases along the length of the small intestine

The distribution of an enzyme along the gut and the subsequent absorption of products arising from this enzyme activity may be correlated. This aspect has been extensively studied in hamster [34], pig [35,36] rat [37,38] chicken [39,40] man and monkey [41], guinea pig, pigeon and rabbit [42]. In general, the enzyme activities are maximally present in jejunum with decreased activities in duodenum and ileum. However, there are certain deviations. Trehalase of pig intestine is equally active in both proximal jejunum and distal ileum. In rabbit while maltase is low in duodenum and ileum compared to jejunum, glucoamylase activity is distributed uniformly throughout [42]. In the newborn human the activities are more or less uniformly distributed [43]. In pigeon and adult human the activities are maximal in duodenum and proximal jejunum. The maximal sites of absorption of the products of enzymic action follow rather closely the distribution of the enzyme activities along the intestine, suggesting the proximity of the two systems [44].

## Isolation of the enzyme activities

Solubilisation using proteases: To understand more about the mechanisms involved in the terminal stages of digestion and absorption, it became essential to isolate the enzyme activities and to study their molecular nature. Since these are all membrane bound, the first step was to evolve suitable methods of solubilisation. Several procedures have been tried with varying degrees of success, like repeated freezing and thawing, use of bicarbonate, acetone drying followed by aqueous extraction, n-butanol extraction and use of enzymes. Lecithinase, lipase and amylase were ineffective in the case of both swine [45] and rabbit [46] and presumably so in other cases. In the case of swine, pig and rat <sup>membranes,</sup> trypsin was found to be effective, but it was not in the case of rabbit and human <sup>membranes</sup> [47]. Deoxycholate was shown to be effective in solubilising more than 50% of disaccharidase activity in swine and rabbit <sup>?</sup> [45,46]. The solubilised invertase activity was found to be protected against protease damage by phosphate, Tris and borate buffers, but not by veronal. Semenza and Auricchio [48] were the first to solubilise disaccharidases using papain for their separation using chromatography. In 1963 Auricchio et al [47] published a procedure to solubilise the human intestinal disaccharidases using papain. While maltase, isomaltase, invertase, lactase and cellobiase were completely solubilised,

trehalase remained <sup>insoluble</sup> ~~un-solubilised~~ and lactase and cellobiose <sup>were</sup> ~~got~~ partially inactivated. Protection against the loss of maltase activity was provided by  $K^+$  but not by  $Na^+$ . Ever since its use in solubilisation was demonstrated, papain became the protease of choice for the purpose in subsequent studies. With hamster, rat, rabbit, pig, monkey and human, elastase has been shown to be as effective as papain in solubilisation, and it was implicated in the degradation of membrane proteins and their rapid turnover [49].

Solubilisation using detergents: While papain solubilisation was successful in the release of enzyme activities, use of detergents as effective solubilisers was shown as early as in 1958 [45] in the study on swine, and later in rabbit [46]. Before the superiority of using a non-ionic detergent (Triton X-100) was brought out in their systematic study [50] on rat liver plasma membrane enzymes, Gitzelmann et al [51] used Triton X-100 in their study on rabbit small intestinal disaccharidases, and Eggermont and Hers [52] demonstrated its usefulness in solubilising maltase-isomaltase and maltase-sucrase and glucoamylase of the human intestinal mucosa. Maroux et al [53] used Triton X-100 for the first time in intestinal mucosal protein purification from hog intestinal brush border and subsequently it found its use in rabbit [54], rat [55] and pig [56]. SDS was shown to be

more effective than Triton-X 100 in releasing the activities even at lower concentrations. The activities were, however, found to be less stable in SDS medium compared to Triton-X 100 and hence the latter was preferred [57,58]. Colbean and Maroux [59] used Emulphogen BC 720 to solubilise alkaline phosphatase.

Purification of solubilised enzyme: In most cases, the purification of the solubilised proteins involved different combinations of salting out, gel filtration, preparative gel electrophoresis and ion exchange chromatography procedures. The first purification procedure for sucrase-isomaltase [61] involved urea extraction followed by papain solubilisation and chromatography on Sephadex G 200 and Biogel P 300. Preparation of lactase and glucoamylase from baby rat small intestine by Schlegel-Hauteur et al [62] involved chromatography on Sepharose, Sephadex and DEAE cellulose and Kolinska and Kraml [63] employed only Sephadex G 200 and DEAE cellulose to purify sucrase-isomaltase and glucoamylase. Ethanol precipitation after solubilisation was followed by DEAE cellulose, Sephadex G 200 and preparative electrophoresis in the case of human intestinal glucoamylase purification [64]. Additional steps like heat treatment and ammonium sulfate precipitation were followed in the case of lactase-phlorizin hydrolase purification from rabbit [64] and glucoamylase from monkey [65]. An elegant purification procedure of rabbit

intestinal glucoamylase-maltase complex was a single specific affinity step using Sephadex G 200 [65]. Recently <sup>the</sup> an immunoadsorbent method was used for purification of pig intestinal glucoamylase-maltase complex [56]. The method of solubilisation, either using papain or Triton X-100 does not alter the purification procedure generally. In the case of detergent solubilised enzymes, the detergent is ultimately removed either by butanol extraction [67] or ice-cold acetone precipitation [54] or washing the affinity gels with large volumes of the detergent free buffer before elution [68]. The purified enzymes have been shown to be almost completely homogeneous in PAGE (and free of any major heterogeneity)

### Studies on the purified enzyme systems

Mode of attachment to the membrane: The general belief that the enzyme activities are membrane bound came from evidences<sup>§</sup> from different lines of investigations detailed above. Though their external localisation was well established by electron microscopy and the solubilisation studies [69,70], the exact nature of their association remained obscure and is not completely understood even today in certain cases. Solubilisation using protease and detergent became an important tool to gain a breakthrough

into this problem. Since the former releases the protein presumably by virtue of its proteolytic activity and the latter removes the proteins as a whole, it is expected that the two forms (referred to as detergent form and protease forms) should differ in molecular details and this difference will reveal the nature of the peptide called anchor peptide which is not accessible to protease activity because of its association with the membrane. The early observation that the form of aminopeptidase released from pig brush border by Triton X-100 is different from that released by papain was extended to the hydrolases from pig, rat and rabbit [71]. Among the glycosidases sucrase-isomaltase is the best studied system with regard to this problem. It has been clearly shown in the brilliant studies by Semenza and his associates [2,72,73] that it is anchored by a hydrophobic segment which is less than 10% of the total protein mass of the isomaltase unit (the sucrase unit being not involved). However, similar studies on rat intestinal glucoamylase-maltase complex did not reveal the presence of any such peptide [55]. In the case of pig glucoamylase-maltase complex there is adequate evidence for its presence but it has not been isolated and identified [56]. This mode of attachment is not uncommon in other classes of membrane bound enzymes like leucine amino peptidase [74], cytochrome P 450, glycophorin, neuraminidase, etc., [75]. The study from such systems reveal



certain general characteristics of the anchor peptide. The anchor peptides are generally 20-30 amino acids long, predominant in hydrophobic amino acids like leucine, valine and isoleucine and are deficient in acidic and basic amino acid and exhibit either  $\alpha$ -helical or  $\beta$ -pleated sheets within the membrane [75]. Owing to the presence of this peptide and its detergent binding ability, it is often found that the detergent forms have higher  $M_r$  (about 100,000 in the case of Triton solubilized enzymes) larger Stokes' radius (almost a factor of 2), show charge shift in immunoelectrophoresis, possess affinity to hydrophobic gels and aggregate on removal of the solubilising detergent. Chemically, the protease form will lack this peptide portion, and hence show a new C- or N-terminal depending on its insertion in the sequence, the latter being more common among brush border enzymes [4]. The majority of the brush border (intestine and kidney) hydrolases seem to be different in their mode of insertion from the other intrinsic membrane proteins. They are attached to the membrane by their N-terminal side while the other intrinsic proteins like glycophorin [76] alkaline phosphatase [59] are associated by their C-terminal. This difference according to Brunner et al [73] has biosynthetic implications and explains the external localisation of the major part of the molecule, unlike the others (C-terminus linked) which are mostly buried in the membrane [64]. The two forms of

rat glucoamylase-maltase complex were shown to be identical except in one behaviour, i.e. the aggregation of the aged detergent form. However, very recently [77]<sup>\*</sup> the isolation of the detergent form of the rat enzyme with an additional (protease sensitive) peptide has been reported. Obviously there are diverse ways in which proteins can be bound to the membrane and more careful studies are needed to unravel their association with the membranes.

### Characterisation of individual enzyme system

Heterogeneity in enzyme activities: Early studies identified glycosidases viz. maltase, invertase, lactase and trehalase, phosphatase and peptidase activities associated with the brush border preparations. Heat inactivation, gel filtration and ion-exchange chromatography employed in their isolation indicated that these were present in multiple forms. In the case of the human, maltase was shown to be present in as many as five forms [78], while later studies [79] confirmed only four forms. In many animals there are three maltases, and in rabbit and monkey of the three forms only two are predominant [80,42]. With the characterisation of the isolated systems it became apparent that each maltase activity is characteristically associated with another disaccharidase or oligosaccharidase

---

\*The paper seen in title form only

activity. Thus, the heat labile maltase (called maltase I) was found associated with invertase and isomaltase activities while the heavy and heat stable maltase (maltase III or II, depending on the animal) was found to be associated with glucoamylase activity [57,81-84]. The existence of two  $\beta$ -galactosidases (lactase activity to be more precise in animal systems) in the intestinal mucosa, a soluble enzyme with an acid optimum pH and a particulate enzyme with pH optimum around 6.0 has been reported in many animal species - rat, rabbit, cat, monkey and man [85-90] - while purification of a third  $\beta$ -galactosidase with low optimum pH was effected in human small intestine [91-92]. The lactase activity of monkey [93] and of human was further resolved into two fractions chromatographically. Our knowledge at present on these different forms has increased sufficiently and the molecular details ~~flowing, slowly and steadily about them~~ demand consideration of each system individually here.

Sucrase-isomaltase complex: This is identifiable with the heat labile maltase I. This is perhaps the best studied system among the glycosidases of intestinal mucosa. Though this has been purified from various animals [51,60, 94-97] the one from rabbit has been studied extensively with respect to its molecular and other details. This

complex is a glycoprotein containing about 15% by weight of carbohydrate. Its molecular weight is 220,000 and apparently consists of two non-identical peptides of  $M_r$  110,000-120,000 both having maltase activity but in addition, one has sucrase activity and the other isomaltase activity [98]. The two activities are separable either by mild alkaline treatment [99], citraconylation [100] or tryptic digestion [101]. Both have similar amino acid composition tryptic peptides indicating high structural similarities but, do not recombine after separation, indicating induced structural alterations preventing their reassembly [99]. The whole assembly is bound to the membrane by means of an anchor peptide, the N-terminal sequence containing about 140 residues of isomaltase subunit and sucrase is non-covalently attached to isomaltase and does not take part in membrane association [73]. The anchor peptide was difficult to ~~be isolated~~ and characterised ~~owing~~ to its strong association with the glass and plastic walls, leading to poor recoveries. It was suggested by Brunner et al [73] that its molecular weight is about 17,000 and <sup>that it</sup> is heterogeneous at the C-terminal side. The N-terminal sequence of the detergent solubilised isomaltase subunit has a long (in fact, the longest among the known membrane bound systems) stretch of extremely hydrophobic sequence from residues 12 to 31 [73]. The presence of an anchor peptide at the N-terminal has interesting biosynthetic implications.

Removal of detergent (Triton X-100) from the detergent form leads to aggregation of the form (diameter 435 Å) in which three different assemblies of the enzyme could be identified [102]. The individual molecule measured 155 Å in length and its axial ratio was 4. The two subunits, arranged lengthwise, are similar in size and shape, approximating prolate ellipsoid with major and minor axes measuring 65 Å and 45 Å respectively and the distance between their centres being about 85 Å and different orientations of the subunits with respect to each other indicated flexibility in the linkage [102]. As is the case with many other membrane bound enzymes [75], it has not been possible to obtain this system in crystalline forms to subject to X-ray analysis and study at atomic level.

The detailed steady state kinetics worked out revealed ping-pong bi-bi mechanism for its action on disaccharides. The activities are activated by  $\text{Na}^+$  ions allosterically, showing homogeneous cooperativity, either K type or V type depending on the species. The activities are heat labile and susceptible to proteolytic damage in the absence of  $\text{K}^+$  [103]. Each subunit has its own  $\text{Na}^+$  binding site [99]. Tris is a competitive inhibitor for both the activities and it was suggested that it competes for the glucose subsite with the substrate [103]. A recent study on the mode of action of rat intestinal sucrase-

isomaltase on  $\alpha$ -limit dextrin [104] revealed some very interesting points. Isomaltose is a poor substrate for isomaltase though it is mostly involved in the hydrolysis of  $\alpha$ -(1 $\rightarrow$ 6) bond. On the other hand  $\alpha$ -limit dextrin is a very good substrate ~~for~~ it, and a model substance, used  $6^3$  maltotriosyl maltotriose, clearly indicated its stepwise degradation from the non-reducing end to glucose in a complementary manner by both sucrase and isomaltase sites. On the basis of substrate specificity it appears that isomaltase is a misnomer and it should be more appropriately called  $\alpha$ -dextrinase. The ability of this disaccharidase to transport its product across the artificial lipid membrane [105] provided an attractive hypothesis, and indicated the possibility of such a mechanism operating in the brush border. However, since the enzyme used in these studies was the protease form devoid of natural membrane associated peptide, its association with the membrane could not be natural [4], and in fact recent data indicate that the protease form fails to attach to the liposomal membrane [2].

The human intestinal sucrase-isomaltase complex [106], is an elongated molecule with an axial ratio of 8, consisting of two non-identical subunits of  $M_r$  130,000 and 120,000 [87]. separable by urea or guanidinium chloride in presence of sulfhydryl compounds with their activities intact [107].

The evidence for the actual existence of 'free-sucrase' and 'free-maltase' in human intestine, contrary to the thinking that they could have been released by papain after solubilisation [108], was provided by Skorbjers et al [109] in human intestine.

Glucoamylase-maltase complex: Prompted by the work of McGeachin and coworkers [110,111] who showed that rats even after the removal of the pancreas and salivary glands could digest starch normally owing to the presence of intestinal glycosidases, Dahlqvist and Thomson [112] purified two intestinal amylases and showed that one had  $\alpha$ -amylase type of activity and the other glucoamylase type of activity. Since then this complex was identified with both heat stable and fast sedimenting or high molecular weight maltase II or III, depending on the species [57,81-84]. This complex has been studied fairly well in the case of rat [55,77,113,114], rabbit [66,115,116], human [63] and pig [56]. While human, rabbit and pig intestinal glucoamylase maltase complexes have  $M_r$  210,000, 760,000 (this report) and 240,000 respectively, the rat enzyme was shown to have a  $M_r$  of 500,000. The complex band pattern of rat enzyme obtained on SDS PAGE at low pH values and high temperatures and N-terminal analysis of these bands, suggested that the enzyme is an oligomer of two subunits of  $M_r$  135,000 and 245,000. However, the

evidence on the oligomer composition is not clear-cut [113]. The rabbit enzyme did not dissociate at all under any of the usual dissociation conditions involving SDS and guanidine hydrochloride, etc., remarkable for a very large polypeptide [116]. Its behaviour during gel filtration was unusual, in that, it eluted much earlier than expected like a molecule of  $M_r > 900,000$  while its  $M_r$  is only 760,000 according to approach to equilibrium method (this Thesis). This clearly indicated a very asymmetric and elongated shape of the enzyme [117]. The pig enzyme has two polypeptide chains of  $M_r$  135,000 and 125,000 [56]. The two activities have not been separated at all in any of the cases, as <sup>has</sup> have been done with sucrase-isomaltase. Detailed kinetic studies with the rabbit enzyme [115] suggest the presence of multiple substrate and inhibitor binding sites. But, in the case of human enzyme, the two activities seem to belong to the same active site [63]. There is little information regarding the number and arrangement of subunits and interactions between the subunits. In the case of rat the detergent and protease forms did not show any notable difference and seemed identical. The detergent form on ageing showed undissociable aggregation suggesting the possibility of a very small hydrophobic peptide at the C-terminal side, since the N-terminal amino acids were identical. No detergent binding ability could be demonstrated, in the case of



detergent form [55]. On the other hand, the detergent form of pig-enzyme shows charge shift during immuno-electrophoresis and elutes ahead of protease form with difference in  $M_r$  of about 100,000 expected for <sup>the</sup> Triton solubilised form indicating the possibility of an anchor peptide involved in its membrane association [56]. But, the isolation and characterisation of the anchor peptide has not been attempted. With no agreement between these two findings, it was difficult to suggest a possible mode of its attachment to the membrane. Very recently Lee and Forstner [77] have reported that the detergent form could be isolated with an intact additional peptide portion, if the solubilisation was performed with protease inhibitors and this peptide is possibly chopped off during the normal course of solubilisation which leads to an apparent identity of the two forms.

The enzyme has been studied in detail with respect to its specificity, inhibition pattern, etc. in rabbit [116], pig [56], human [63] and monkey [118]. Maltose, starch and amylopectin are the best substrates for the enzyme. Oligosaccharides are also hydrolysed. The human enzyme is most active on maltonanose, and oligosaccharides with higher or lower degree of polymerisation have lower activities [63]. Generally, the isomaltase activity is about 1% of maltase

activity and the activity is improved if the isomaltose unit is present in a larger molecule [56]. The enzyme while specific for  $\alpha$  linkage shows lack of specificity for aglycon part, which could be either glucose or even a phenyl moiety. The bonds cleaved can be either  $\alpha$ -(1  $\rightarrow$  4),  $\alpha$ -(1  $\rightarrow$  3),  $\alpha$ -(1  $\rightarrow$  2) or  $\alpha$ '-(1  $\rightarrow$  6) (in the order of activity) [115,56]. There seems to be some importance for the anomeric hydroxyl in disaccharides hydrolysed by this enzyme because, if it is blocked or involved in glycosidic bond as in the case of sucrose, trehalose and maltosaccharides, they are either inhibitors or poor substrates [56]. During starch hydrolysis the enzyme releases glucose residues one by one from the non-reducing end and the only product, identifiable is glucose though there was a faint maltose spot observable after 45 min of hydrolysis [112]. There is contrast with regard to the action pattern of the enzyme when compared to glucoamylase from mould. The mould enzyme exhibits lower activity towards maltose, compared to higher oligosaccharides [118]. On the other hand intestinal glucoamylase exhibits maximum activity towards maltose. Though there is a clear indication in the detailed kinetic study by Sivakami and Radhakrishnan [115] for the presence of multiple substrate and inhibitor binding studies it is not clear if they are arranged in the linear fashion suggested for fungal glucoamylases based on their action pattern [118]. Some interesting aspects

of the action pattern of the rabbit enzyme and a speculative model for the active site are given in this thesis.

Lactase-phlorizin hydrolase complex: This is one of the intestinal glycosidases which has not been probed adequately for molecular details. Since the time Malathi and Crane [119] reported that phlorizin hydrolase activity is distinct from the brush border lactase, the relationship between the two activities in the complex has been ~~the~~ <sup>subjected</sup> ~~to a lot of study~~ <sup>of many studies</sup> at the kinetic level. There <sup>is</sup> ~~are~~ evidence that both the activities are present in the same protein or protein complex [61,120,121] with at least two catalytic sites. In <sup>the</sup> infant rat the sites appear to be independent [122] whereas in the case of human and hamster and rabbit there appears to be an interaction [120,121,123]. However, in monkey there seems to be only one site for both ~~the~~ activities [123]. An interesting feature of this enzyme is its taxonomy and developmental pattern. In general, both lactase and phlorizin hydrolase activities are relatively higher in the infant animals than in adults and the activities can be under same or different biological control mechanisms [38]. It is likely that there are two separate polypeptides forming an oligoenzyme structure [122].

There is also an acid phlorizin hydrolase activity for the enzyme which is stimulated by linear 4 carbon dicarboxylic acids, the most effective being L(+)-tartaric acid and the stimulated activity can be inhibited by other organic acids like pyruvic acid which do not have any effect on the unstimulated enzyme [123]. A possible physiological role that has been attributed to this complex is the hydrolysis of glycosyl ceramides present in milk [124]. This activity can be associated with either phlorizin hydrolase [124] or lactase [123].

This complex does not have maltase activity and it is specifically a  $\beta$ -glycosidase. It is essentially a disaccharidase with about 1% of  $\beta$ -galactosidase activity. Cellobiose is also hydrolysed at a considerable rate though, it does not have galactosyl moiety which would mean that the enzyme is specific ~~about~~<sup>for</sup> the glycone and the  $\beta$  linkage. Though it is not specific towards the aglycon part, nevertheless, it determines the rate. In higher animals, a  $\beta$ -galactosidase activity does not necessarily correspond to lactase activity as in microbial systems.

## HYDRODYNAMICS AND QUATERNARY STRUCTURE OF MACROMOLECULES

### Quaternary structure of proteins: a bird's-eye view

Many proteins whose  $M_r$  is greater than about 60,000 have more than one polypeptide chain either identical or non-identical [125]. Larger proteins with subunit structure exhibit a quaternary structure which adds versatility to their action as compared to single polypeptides of the same size [126] and it also serves to minimise to a great extent, the errors that might creep in during their biosynthesis especially at transcriptional level [127]. The advantages of proteins with a quaternary structure can be appreciated better especially when viewed from the point of their functions. These functions vary widely and the proteins with quaternary structure are well adapted to suit the function. This class of proteins <sup>includes</sup> ~~comprise~~ of structural proteins like collagen and many key enzymes in metabolic pathways, often consisting of multienzyme systems. Large protein assemblies like ribosome owe their function to the quaternary structure [126].

Within the structure the individual polypeptides are associated in a specific manner even if the linkages are not covalent. The forces involved may be so weak that the

complex could be reversibly dissociated even to the monomers level simply by dilution [128], or binding of a monovalent cation [129] or anion [130] or cofactors [131] or substrates [132]. This reversible association and dissociation play an important role in the function of these proteins. On the other hand, many of these proteins possess highly associated polypeptides which cannot be dissociated easily but, with detergents like SDS or denaturants like urea and guanidinium chloride [133-135]. In others especially the structural proteins the polypeptide chains may be covalently linked.

Over the years, by an analysis of the quaternary structures with respect to the number and nature of polypeptide chains and the geometry of their ensemble, certain general features have emerged [136]. A large proportion of these proteins are made of an even number of identical polypeptides and are arranged to generate a close set of geometries, symmetrical around a central point. Recently, however, it has become apparent that some proteins with asymmetrically arranged subunits can exist and even in a crystalline form [137].

A study of quaternary structure involves various aspects [137], which include: (a) identification of the nature and number of polypeptide chains, which is easily

performed by dissociating the complex either with SDS, urea or guanidine HCl in <sup>the</sup> presence or absence of sulphydryl compounds and subsequent estimation of the size by electrophoresis, gel filtration, analytical ultracentrifugation or less commonly, using hybridisation technique [138]; (b) establishing the geometry of the ensemble which in the case of crystallisable complexes involves low-resolution X-ray diffraction studies and in the case of non-crystallisable ones, a small angle X-ray scattering technique or high resolution transmission electron microscopy aided by image reconstitution techniques and hydrodynamic studies along with theories of various model systems; (c) a study of subunit interactions which can be accomplished only for crystallisable complexes by high resolution X-ray diffraction techniques, the best example being haemoglobin.

A structural complexity that is seen in some proteins with quaternary structure is the presence of a functional unit or 'protomer' which is not easily dissociated further into polypeptide chains but which combines in a particular geometrical pattern to give rise to the final complex [136].

#### Methods available for noncrystallisable proteins to study their quaternary structure

The subunit arrangement and their interactions have not been well investigated for many of the membrane bound

proteins, mainly because, they could not be isolated as crystals suitable for X-ray studies [75]. One advantage especially in the case of intestinal disaccharidases, is that they are large enough ( $M_r > 200,000$ ) to be investigated using high resolution electron microscopy, which enables an evaluation of structural details at about 20 Å resolution. This will definitely allow one to predict the plausible arrangement of subunits, especially using image reconstitution studies [139]. Proteins less than about  $M_r$  100,000, are difficult to be analysed for subunit details by electromicroscopy. In such cases their behaviour in solution is a useful aid to make prediction about their shape and if the number of subunits <sup>is</sup> are known from other physicochemical or chemical methods, it is relatively easy to predict their actual arrangement, thanks to the rapid development in theoretical models for hydrodynamic particles [140]. The combination of solution studies with electron microscopy has many advantages. Primarily it is a useful cross-check for the structure derived from the electronmicroscopic images, and if the structure from electron microscopic studies is well founded, then it helps to see if the predicted behaviour of hydrodynamic model is in keeping with the true behaviour of the molecule. Additional information like molecular weight, water of hydration etc. can be obtained from solution study.



Since we have used such an approach and since its development especially on the prediction of actual structure from experimental measurement is of recent origin and has not been fully exploited, (except to make some comments on axial ratio) it is proposed to review the recent knowledge on the subject and highlight the potentiality of the approach.

#### Hydrodynamic studies-theoretical principles of various model systems:

This study is pertaining to the motion of the macro-molecule or any other hydrodynamic unit, in solution and the methods involve physical measurements of such a motion. Since the methodology is ~~of~~ old ~~origin~~ and well studied and great details are covered in many excellent reviews and text book chapters [141 - 153], only the information obtainable on shape and assembly of subunits in a complex from hydrodynamic study, pertaining to ~~the~~ recent development<sup>r</sup> will be covered here.

Shape factors: There are two important shape factors,  $f$  and  $v$ . The former ( $f$ ), called frictional coefficient, is obtained from both sedimentation coefficient and diffusion coefficient measurements, by the relations

$$f = \frac{M(1-\bar{v}\rho)}{NS^0} = \frac{RT}{ND^0}$$

The latter ( $\nu$ ), called viscosity increment is obtained from intrinsic viscosity by the relation.

$$[\eta] = V_h \nu$$

In the case of spherical molecules  $f$  is related to the size of the sphere by Stokes' equation.

$$f = 6\pi\eta r_0,$$

and analogous equations for prolate ellipsoid, oblate ellipsoid and long rod, in terms of their axial ratio and size are complicated [152].

Theory of equivalent ellipsoids: Perrin employed a quantity called frictional-ratio, that is the ratio between  $f$  and  $f_0$ , which is the frictional coefficient of an equivalent sphere of radius  $a_0$  and volume,  $V_0$ . Now  $f/f_0$  is independent of the size of the particle and is a function of axial ratio only [154].

$\nu$ , on the other hand, is a function of axial ratio only and appropriate expressions in terms of axial ratio have been worked out by Simha [155,156].

Actually, <sup>F</sup>frictional ratio and viscosity increment are functions of not only shape but also the hydration of the hydrodynamic particle. Hence it is not possible to weigh the relative contributions from the measurement of one of them. As an alternative, Oncley et al [156] suggested that either a typical value of water of hydration (0.25 g/g of protein) is assumed and the axial ratio is read from a contour of axial ratio vs frictional ratio or viscosity increment for different hydration values; or, the hydrated volume  $V_h$  is replaced by partial specific volume  $\bar{v}$  so that  $[\eta] = \bar{v} \nu$ , which straight away yields  $\nu$  and hence the axial ratio. Yet another way of interpreting the data would be to assume either no hydration or sphericity and express dimensions corresponding to maximum asymmetry or maximal hydration respectively. Sheraga and Mandlkern, [158] strongly objected to such arbitrary assumptions and pointed out that these assumptions are unwarranted if one combined two different hydrodynamic parameters and solved two simultaneous equations, to obtain both asymmetry and hydration factor. They introduced a factor called  $\beta$  given by the relation

$$\beta = \frac{n_o [\eta]^{1/3} M^{1/3}}{f} \quad [f \text{ is obtained either from } S^0 \text{ or } D^0]$$

$\beta$  is a function only of axial ratio and has a characteristic value of  $2.25 \times 10^6$  for spheres, random coils and oblate ellip-

soids, and in the case of prolate ellipsoids it increases rather insensitively in relation to their axial ratios. Owing to this insensitivity, it requires very accurate data for its evaluation and hence is unsuitable for the purpose. However, this insensitivity was used with advantage in computing molecular weight from viscosity and transport data. Holtzer and Lowey [159] pointed out that even this estimate could be subject to error if the true molecular shape is not the same as the assumed ellipsoid. So, at present the use of  $\beta$  is restricted to finding out if the hydrodynamic particle is a prolate ellipsoid or an oblate ellipsoid. There are other criticisms questioning the wisdom ~~in~~<sup>of</sup> combining two different experimental quantities [146,147] since, the shape assumed could be different in these measurements, especially for flexible molecules.

A close approximation to the equivalent ellipsoid is a cylinder of the same length and volume as the ellipsoid [160]:

$$V_e = 4/3 \pi a^2 b = \pi r^2 L$$

String of beads (Kuhn's model): Hydrodynamic behaviour of approximate representation of a rod as a string of beads of radius 'r' with surfaces separated by distance equal to the bead diameter was theoretically worked out by Kuhn [161] and the following relations were derived:

$$\eta_{sp} = \pi/48 GS^3 \text{ and } D = KT/(3\pi/2)\eta_0 S$$

where  $\eta_{sp}$  is the specific viscosity,  $G$  is the number of particles/ml,  $S$  is the length of the model. Volume of the model is given by:

$$V = (\pi/12)(d^2 s)$$

where  $d$  is the diameter of a bead and the number of beads in the model is  $S/2d$ .

This model was used by Shulman [162] to derive the shape of fibrinogen molecule from its sedimentation and viscosity data. He used the relations:

$$\nu = \frac{1}{4} (S/D)^2$$

$$f/f_0 = (S/2d)^{2/3}$$

and showed some agreement between its electron microscopic appearance and shape derived using  $\nu$ , but not  $f/f_0$ . However, there was uniformly lack of agreement between the shapes derived from  $\nu$  and  $f/f_0$  using other model systems.

String-of-beads(Kirkwood's model):Kuhn's model did not achieve much popularity, but it lent support to the view that  $[\eta]$  is proportional to the first power of molecular

weight. A glaring omission that led to the failure in predicting correct molecular weight, especially of large molecules was the hydrodynamic interactions between the monomers/subunits in a chain. It is obvious that in large molecules the interior elements will be hydrodynamically shielded and their effect on the motion of the molecule will be insignificant. The theories developed later took into account this interaction. Debye and Brinkman [163] described a molecular model consisting of a sphere containing a uniformly distributed system of resisting points equal in number to the number of monomer units and obtained an agreement with the experimental observation. In the relation

$$[\eta] = kM^a, \text{ 'a' decreases from 1.0 to 0.5 as}$$

the molecular weight increases. A popular model, based on theories which took into account hydrodynamic interactions between units, was developed by Kirkwood [164]. This is a more accurate version of Debye's model. Kirkwood treated the rod like particles as a string of spherical beads, aligned in a row, with beads touching each other and their centres separated by a distance equal to the diameter of a bead. The sedimentation coefficient and intrinsic viscosity of such a geometry is:

$$S^0 = [ (1-\bar{v}\rho_0)d^2 \ln J ] / 18\eta_0$$

$$\text{and } [\eta] = (24 J^2) / (9000 \cdot \rho \cdot \ln J)$$

where  $\rho$  is the density of the particle,  $J$  is its axial ratio and  $d$  is the diameter of each bead.

String-of-beads vs equivalent ellipsoid: Holtzer and Lowey [159] obtained the  $\beta$  value from these expressions for this model and made a comparison with the  $\beta$  values obtained from a similar expression for ellipsoidal model. They indicated that  $\beta$  value obtained would depend on the model chosen and hence would affect the calculated  $M_r$ . They traced the origin of this difference to the frictional coefficient of the models. A rigid string of spherical beads offer a significantly greater frictional resistance to translation than a similar ellipsoid. The molecular weights obtained from  $\beta$  values based on Kirkwood's model for some long chain molecules like light meromyosin, paramyosin and collagen were in good agreement with their absolute  $M_r$ , unlike the values based on  $\beta$  from equivalent ellipsoidal model. However heavy myosin did not show a good correlation with Kirkwood's model, but agreement was good with the ellipsoid.

Holtzer and Lowey [165] had previously applied Kirkwood's model to myosin molecule and obtained its dimensions, which were close to the ones obtained from light scattering experiments.

$$S^0 = [\rho (1 - \bar{v}\rho_0) d^2 \ln J] / 18\eta_0$$

$$\text{and } [\eta] = (24 J^2) / (9000 \cdot \rho \cdot \ln J)$$

where  $\rho$  is the density of the particle,  $J$  is its axial ratio and  $d$  is the diameter of each bead.

String-of-beads vs equivalent ellipsoid: Holtzer and Lowey [159] obtained the  $\beta$  value from these expressions for this model and made a comparison with the  $\beta$  values obtained from a similar expression for ellipsoidal model. They indicated that  $\beta$  value obtained would depend on the model chosen and hence would affect the calculated  $M_r$ . They traced the origin of this difference to the frictional coefficient of the models. A rigid string of spherical beads offer a significantly greater frictional resistance to translation than a similar ellipsoid. The molecular weights obtained from  $\beta$  values based on Kirkwood's model for some long chain molecules like light meromyosin, paramyosin and collagen were in good agreement with their absolute  $M_r$ , unlike the values based on  $\beta$  from equivalent ellipsoidal model. However heavy myosin did not show a good correlation with Kirkwood's model, but agreement was good with the ellipsoid.

Holtzer and Lowey [165] had previously applied Kirkwood's model to myosin molecule and obtained its dimensions, which were close to the ones obtained from light scattering experiments.



The relationships used were

$$[S] = [(1-\bar{v} \rho_o) d^2 / 18 \cdot \bar{v} \cdot \eta_o] \ln(6M\bar{v}/N\pi d^3)$$

$$[\eta] = 24 \bar{v} J^2 / 9000 \cdot \ln J$$

$\rho_o$  and  $\eta_o$  = density and viscosity of solvent.  $d$  = mol. diameter  $J$  = axial ratio and  $\bar{v} = (N\pi d^2 L)/6M$

Stern [166], made a comparative study between equivalent ellipsoid theory and Kirkwood's model. From the expression for  $[\eta]$  and  $[S]$  in both the model systems, he obtained

$$L_{SB}^2 = \frac{6750 \eta_o [\eta] [S]}{(1-\bar{v} \rho_o)} \quad (\text{for axial ratios} > 20)$$

$$L_E^2 = \frac{1800 [\eta] [S] \eta_o}{\epsilon_E (1-\bar{v} \rho_o)} \quad (\text{for all axial ratios})$$

$$\epsilon_E = \frac{F_E^r}{J_E^{4/3}}$$

$$F_E = f_o / f$$

the subscript SB and E respectively mean string-of-beads and equivalent ellipsoid model.

Values of  $\epsilon_E$  and  $J_E$  have been tabulated [166]. For the estimation of lengths of a macromolecule, while in the case of ellipsoidal model one should have a prior knowledge of axial ratio, no such requirement is necessary in the case of SB model. Stern [166] also concluded that the spherical bead model gave valid estimates of  $M_r$  for rigid helical macromolecules of high axial ratio. According to him from the deviation of the length measured using light scattering and the one calculated using either string-of-bead model or ellipsoid model one can pick up the correct model.

One valid reason for the lack of a sensitive variation of  $\beta$  with respect to axial ratio, could be that relative weightage for  $[\eta]$  is poor, being  $[\eta]^{1/3}$  in the expression of  $\beta$ . In fact  $[\eta]$  is the more sensitive parameter of shape than frictional ratio. Stern's expression for  $L$  gives an equal weightage for  $[\eta]$  <sup>and  $[S]$</sup>  and hence could be used with a better reliability and confidence.

Once-broken-rod, a model for denatured states: Since the rigid rod and random coil models were suited for native and completely denatured states, the model of once broken rod was treated by Hyuk Yu and Stockmayer [167] to include the case of partially denatured macromolecules (like DNA). The contribution to changes in hydrodynamic parameters by such flexibilities at or near either end of a rod is

insignificant. For the model chosen, i.e. centrally placed break, it was predicted that  $[\eta]$  would be 15% lower than the native behaviour and this was actually seen in the behaviour of poly- $\gamma$ -benzyl-L-glu polymer chains linked by a flexible bifunctional initiator trimethylene diamine [168]. In the case of chains with flexible joints away from the centre and with segment lengths  $L_f$  and  $L(1-f)$ , the following relationship holds

$$[\eta] \text{ once broken} / [\eta] \text{ rigid} = 1 - 0.60f(1-f)$$

It was pointed out by Zwanzig [169] that a defect in Kirkwood's theory led to inaccurate results in some cases; like the correct  $D$  for a rigid circular ring molecule is actually 11/12 of that predicted by theory. But, correct values will be got for long rigid rods. Hearst and Stockmayer [170-173] studied in detail the hydrodynamic behaviour of cylindrically symmetrical models with rigidity intermediate between flexible coil and rigid rod or ellipsoid.

Hydrodynamics of all shapes (Shell model): In all the cases discussed above, the macromolecular shapes have been modeled into a few restricted classes <sup>as</sup> like spheres, ellipsoids (prolate or oblate), cylinders, rigid string of spherical beads. But, the actual shape<sup>s</sup> of macromolecules

are so varied, from linear to subunits arranged in strict regular geometrical patterns with spherical, cubical, di- and polyhedral symmetries. To account for the hydrodynamic behaviour of these and to predict the actual shape the first attempt was made by Bloomfield et al [174]. Confirming the validity of Kirkwood theory they modified Kirkwood's model to consider even subunits of different sizes. They proposed a shell model, according to which a large number of small and identical spheres (subunits) are arranged to outline the overall particle shape. For a structure composed of identical subunits of effective radius  $r_1$  arranged in a rigid geometrical array with a uniform spacing  $r$ , the frictional coefficient is given by

$$f = n [1 + (\zeta/\zeta_0) r_1/r] \sigma(n)]^{-1}$$

where  $\zeta$  and  $\zeta_0$  are frictional coefficients of individual subunits and that of equivalent sphere,  $\sigma(n)$  is a geometrical factor determined by the arrangement of subunits. This model was applied to macromolecules of known size and shape <sup>such as</sup> ~~like~~ haemocyanin, phycocyanin, fibrinogen, slow form of  $T_2$  bacteriophage, tobacco mosaic virus (TMV), fast form of  $T_2$  and  $\lambda$  ghosts [175]. There was an 'excellent' agreement in the case of haemocyanin and 'good' agreement in the case of phycocyanin, TMV, fast form of  $T_2$  and  $\lambda$  ghosts. However,

a good agreement was not seen in the case of fibrinogen, slow form of  $T_2$  and bacterio phage.

Hydrodynamics of all shapes (Subunit model): In a series of articles, Jose Garcia de la Torre and Bloomfield, [176-179] reported their study using another model system called subunit model, in which the particles are built up by using a definite number of spherical subunits having different sizes. Kirkwood's theory was actually based on the formulations of hydrodynamics developed by Oseen and Burgers [180]. According to them the subunits were regarded as point sources of friction regardless of the shape, while it is true that the hydrodynamic forces are distributed on the subunit surfaces. Rectification of this and other flaws [181-183] in the original theory led to an improved hydrodynamic theory. In some cases even negative diffusion coefficients were predicted owing to the strength of hydrodynamic interactions of these point sources. Using the improved theory, it was shown that the <sup>transport behaviour of</sup> bead model of a rod like molecule <sup>would be</sup> ~~behaved in its transport behaviour~~ intermediate between an ellipsoid and a cylinder.

$$D = \left( \frac{KT}{3\pi\eta_0 L} \right) \left[ \ln L/a + \gamma \right], \gamma = 3/8 \text{ and } L = na$$

$L$  = length

$a$  = diameter of a bead

$n$  = number of beads

They [179] reported a simple and improved version of a theory to calculate  $[\eta]$  and published tables containing frictional coefficients and intrinsic viscosity values for a number of common structures usually assumed by macromolecules and their assemblies. Application to hemierythrin and aspartate-transcarbamylase and once-broken-rod clearly demonstrates not only their usefulness but also their potentiality to predict the correct hydrodynamic behaviour of the molecules. They also stress the importance of combining two hydrodynamic quantities, translational and viscosity parameters to get  $\beta$  values. Such  $\beta$  values for various structures have been tabulated.

Hydrodynamics of all shapes (Improved subunit model):

While their predictions were in good agreement with experimental values for structures with sizable axial ratios, error was unavoidable in the case of prolate ellipsoids with short axial ratios [184]. This problem <sup>results from</sup> is owing to the considerable concentration of the frictional resistance in the central bead which occupies a large fraction of the volume of the particle. <sup>Thus</sup> So, in order to improve upon the results it was necessary to move the frictional elements to the surface of each sphere with an array of smaller spheres, replacing larger ones. But <sup>this</sup> this inevitably increases the computation and hence computer time [184].

Bernal and Garcia [185] made use of the point just mentioned and worked out the improved values for various geometrical shapes (to save the computer time, subunits have been replaced by only a few (5-8) small spheres). They have tabulated both  $f$  and  $[\eta]$  for various shapes of macromolecules [185].

Frictional coefficient and geometry of oligomers:

A recent review [186] on this aspect gives an excellent guideline to arrive at the geometry of an oligomeric protein from its frictional property. Taking into account the rugosity of proteins, arising from the processes on its surface and assuming that the subunits in an oligomeric proteins are hydrodynamically independent, a useful relationship (given below) connecting the sedimentation coefficient and geometry of an oligomer was arrived at.

$$\frac{S_n \bar{v}^{1/3}}{(1-\bar{v}\rho)} = 0.01 M^{2/3} F_n$$

$$F_n = n^{1/3} (\zeta/f_n)$$

where  $S_n$ ,  $f_n$ ,  $M$ ,  $\bar{v}$  and  $F_n$  are respectively the sedimentation coefficient (in water at 20°C) frictional coefficient, molecular weight, partial specific volume and geometric factor of an oligomer.  $\zeta$  and  $n$  are respectively the frictional

coefficient and number of subunits.  $F_n$  <sup>value</sup> for various possible geometries up to a tetramer have been tabulated and the possible geometry can also be read from the graph provided [186].

$F_n$  can also be approximately calculated for any geometry using the following relation derived from Kirkwood's formulation [186]

$$F_n = n^{-2/3} \left( 1 + \frac{a}{n} \sum_{i=1}^n \sum_{\substack{j=1 \\ i \neq j}}^n r_{ij}^{-1} \right)$$

$r_{ij}$  is the distance between subunits of equal size and radius 'a'. The correlation between  $F_n$  values arrived at by these two different methods for various proteins with known quaternary structure was found to be good.

Using the shell model with spherical beads of 1.4 Å radius and Kirkwood's formulation Teller et al [186] found out that the correct frictional coefficients are calculable only when hydration of charged residues is taken into account. According to them the frictional properties are dependent on overall dimensions, rugosity of the surface and hydration at charged residues on the surface.

Surface area of proteins: The empirical relationship connecting surface area and sedimentation properties of mono-



meric proteins is given by

$$S\bar{v}^{1/3} (1 - \bar{v}\rho) = kA_s$$

Where  $A_s$  is the accessible surface area in  $\text{\AA}^2$  and  $k = 8.9 \pm 0.7 \times 10^{-4} \text{ S.cm/g/\AA}^2$ . From this relation one can calculate the accessible area of a protein and for a number of proteins this has been found to be a simple function of  $M$  and appears to be an invariant property of protein folding [188]. The  $\log A_s$  vs  $\log M$  is linear with a slope of 0.70

$$\text{and } A_s = 11.1 \times M^{2/3}$$

For a spherical molecule it can be shown that

$$A_s = 5.6 \times M^{2/3}$$

The experimental value is almost twice ~~that~~ of the calculated <sup>value</sup> ~~and this is~~ owing to the fact that folded proteins have nearly twice the area of the sphere of same mass and density. Presence of crevices seems to have negligible effect on  $A_s$ . It is to be appreciated that hydrodynamics offers a simple and straight forward method to arrive at the shape and geometry of an oligomer especially after the advent of modifications in older theories and its intelligent applications to predict the hydrodynamic behaviour of all possible shapes known in biological systems. The <sup>task</sup> ~~job~~ is simplified to

the extent that one should measure rather accurately either frictional coefficient or intrinsic viscosity of an oligomer, whose subunit-stoichiometry is known, and compare the values given for various geometries in reference [185] and choose the best fit, or calculate the geometrical factor from *the* frictional coefficient and know the best fitting geometry from the table or graph provided in <sup>the</sup> reference [186]. If the probable geometry is available by other direct methods like electron microscopy or small angle X-ray scattering, one can cross check if the probable geometry is true hydrodynamically also.

## QUATERNARY STRUCTURE AND ELECTRON MICROSCOPY

### Negative stain techniques

The high resolution technique using negative staining is an alternative to X-ray analysis, in the case of proteins ~~which~~<sup>that</sup> cannot be crystallised to suit X-ray work. In the past few decades this area of electron microscopy has shown considerable development in specimen preparation for high resolution work and in image reprocessing technique. The recent image reprocessing techniques enable one to obtain the original three-dimensional picture of the macromolecule from its two-dimensional image, a task rendered difficult due to the large depth of focus in E.M. Since there are

some excellent reviews [139,190] and illustrative examples [191,192] in the literature, only some aspects relevant to the work reported in this Thesis will be summarised below.

Conventional methods: It was accidentally found by Farrent [193] that certain molecules were in negative contrast in his micrographs obtained after positive staining. Similar observation<sup>s</sup> was made by Hall [194], while studying positively stained virus particles. Its routine use and superior quality of the pictures were brought out by Brenner and Horne [195]. One of the advantages of this staining method is that when protein molecules are dried within the matrix of negative stain, surface tension forces are dissipated against<sup>th</sup> stain bed surface, minimising distortion of the ultra-structure of the specimen. In the conventional negative staining techniques the proteins along with a suitable negative stain are placed on a support film, prepared either of plastic or carbon on a copper grid. When the stain dries ~~out~~, the specimen is subjected to electronmicroscopic investigation. Though the procedure looks very simple and straight-forward, one should bear in mind<sup>th</sup> the artefacts<sup>s</sup> which might arise owing to either improper stain and support film interactions or nonuniform layering of stain, or formation of stain microcrystals which interfere with the quality of<sup>th</sup> image and its interpretation [196]. Better negative

stains do not usually possess this <sup>disadvantage</sup> evil and give a very thin film on the surface of the membrane. The membrane is thought to be a 'necessary evil' [196] because it limits the resolution and is a candidate for artefacts, while providing mechanical strength to the specimen. Though there are several compounds of heavy elements like tungsten, uranium, molybdenum, etc., available, phospho-tungstic acid and uranyl acetate are the two most popular negative stains, the latter is preferred for high resolution work owing to its smaller size compared to PTA.

Techniques without support membranes: <sup>suggestion</sup> A hint to do away with the necessary evil was obtained from the early work of Hexley and Zubay [197], when they found better clarity and quality of pictures obtained from areas not covered by support film. In other words, the molecules in holes of otherwise uniform membrane gave rise to superior images. It is remarkable that these films formed across the holes are resistant to washing from one side. Though holey carbon and plastic membranes became a fashion, there was not any major attempt to remove the membrane completely, until Malech and Albert [198] reported a very novel method in which thoroughly cleaned grids of 400 or 500 mesh were floated on a mixture containing 1% PTA (final) pH 7.3, 10 µg/ml . bacitracin and the specimen. After a brief

wash, the dried grids were examined under E.M. The protein-stain-bacitracin combination seems to be essential for the formation of stable films under the electron beam. This method was shown to be useful for molecules in the  $M_r$  range of  $10^5$ - $10^6$  because smaller and larger molecules crossing this range did not yield stable membranes. The images were claimed to be superior and artefact free. Apart from other claims the simplicity of the method and the ability of the proteins to make stable films did <sup>much to credit</sup> more credit to the method and questioned the inevitability of the support film. We were prompted by this observation and recently found out that our protein, falling in the size range recommended, had the ability to form stable films with uranyl acetate stain (2%, pH 4.0). (See page 70).

Sandwich techniques: Another major variation in the negative staining technique, was introduced by Lake et al [199]. The carbon film was floated on the enzyme solution followed by its floating on the stain solution. Later it was lifted with the grids. Lake et al [199] found that the molecules in areas where the carbon support film had folded on itself gave superior quality pictures and thus developed a double layer carbon technique as a modification of the single carbon layer technique [200]. A review of this method and its use in immuno electronmicroscopy work has been published [200a].

Image reconstitution: The difficulty in interpreting the images formed as two dimensional projections of the three dimensional objects is to an extent rendered easy by the presence of a population of molecules oriented in different ways. With an intelligent guesswork one can identify with relative ease the gross geometrical pattern of the subunit arrangement, from these different orientations, owing to the presence of symmetry axes in the design of the macromolecules. A useful technique which may further aid this process is photographing the molecules normal to the beam and at an angle slightly tilted to the normal. This gives a stereoscopic pair of images of the molecule and comparison of related views reveals the gross three dimensional appearance of the molecule. There are image reconstitution methods available to envision the original structure which led to the particular image[139, 190].

## MATERIALS AND METHODS

## MATERIALS

Chemicals: The chemicals and materials commercially obtained are grouped together with the supplier's name in parenthesis. All chemicals not listed were of the analytical or the best available grade.

Sepharose 4B-200 (40-150 $\mu$ ), Octyl-Sepharose CL-4B, Phenyl-Sepharose CL-4B, Sephadex G200 (40-120 $\mu$ ) and blue dextran (Pharmacia Fine Chemicals, Uppsala, Sweden).

Dowex-50 (50x8, 200-400 mesh) H<sup>+</sup> form, Dowex-1 (1x4, 100-200 mesh) Cl<sup>-</sup> form, papain (2xcrystallised), glucose oxidase, horse radish peroxidase, o-dianisidine, trypsin (TPCK treated), carboxy peptidase A, acrylamide, bis-acrylamide, TEMED, riboflavin, TRIS buffer, bovine serum albumin (crystalline), guanidinium chloride, sodium dodecyl sulfate (recrystallised from methanol), dansyl chloride, dansyl amino acids, dipeptides, tripeptides, N-ethyl morpholine,  $\beta$ -mercaptoethanol, p-hydroxy mercuribenzoate, p-nitrophenyl- $\alpha$ -glucoside, glucono- $\delta$ -lactone, phenyl- $\alpha$ -glucoside, amylose, amylopectin, Coomassie blue R 250, Coomassie blue G 250 (Sigma Chemical Company, MO, U.S.A).



Triton-X100, enzyme grade sucrose and urea (Eastman Kodak Company, Rochester, New York, U.S.A); soluble starch (E Merck, Darmstadt, W. Germany); Freund's complete adjuvant (Difco Laboratories, Detroit, Michigan, U.S.A); Azocoll (Calbiochem, Los Angeles, California, U.S.A). .

Micropolyamide sheets, 15 cm x 15 cm, coated on both sides without bonding agent (Schleicher and Schull, D-3354, Dassel, W. Germany).

Polyamide powder was a gift from Dr. Keshav Datye, U.K. and  $\beta$ -limit dextrin from Dr. R.P. Sharma, University of Hyderabad, Hyderabad, India; bacitracin was a gift from Prof.L.K. Ramachandran, Osmania University, Hyderabad.

### Instruments

Beckman Model E analytical ultracentrifuge equipped with Schlieren Optics, RTC unit and electronically controlled speed regulation was used for sedimentation velocity, sedimentation equilibrium and diffusion experiments. The plates read on a microcomparator (Gaertner Scientific Corporation, Chicago, ILL.U.S.A).

Viscosity was measured using Ubbelohde semi-micro type viscometer.

Automatic amino acid analysers used were: Bechman model 116C, Kontron and LKB (alpha plus).

Isoelectric focusing was performed in an LKB Multiphor unit Model 2117 fitted with a cooling system.

Gilford spectrophotometer-250 (Gilford Instruments LAB, U.S.A) fitted with thermo programmer and Shimatzu spectrophotometers (Japan) were used to record the absorption spectra.

Fluorence spectra was recorded on Fluorescence spectrophotometer (Hitachi, Japan).

Mineralight UV SL.25(Ultraviolet products, U.S.A), was used as a source of both long and short wave UV to view the fluorescent dansyl derivatives on TLC.

## PURIFICATION PROCEDURE FOR THE PROTEASE AND DETERGENT FORMS OF THE ENZYME

### Preparation of particulate fraction:

The procedure was essentially according to Sivakami and Radhakrishnan [66] with slight modifications. Rabbits, about forty in number per batch, were sacrificed by decapitation. The intestines were removed, washed thoroughly with ice-cold isotonic solution of KCl (1.15% w/v), cut open lengthwise and the mucosa was scraped with a microscope slide by running it over the mucosal surface gently under ice-cold condition. The scraped mucosa was weighed, suspended in sufficient volume of cold ( $4^{\circ}\text{C}$ ) potassium phosphate buffer (0.01 M, pH 7.0) and homogenised using either a Waring blender worked at top speed for 5 sec, or a mechanical grinder consisting of a motor drive, a glass grinding chamber of volume, 30 ml, and a teflon pestle, to give a 20% (w/v) homogenate. The homogenate was centrifuged at 20,000 g for 30 min and the resulting pellet was resuspended in half the original volume ~~with~~ cold potassium phosphate buffer (0.01 M pH 7.0; hereafter referred to as K-phosphate buffer), using a tissue-grinder. The resuspended pellet was divided into two approximately equal parts. One part was <sup>subjected to</sup> ~~subjected to~~

solubilisation with papain and the other was treated with Triton-X100, a neutral detergent.

### Purification of the papain form of the enzyme

The first resuspended pellet fraction was adjusted to a final protein concentration of 10 mg/ml with K-phosphate buffer, and papain and  $\beta$ -mercaptoethanol were added to a final concentration of 0.5 mg/ml and 0.01 M respectively and incubated at 37°C for 90 min with continuous stirring. At the end of this period, the proteolytic activity was arrested with iodoacetamide (0.01 M, final) and the suspension was centrifuged at 100,000 g for 1 hour. The supernatant fraction was passed through a Sephadex G-200 column, previously equilibrated with K-phosphate buffer in the cold room. The bed volume of the gel was calculated on the basis of a predetermined ratio; 10 units of enzyme per 1 ml bed volume of gel, [66]. The flow rate was maintained at 20 ml/hour. After the collection of the breakthrough fraction, the column was washed with 25 bed volumes of K-phosphate buffer. The column was brought to room temperature and the bound enzyme was ~~subjected to substrate~~ elution with 0.1 M maltose dissolved in K-phosphate buffer. The eluted enzyme collected in three single bed-volume fractions was dialysed in the cold room against double glass distilled water to remove

maltose. Pilot experiments had shown that substrate elution of the enzyme at room temperature was superior to elution in the cold room in terms of recovery.

#### Purification of the Triton form of the enzyme

The second resuspended pellet fraction was adjusted to a final protein concentration of 5 mg/ml with K-phosphate buffer and Triton-X100, final concentration of 0.5% (v/v) containing NaCl 0.01 mM, final. At the end of 90 min at 4°C, the suspension was centrifuged at 100,000 g for 1 hr. The supernatant fraction was mixed with Sephadex G-200 beads previously equilibrated with the buffer containing 0.5% (v/v) Triton-X100 NaCl, 0.01 mM. The amount of the gel, as in the previous experiment, was calculated on the basis of 1 ml/10 units of enzyme. The mixture was kept at 4°C, with frequent manual shaking, for about 24 hours (also see page 90). Then the gel was allowed to settle and the supernatant was decanted. The settled gel was washed thrice with the equilibration buffer, each time using twice the bed volume. The washed gel was packed into a column and further washed with 25 bed volumes of 0.01 M K-phosphate buffer, pH 7.0, at a flow rate of 20 ml/hour. The bound enzyme, after bringing the column to room temperature, was eluted with 0.1 M maltose contained in the wash buffer,

free of Triton-X100. Single bed volume fractions were collected and dialysed against double-distilled water to remove maltose.

In both the cases, the fractions containing enzyme activity were combined and concentrated by freeze drying to a final concentration of about 10 mg/ml and once again thoroughly dialysed against the K-phosphate buffer.

## PHYSICAL METHODS

### Gel filtration

Sephacrose-4B was packed into a 300 ml column, taking necessary precautions recommended by the manufacturer and equilibrated with a single bed volume of 0.01 M K-phosphate buffer, pH 7.0, containing 0.1 M NaCl. The enzyme sample (3.0 ml; 1 mg/ml protein) was loaded carefully on top of the gel and eluted with the equilibrating buffer at a flow rate of 6 ml/hr. Fractions (3.0 ml) were collected using an automatic fraction collector. Packing was done at room temperature and the other operations were done in the cold room at 4°C. The enzyme was detected by assay and the fractions containing activity were pooled and preserved.

## Gel electrophoresis

### Non-denaturing type (Davis[201])

Gel composition: Stacking gel, 3.3% acrylamide; acrylamide: bis-acrylamide 40:1; stacking gel buffer, Tris-HCl, pH 6.9; running gel buffer, Tris-HCl, pH 8.3; gel electrophoresis buffer; boric acid-borax, pH 8.3; Sample: the two forms of the enzyme - native, heat treated, papain, trypsin, and chymotrypsin treated; in each case 50 µg enzyme was used if the staining was Coomassie Blue R250 or 5 µg if it was silver staining.

Run condition: 4 mA/tube for cylinder (constant current) and 50 mA in the case of slab. Run usually was stopped when bromophenol blue reached just one cm above the bottom.

Staining: for cylindrical gels - Coomassie blue R250 (see page 62) and for slab gels - silver staining was according to Sammans [202].

### Denaturing type-SDS PAGE (Weber and Osborn [203]):

Gel composition: running gel, 5% acrylamide and 0.135% bis-acrylamide; running gel buffer, 0.1 M sodium phosphate buffer, pH 7.2 containing 0.1% SDS. Gel electrophoresis buffer: 0.1 M sodium phosphate buffer, pH 7.2 containing 0.1% SDS.

**Sample:** The enzyme (50  $\mu$ g) was treated with 1% SDS under a variety of conditions such as heating at 100°C for 2,5, 10,20 and 30 min in the presence of 1% SDS; guanidine hydrochloride (6 M) treated enzyme was heated with 1% SDS up to 15 min 100°C, after completely removing guanidine hydrochloride by dialysis.

**Run condition:** Allowed to run at 8 mA/tube (in the case of cylindrical gels and 50 mA in the case of slab) till Brom-phenol blue reached just one cm above the bottom.

**Staining:** Coomassie blue R250 (for cylinders) and silver staining for slabs [202]. (staining was done after removal of SDS by repeatedly rinsing the gels with 50% methanol and 10% acetic acid).

#### Denaturing type-SDS PAGE (Lamelli [204])

**Gel composition:** Stacking gel, 5% acrylamide and bis-acrylamide in 0.07 M Tris-EDTA buffer, pH 6.8, containing 0.1% SDS; resolving gel, 10% acrylamide and acrylamide: bis-acrylamide, 33:1 in 0.2 M Tris-EDTA buffer, pH 8.8 containing 0.1% SDS. Gel electrophoresis buffer: 0.05 M Tris-glycine, pH 8.8 containing 0.1% SDS and 0.75% sodium EDTA.

**Samples:** As in the case of previous system.



Run condition: Constant voltage (100 V) till bromphenol blue reached one cm above the bottom.

Staining: Silver staining [202].

Denaturing type - Acetic acid PAGE [205]

Gel composition: 12 ml of 5% acrylamide and 0.8% bis-acrylamide in 1.5% acetic acid were polymerised by the addition of 0.12 ml of 10% ammonium persulfate and 0.12 ml of 10% TEMED and keeping at 50°C for 1 hr in an oven. Electrophoresis buffer, 1.5% acetic acid solution.

Sample: Aliquots of enzyme (50 µg) were treated with 0%, 10%, 50% and glacial acetic acid at room temperature as well as at elevated temperatures (60°C and 100°C) for varying intervals of time (5, 10 and 15 min). Treated samples were dried in vacuo and dissolved in 100 µl of electrophoresis buffer prior to loading.

Run condition: Pre-run for 2 hrs at 20 V cm<sup>-1</sup> and electrophoresis for 20 min at 40 V cm<sup>-1</sup>.

Staining: Coomassie blue 250.

Denaturing type-phenol-acetic acid-urea, PAGE [206]

Gel composition: Solution containing 6% acrylamide, 0.23% bis-acrylamide, 28% urea and 37% acetic acid, was mixed with a solution containing 1.6% ammonium persulfate in 60% urea in a ratio of 3:1 by volume and 0.02 vol of TEMED was added to initiate polymerisation. Polymerisation usually took about an hour at room temperature. Electrophoresis buffer: 10% acetic acid.

Samples: Aliquots (50 µg) of enzyme solution were treated with a solution containing 20% acetic acid, 24% urea, 40% phenol and 5% β-mercaptoethanol, both at room temperature and at 100°C for 15 min.

Run conditions: Gels were initially run in a current of 1.5 mA/tube for 1 hr, followed by 4.0 mA/tube for 4 hours.

Staining: Coomassie blue R250

General staining procedure

The cylindrical gels in almost all the cases were stained with ~~Coomassie blue R250~~ by soaking the gels for 2 hrs in a stain solution composed of 0.25% (w/v) Coomassie blue R250, 40% (v/v) methanol and 10% (v/v) acetic acid.

At the end of 2 hrs, they were removed and destained by a diffusion method, which involved soaking the gels in 50% methanol and 10% acetic acid initially a few times followed by gently stirring in a solution of 10% methanol and 10% acetic acid. Mixing of Dowex-1 resin, chloride form, to the latter (1 gm/100 ml of destaining solution) [206] and heating to 60°C not only removes the dye rapidly but also leaves the destaining solution fresh for repeated use.

### Isoelectric focusing

Acrylamide (29.1% w/v, 10 ml), bis-acrylamide (0.9% w/v, 10 ml), glycerol (87% v/v, 7 ml) and ampholine of pH range 3.5-10.0 (2.8 ml) were mixed and made up to 60.0 ml with double distilled water and degassed for 10 min. Polymerisation was started by the addition of 1.5 ml of 1% ammonium persulfate. The contents were stirred and cast into a slab of 1.5 mm thickness. Aliquots ranging from 25-60 µg of enzyme in 0.01 M potassium phosphate buffer, pH 7.0 were loaded into wells cut out near the anodal end. Anode and cathode solutions were 1 M  $\text{H}_3\text{PO}_4$  and 1 M NaOH respectively. The run was conducted at <sup>✓</sup>constant current (30 mA) mode while the voltage varied from 300 volts to 1,200 volts gradually <sup>c t</sup> in a duration of 3 hours. At the end of the run the gel slab was transferred carefully into

a tray containing 0.3 g of Coomassie brilliant blue G 250 in 400 ml of 4.13% (w/v) perchloric acid solution and left overnight for staining. Destaining was effected by rinsing the gel thrice with 4.13% perchloric acid, for 5 min each time. Throughout the run a temperature of 4°C was maintained by means of a cooling system.

### Hydrophobic chromatography

The hydrophobic gels, phenyl-Sepharose and octyl-Sepharose were packed into a 1 ml column and equilibrated with 10 ml of 0.01 M potassium phosphate buffer, pH 7.0. Triton solubilised enzyme (20 µl containing 42 µg) was applied and 0.1 ml fractions were collected when the equilibrating buffer was passed at a flow rate of 1 drop/12 sec. Fractions were collected and assayed for glucoamylase activity. Between breakthrough and washing 1 hour was allowed for the interaction of the enzyme with the gel.

### Analytical ultracentrifugation

Sedimentation velocity: Single sector cell (4°, 12 mm) was used for isolated samples (Fig. 2a) and <sup>a</sup>single sector cell along with wedge-shaped cell was used whenever the aim was to compare two samples accurately (Fig.15). The samples,

Triton form and papain form were centrifuged mostly at 60,000 rpm and the position of the boundaries were photographed and simultaneously temperature was recorded every 10 min, till the run was stopped when the peak approached the bottom of the cell. The mobility was calculated from the distance travelled by the peak in a certain time and the average temperature during the run was taken as the temperature of the run. Apparent sedimentation coefficient was calculated from the relationship

$$S_{app} = \frac{\Delta X}{\omega^2 \cdot x \cdot \Delta t}$$

where  $X$  is the migration along the axis in a time interval

$\omega^2 x$  is the radial acceleration.

Apparent sedimentation coefficients were corrected to 20°C and in water using the relationship,

$$S_{20,w} = S_{app} \left( \frac{\eta_t}{\eta_{20}} \right) \left( \frac{\eta_{so}^{\rho}}{\eta_o} \right) \left( \frac{1 - v\rho_{20,w}}{1 - v\rho_t} \right)$$

$S_{20,w}^0$  was obtained from the corrected sedimentation coefficients at three different protein concentrations (3.0, 5.0 and 10.0 mg/mol) and by extrapolating the straight line resulting from the plot of  $S_{20,w}$  vs concentration (Fig.2b) to zero concentration.

Sedimentation equilibrium: Archibald's [208] approach to equilibrium method was followed observing the necessary precautions suggested by LaBar [209]. Single-sector cell ( $4^\circ$ , 12 mm) was used for the equilibrium run and double-sector synthetic-boundary cell was used for synthetic boundary run to determine the original concentration of the protein. About 10 mg/ml of the enzyme solution in 0.01 M potassium phosphate buffer of pH 7.0 was used. The rotor speed was maintained at 4,400 rpm and the photographs of the boundary pattern at the meniscus were taken at 15 min intervals. After the equilibrium run was over, the cell was shaken well and the enzyme solution was sucked out to fill up one of the chambers of the synthetic boundary cell, while the other contained the buffer in which the enzyme was dissolved. The rotor was rotated at 6,000 rpm when the buffer overlayered on the enzyme solution through a capillary connecting the two chambers. The first photograph was taken as soon as the boundary was formed and the next ones followed at 15 min intervals. The rotor temperature was maintained at  $24^\circ\text{C}$  during the run and the phase-plate angle ( $80^\circ$ ) was unchanged for both the runs.

The molecular weight was calculated from the relation-

shy ;

$$M_r = \frac{RT}{(1-\bar{v}\rho)\omega^2} \cdot \frac{(dc/dx)_m}{X_m C_m}$$

ship where  $(dc/dx)_m$  is the concentration gradient, at the meniscus,  $X_m$  is the radial distance of the meniscus from the axis of rotation.

Diffusion: This is essentially a synthetic boundary run, conducted as described under sedimentation equilibrium. To evaluate  $D_{2O,w}^0$  the experiment was performed at three different concentrations of the enzyme (3,5 and 10 mg/ml). The apparent diffusion coefficient was obtained using the relationship [210] where, A and H are area and height

$$D_{app} = \frac{(A^2/H^2)}{4\pi t}$$

respectively of the peak, at time t.

$D_{app}$  was corrected to the standard condition of 'in water at 20°C', according to the relation

$$D_{2O,w} = D_{app} \left( \frac{293}{293+t} \right) \left( \frac{\eta_{solv}}{\eta_w} \right) \left( \frac{\eta_{t,w}}{\eta_{2O,w}} \right)$$

$D_{2O,w}^0$  was evaluated as a Y-intercept of the straight line resulting from the plot of  $D_{2O,w}$  vs concentration.

### Partial specific volume

Partial specific volume of the papain form of the enzyme was calculated from the available chemical composition

reported by Sivakami and Radhakrishnan [116], partial specific volume of individual amino acids taken from Cohn and Edsall [149], and those of carbohydrates from Gibbons [211], and using the relation

$$\bar{v} = \sum v_i \omega_i / \sum \omega_i$$

where  $v_i$  is the specific volume of the  $i$  th amino acid.

$\omega_i$  is the weight proportion of the  $i$  th amino acid.

The partial specific volume of the Triton form of the enzyme, assumed to be the same as that of the papain form.

### Viscosity

Viscosity measurements were made with a semi-micro type Ubbelohde viscometer. Since viscosity is sensitive to temperature fluctuations, the experiments were performed, immersing the viscometer in a constant-temperature water bath provided with an efficient temperature control system which maintained the temperature at  $24.00 \pm 0.02^\circ\text{C}$ . The viscometer constants were verified by measuring the viscosity of double distilled water at three different temperatures. Time of flow of double distilled water was  $228.3 \pm 0.1$  sec



at  $24.00 \pm 0.02^{\circ}\text{C}$ . Great care was taken to prepare solutions free of dust particles which would give rise to erroneous results. The solutions were rendered dust-free by centrifuging in a table-top centrifuge followed by millipore filtration. The viscosity of the buffer, 0.01 M potassium phosphate buffer, pH 7.0 containing 0.02% sodium azide in which the enzyme was dissolved, was measured first followed by enzyme solutions at various concentrations, starting at 12 mg/ml. The viscometer had an in-built provision for dilution. Dilutions were made with the buffer equilibrated at the same temperature. After every dilution, 10 minutes were allowed for thermal equilibration. Measurements were repeated till concordant values within  $\pm 0.1$  sec were obtained. The relative viscosity was obtained from the relation,

$$\frac{\eta}{\eta_0} = \frac{\rho t}{\rho_0 t_0}$$

where  $\eta$ ,  $\rho$ , and  $t$  are the viscosity, density and time of flow, respectively for the enzyme solution;  $\eta_0$ ,  $\rho_0$  and  $t_0$  are the corresponding parameters for the buffer. Intrinsic viscosity was obtained as a common Y intercept of two lines, from the plots of  $\ln \eta_{\text{rel}}/C$  vs  $C$  and  $\frac{\eta_{\text{rel}}^{-1}}{C}/C$  vs  $C$  [146]. The concentration of the protein ( $C$ ) was determined by Lowry's method of protein estimation.

## Electron microscopy

Clear and dust free samples of the two forms of the enzyme prepared as described earlier, were appropriately diluted with double distilled water so as to give a uniform and well separated images of the molecules in the electron-micrograph. A few  $\mu$ l of the sample <sup>h</sup>were applied on to a copper grid (200 or 400 mesh) coated with Formvar stabilised with a thin layer of carbon. The excess liquid was drained off with a blotting paper from an edge of the grid and before the sample on the grid dried, a few  $\mu$ l of 2% uranyl acetate stain was applied on to the grid. After a few minutes (usually 5 min) of staining, the grids were dried and viewed under electron microscope operated at 80 kv.

During our investigation it was observed that the enzyme and uranyl acetate stain combination formed membrane/film over naked 400 mesh copper grids. It withstood the electron beam (80 kv) fairly well, though there was some drift observed on exposure to the beam, which disappeared subsequently. In this method, naked copper grids (400 mesh) were either floated on the enzyme solution (50  $\mu$ g/ml) for a few minutes and then removed, blotted off and placed in a 2% uranyl acetate stain solution for 6 min or floated directly on enzyme stain mixture. The blotted and dried grids were viewed under <sup>h</sup>electron microscope operated at

80 kv. Several windows were either partially or fully covered with membranes attached to the edges (see electron micrograph, Fig. 18 ). While some of the membranes were unstable to the electron beam, many were stable after initial drift. The images were of a better quality, compared to the one obtained from Formvar coated grids. Areas were selected and photographed at focus, under-focus and over-focus conditions. It is also interesting to note that such membranes formed even with soluble glucoamylase-maltase-anti glucoamylase-maltase complex ( Fig.36 ).

## CHEMICAL METHODS

### Amino acid analysis

The enzyme (100 µg) was digested with 6 N HCl at 110°C for either 24 hours or 48 hours in a tube sealed under vacuum. The seal was broken open at the end of the digestion and the acid was evaporated in vacuo over moist NaOH pellets. The residue was washed thrice with glass double distilled water and analysis was carried out with an automatic amino acid analyser.

## Analysis of N-terminal amino acid

Identification of N-terminal amino acid: For the identification of the N-terminal amino acid, the enzyme (100 µg) in double distilled water (100 µl) was denatured by heating at 100°C for 15 min in the presence of 1% SDS. After cooling, dimethyl formamide (100 µl), 1 M NaHCO<sub>3</sub>-Na<sub>2</sub>CO<sub>3</sub> buffer, pH 8.5 (100 µl) and 100 mg/ml dansyl chloride solution in acetone (10 µl) were added and kept at 37°C for 30 min [212,213]. The reaction mixture was then dialysed against several changes of double distilled water till dansic acid and other fluorescent side products were completely removed. The retentate was hydrolysed with 6 N HCl at 110°C for 18 hours in a sealed tube. The hydrolysate was evaporated to dryness in vacuo over moist NaOH pellets and washed thrice with double distilled water followed by a wash with 50% pyridine. The washed residue was dissolved in 10 µl of 50% pyridine and about 2 µl of this was applied in a corner of one side of a polyamide sheet coated on both sides (5cmx 5cm) while standard DNS-amino acids were spotted on the same corner on the other side. The thin layer chromatogram was developed in the first direction with 3% formic acid [213] and in the second direction with benzene-acetic acid (9:1, v/v) [214]. Care was taken to see that the chromatogram was completely dried and freed of first solvent

before running in the second solvent. The plate was dried and viewed under an UV lamp. By comparison with the standard DNS-amino acid spots (on one side) the N-terminal(s) were identified.

Quantitation of N-terminal amino acid: In the quantitation of N-terminal amino acid the dansyl-labelling procedure was essentially the same as the one followed for its identification, except that each step was carried out carefully avoiding transfer and other losses. Aliquots of enzyme solution containing 200 and 300  $\mu\text{g}$  of the enzyme were dansylated as described above but hydrolysed with 6N HCl for only 6 hours at  $110^{\circ}\text{C}$ , to prevent excessive damage caused by the conditions of conventional acid hydrolysis to the released dansylated N-terminal amino acid, which has been shown to be released faster than many other amino acids in the protein/peptide [24a]. The hydrolysate was dried in vacuo over moist NaOH pellets and washed with double distilled water, followed by 50% pyridine. The washed residue was dissolved in 50% pyridine in 50  $\mu\text{l}$  and loaded on to a column of polyamide powder (1 ml bed volume), previously washed and equilibrated with a mixture of benzene and acetic acid (9:1). Elution was effected with the same solvent system and the fluorescent zone which eluted first and much ahead of others from the column was collected and analysed by TLC on polyamide sheet (see previous section

for details). The collected fraction was made up to 5.0 ml with the solvent system and the amount of the derivative was estimated both fluorimetrically and spectrophotometrically (Figs. 9, 10), with reference to a weighed amount of an authentic sample of dansyl derivative of the N-terminal amino acid, treated identically as the sample.

#### Analysis of C-terminal using carboxypeptidase A

To identify and estimate the C-terminal amino acid and to unravel the partial sequence of the C-terminal of the enzyme simultaneously, the enzyme (600  $\mu$ g) was denatured by heating at 60°C for 1 hour with 6 M guanidium chloride in Tris-HCl buffer (0.3 M, pH 8.5). The denatured enzyme was dialysed thoroughly till it was ~~rid~~<sup>free</sup> of guanidium chloride, and evaporated to dryness. The dry residue was dissolved by heating at 100°C for 5 minutes in 200  $\mu$ l of 0.2 M N-ethylmorpholine acetate buffer, pH 8.5 containing about 2 M urea. Activated carboxy<sup>peptidase</sup> A [215] was added to give a protein to protease ratio of 40:1 by weight, and incubated at 37°C. Aliquots, corresponding to 120  $\mu$ g of the enzyme were removed at 0, 5, 15, 45 minutes and 2 hours and the proteolytic activity was arrested immediately with glacial acetic acid (10  $\mu$ l). The aliquots were then analysed for the released amino acids, in an automatic amino acid analyser.

Ideally, the C-terminal amino acid will correspond to that particular amino-acid which shows a maximum rate of release followed by the next. The stoichiometry of the C-terminal amino acid is established from its amount (in moles), corresponding to the complete release [visualised by the plateau region in the time vs amount of aminoacid released curve (Fig.11)] for the quantity (in moles) of the enzyme taken

#### Peptide mapping of a tryptic digest

The enzyme (100  $\mu\text{g}$ ) was denatured by heating at  $60^{\circ}\text{C}$  for 1 hr with 0.3 ml of 0.3 M Tris-HCl (pH 8.4) buffer containing 6 M guanidium chloride. The denatured enzyme was thoroughly dialysed against double distilled water and the retentate was evaporated to dryness. The dried and denatured enzyme was dissolved in 100  $\mu\text{l}$  of 0.2 M  $\text{NaHCO}_3$ - $\text{Na}_2\text{CO}_3$  buffer, pH 8.5 and 2  $\mu\text{g}$  of trypsin (TPCK treated) was added in two equal parts, one at the start and the other after about two hours. The digestion was allowed to proceed at  $37^{\circ}\text{C}$ . Acetone (100  $\mu\text{l}$ ) and dansyl-chloride (10  $\mu\text{l}$  of a 100 mg/ml stock solution in acetone) were added to the digest at the end of 4 hours and incubated at  $37^{\circ}\text{C}$  for another 30 min. The pH of the reaction was then lowered to 4.0 with glacial acetic acid and the reaction mixture was applied

on to a Dowex-50,  $H^+$  column (bed vol, 0.5 ml) previously equilibrated with 0.01 M acetic acid. Dansic acid, which is a side product was washed out with 0.01 M acetic acid, and when no more blue fluorescence eluted the ion-exchange resin adsorbed dansyl peptides were displaced with 1 M ammonia in 25% acetone as an intense yellow fluorescent zone, which was dried by evaporation and taken in 10  $\mu$ l of 50% pyridine [216]. About 2  $\mu$ l was spotted on both the sides of a polyamide sheet (5cmx5cm) and developed in the first and second directions respectively with 3% formic acid and 9:1 benzene: acetic acid solvent system. After drying the chromatogram, spots were viewed under UV and traced out on a translucent (tracing) paper with a pencil. When a close comparison between the two forms of the enzyme was desired both were spotted on the same plate, one on either side.

## IMMUNOLOGICAL METHODS

### Antibody production

Adult female rats, two in number, were sensitised, each with 250  $\mu$ g of papain solubilised enzyme from rabbit dissolved in 250  $\mu$ l of 0.01 M potassium phosphate buffer, pH 7.0, containing 0.9% NaCl by injecting hypodermally.



A week after, the enzyme (500  $\mu$ g) dissolved in 500  $\mu$ l of 0.01 M potassium phosphate buffer, pH 7.0 containing 0.9% NaCl, was thoroughly mixed with 0.5 ml of Freund's complete adjuvant and homogenised to a white paste (uniform oil-in-water emulsion). To this paste another 0.5 ml of Freund's complete adjuvant was added and mixed to form a uniform oil in water emulsion. This antigen-adjuvant combination was divided into two equal parts and injected to the rats at multiple spots below the skin. This procedure was repeated for three more weeks and in the 5th week after sensitisation the enzyme (500  $\mu$ g/rat) in buffered saline was injected as a booster dose, under the skin just above the intestine. The rats were sacrificed under anaesthetised condition on the 10th day after the booster, and the blood (4 ml/rat) was collected from the artery. The blood, collected in centrifuge tubes, after an hour's standing at room temperature, was allowed to stand in the cold room, overnight without disturbance. Next day, the blood clot was removed by centrifugation, and the clear yellowish supernatant (2 ml/rat) was sucked out with a Pasteur pipette, divided into 0.2 ml aliquots and stored in the frozen condition in plastic vials. The presence of antibodies were checked for by ring-test in which the antigen (papain form of the enzyme) was layered carefully upon the antiserum and allowed to stand at room temperature for about an hour, whereupon the Ag-Ab precipitate formed as a ring in the interface between the two.

### Immuno-diffusion

Agar solution (1%) was prepared by heating to boiling 1.0 g of agar in 100 ml of buffered saline containing 0.02 g of sodium azide. The solution when hot was poured into petri dishes to a few mm height and cast into gels. The agar plates were stored in the cold room and used as and when necessary. In a typical double diffusion experiment, six wells each of 4 mm diameter and equally spaced were made by sucking out the gel, around a central well, at a radial distance of 0.5 cm. Anti-serum was poured in the central well and the antigens were poured in the surrounding wells. Various forms of the enzyme were used for determining antigenicity (native papain and Triton-forms and denatured forms under different conditions and the dansylated protein). The set-up was usually left for 1 hr at room temperature and then for 24 hours in the cold room or in a refrigerator by which time the diffusion of the proteins was complete. From the pattern of the precipitin lines around the central well, conclusions were drawn with regard to the identity of the forms. To enhance clarity and to locate minor components, if any, the gels were also stained with Coomassie blue G 250 after washing the unprecipitated antigen zones with double distilled water. Destaining was done with 10% acetic acid.

### Quantitative immuno-precipitation

In this experiment, a fixed amount of antibody is allowed to react with different amounts of antigen and the precipitates formed are collected and the composition of antigen and antibody in them is <sup>determined</sup> ~~worked-out~~. To 50  $\mu$ l of antiserum in each tube, different amounts of the enzyme (papain form) in the range of 0-240  $\mu$ g were added and all the tubes were made up to the same final volume (0.2 ml) with buffered saline. The precipitation was allowed to take place at room temperature for 1 hr and subsequently for 72 hours in cold room. The precipitates were collected by centrifugation at 5000 rpm for 15 min in a table top centrifuge, and washed with ice-cold saline. The washed precipitates were dissolved in 0.2 ml of 0.05 N NaOH and subjected to protein estimation by Lowry's method. The amount of antigen employed in the reaction vs the amount of protein in the respective precipitate was plotted (Fig.35) and the maximum through which the resulting curve passed was taken as the point of maximal precipitation.

To find out the stoichiometry of antibody binding to antigen it is essential to evaluate the molar composition of the precipitates, i.e., the amounts of antigen and antibody, separately. To achieve this the supernatants

obtained after the removal of precipitates, were assayed for enzyme activity and from the total activity in the supernatant and specific activity of the enzyme the amount of enzyme in terms of protein value in the supernatant, was calculated. The difference between the amount of enzyme employed in the reaction and that recovered in the supernatant gave the amount of the enzyme that was precipitated by antibody. When this was subtracted from the protein value of the precipitate, the amount of antibody in the precipitate was obtained. By assuming an average molecular weight of 150,000 for  $\gamma$ -globulin (antibody) and using 760,000 as the  $M_r$  of the enzyme the molar composition of the precipitates was determined and the stoichiometry was expressed as the number of moles of antibody bound to a mole of antigen.

### Immuno electron-microscopy

To view the complex in an electron microscope and derive useful information it is essential that the complex should be soluble and free from other proteins in the serum. The antigen and antibody complex, was precipitated and separated from other serum proteins. The washed precipitate was brought back to a soluble complex by treating it with 4 M KCl, which brings about the disaggregation of the precipitate, in the presence of excess of antigen. The enzyme

(50  $\mu\text{g}$ ) was precipitated with 50  $\mu\text{l}$  of antiserum. The washed precipitate was shaken vigorously with 0.5 ml of 4 M KCl and left at room temperature for 30 min. The clear solution obtained after this treatment, was mixed with 100  $\mu\text{g}$  of the enzyme and the contents were dialysed overnight against several charges of double distilled water. The retentate in the dialysis bag remained a clear solution. A few micro-litres of this was applied to a naked copper grid (400 mesh) and stained with 2% uranyl acetate (see under electron-microscopy) and viewed in an electron microscope.

## THEORETICAL METHODS

### Size of a macro-molecule

Molecular weight: The molecular weight of a molecule ( $M_r$ ), obtained directly from sedimentation equilibrium experiment, as described above can also be calculated from  $S_{20,w}^0$  and  $D_{20,w}^0$  making use of Svedberg's equation

$$M_r = \frac{RT \cdot S_{20,w}^0}{D_{20,w}^0 (1 - \bar{v} \rho)}$$

Molecular volume: The molecular volume, in turn,, is obtained from  $M_r$  and partial specific volume ( $\bar{v}$ ) of the molecule which is the volume of 1 gm of the molecule in dry state, using the relationship

$$V_M = \frac{\bar{v}M}{N}$$

### Shape of a macro-molecule

The shape of a macromolecule, unlike the molecular weight and volume cannot be obtained directly from the measured hydrodynamic parameters unless certain shape factors are evaluated from them and compared with those of model system of fixed geometrical shapes such as a sphere, a cylinder, an ellipsoid, a string-of-beads whose hydrodynamic behaviour has been studied in detail both theoretically and experimentally, to allow prediction of the shape by comparison. Owing to the restriction in the number of shapes to which such comparisons are possible the derived shape will only be equivalent unless supported by direct observation on the shape of the molecule, such as from electron microscopy and X-ray diffraction. In this study the shape derived from hydrodynamic study has been compared with the one obtained from electron microscopic

studies. In the following section the details of this derivation is given.

Determination of shape factors: Frictional coefficient and viscosity increment are 'two shape factors', widely used in the derivation of shape of molecules. Frictional coefficient, is obtained from both  $S_{20,w}^0$  and  $D_{20,w}^0$  according to the relationship

$$f = \frac{M(1-\bar{v}\rho)}{R.T.S^0} = \frac{RT}{N.D^0}$$

A more useful term, frictional ratio, which is the ratio of the frictional coefficient of the molecule under study to the friction coefficient of an equivalent sphere, is given by

$$f/f_0 = \frac{RT/N.D^0}{6\pi\eta \sqrt[3]{3\bar{v}.M/4\pi.N}} \quad f_0 = 6\pi\eta r_0 = 6\pi\eta \sqrt[3]{\frac{3\bar{v}M}{4\pi.N}}$$

Viscosity increment is evaluated from the intrinsic viscosity using the relationship

$$v = [\eta].V_h$$

where  $v$  is the viscosity increment and  $V_h$  is the hydrated volume of the molecule.

Since the shape factors  $f/f_0$  and  $v$  are functions of hydration value (g. of water associated per gram of the molecule) as well as the shape of the molecule, another shape factor called  $\beta$  was derived by Scheraga and Mandelkern[158] to eliminate the contribution due to hydration, by combining  $S^0$  and  $[\eta]$  or  $D^0$  and  $[\eta]$ , according to the relation

$$\beta \equiv N.S^0\eta_0[\eta]^{1/3} / M.(1-\bar{v}\rho) = N.D^0M^{1/3}[\eta]^{1/3} / RT$$

Though  $\beta$  is unpopular in the elucidation of the dimensions of the molecule owing to reasons discussed elsewhere (page 34) it is used to distinguish between a prolate ellipsoid and an oblate ellipsoid and to calculate the hydration factor by combining, the following equations

$$\beta = \gamma.F(v)^{1/3}$$

$$v = [\eta].V_h.$$

$$\text{where } F = f_0/f \text{ and } \gamma = N^{1/3} / (16200\pi^2)^{1/3}$$

$$\text{hydration factor, } (\phi) = V_h - \bar{v}$$

$\phi$  is then used to find out the contribution of hydration to the values of  $f/f_0$  and  $v$ .



Dimensions of equivalent ellipsoid: For impermeable spherical molecules  $f/f_0$  and  $v$  have values close to 1.0 and 2.5 respectively. Any deviation from this is taken as due to asphericity and the axial ratio is worked out assuming that the molecule is either an ellipsoid or a cylinder. Other evidence to judge if the molecule behaves as a sphere or not comes from gel filtration behaviour. If the molecule is eluted from the gel at the position expected for an equivalent globular shape, it is taken as sphere and if it is eluted earlier, in the absence of any exclusion effects, it is taken as due to elongated shape. If a molecule is shown to be spherical, its only dimension, radius( $r$ ) is obtained by the relation

$$V_M = \frac{4}{3} \pi r^3$$

If it is aspherical, several geometrical shapes are possible. From  $\beta$  value one can decide if it is a prolate or an oblate ellipsoid depending on whether it is above or below a value of  $2.15 \times 10^6$ , characteristic of spherical and prolate ellipsoid of very small axial ratio. The axial ratio of a prolate or an oblate ellipsoid can be obtained from the contours of axial ratio vs hydration factor (calculated as mentioned above or determined independently or assuming a typical value of 0.20 g of water/g of protein) for various

frictional ratios or viscosity increments [157]. Once the axial ratios are known, the dimensions (length<sup>(2b)</sup> and equatorial diameter<sup>(2a)</sup>) are calculated from the following relationship

$$V_M = \frac{4}{3} \pi a^2 b. \text{ for a prolate ellipsoid and}$$

$$V_M = \frac{4}{3} \pi a b^2 \text{ for an oblate ellipsoid.}$$

Dimensions of a cylinder: In the case of a cylinder, the length is taken as that of the prolate ellipsoid of same volume and its diameter is easily obtained from the formula

$$V = \pi r^2 h \text{ where } h = \text{length of the prolate ellipsoid.}$$

Dimensions of Kuhn's string of bead model: In the case of molecules, appearing as a string of identical spherical beads separated by a distance called inter-bead-distance equal to the diameter of the bead, the following relationships were worked out by Shulman [162]. (Page 35).

$$v = 1/4(S/d)^2$$

$$V_M = \frac{1}{12} \pi d^2 S$$

$$n = L/2d$$

where  $S$  is the length of the string;  $d$  is the diameter of a bead and  $n$  is the no. of beads in a string. For these excluding the case of beads separated by certain distance and many other geometrical shapes, owing to the recent development in hydrodynamic theories originally proposed by Kirkwood and his associates, values of frictional coefficient and intrinsic viscosity have been tabulated [185,186]. Combining the formula for the volumes of such geometrical shapes one can easily obtain the dimension of oligomer. The elucidation of geometry of the bead, as given below utilises such an approach.

### Geometry of the bead

To evaluate the bead geometry, the procedure laid down by Teller et al [186] was followed. (Page 44).

Using the relationship,

$$\frac{S_n \bar{v}^{1/3}}{1 - \bar{v} \rho} = 0.01 M_n^{2/3} F_n$$

and known values of  $S_n$ ,  $\bar{v}$  and  $M_n$ , respectively the sedimentation coefficient, partial specific volume and molecular weight of the enzyme, its geometric factor  $F_n$  was calculated. Employing the relationship

$$F_n = n (S/f_n)$$

and known values of  $n$  and  $f_n$  being the number of beads (8) and frictional coefficient of the enzyme,  $\nu$ , the frictional coefficient of a single bead was calculated and its sedimentation coefficient in turn was obtained from Svedberg's equation,

$$\frac{M}{N} \cdot \frac{(1-\bar{\nu}\rho)}{f} = S_{\text{bead}}$$

Since  $S_{\text{bead}}$  is known and  $M_{\text{bead}} = 760,000/8$ , and  $\bar{\nu}$  can be safely assumed to be the partial specific volume of the enzyme,  $F_{\text{bead}}$ , the geometrical factor of the bead was derived from repeating the first step mentioned above.

It is also possible, purely theoretically based on Kirkwood's formulation, to derive approximately the geometrical factor of any model conceived based on other direct or indirect evidence and if the model so derived is compatible with the actual one; thus, the geometrical factor derived from the frictional coefficient using the above procedure and the theoretically calculated should show a good match. The geometrical factor of a model is given by the following relationship.

$$F_n = n^{-\frac{2}{3}} \left( 1 + \frac{a}{n} \sum_{i=1}^n \sum_{\substack{j=1 \\ i \neq j}}^n r_{ij}^{-1} \right)$$

where 'a' is the radius of a subunit  $r_{ij}$  is the distance between the centres of two subunits and  $n$  is the number of subunits constituting the oligomer. In our case, for the model chosen (see page 108),  $a$ ,  $n$  and  $r_{ij}$  were taken as 16.5 Å, 6 and 33 Å respectively.

The electron microscopic appearance helps one to choose the most <sup>probable</sup> possible structure, and also to calculate its dimension. In cases where the appearance coincides with the shape derived from the available model system, it serves as a potent cross-check for the dimensional values obtained hydrodynamically.

## RESULTS AND DISCUSSIONS

## ENZYME PURIFICATION

### Purification of protease and detergent forms

The purification of intestinal glucoamylase-maltase complex is essentially a single step procedure owing to the specific affinity of the enzyme to Sephadex G-200 at low temperatures ( $4^{\circ}\text{C}$ ). It is then possible at least theoretically to achieve nearly 100% yield, if the conditions are properly manipulated. It was found that after homogenisation using a Waring blender only about 70% of the activity in the homogenate pelleted out when centrifuged at 20,000 g for 38 min. On the other hand, homogenisation with tissue grinders, a gentler operation, allowed almost complete pelleting of the activity under identical conditions and was the method of choice for homogenisation. Solubilisation was almost complete using either papain or Triton-X 100 and both forms showed similar affinity to Sephadex G-200. However, <sup>clogging</sup> ~~choking~~ of the column was observed in the case of the Triton form possibly owing to the presence of large mixed (aggregate) micelles of protein and Triton [217]. This occurred after passage of one bed volume of Triton solubilised supernatant and hence was unsuitable for a column procedure. As an alternative, the batch method was equally effective without any significant loss of affinity of the gel. The only step

~~equally effective without any significant loss of affinity of the gel~~ The only step which determines the ultimate yield then is the affinity step. In the range of the amount of enzyme employed [15-150 IU] it was observed that 60% of the loaded activity was bound by the gel, 5 ml bed volume [65] and the remaining 40% which passed unbound did not bind to the gel when recirculated or when passed through a fresh gel. It is possible that the binding is a concentration dependent phenomenon, and the unbound activity in the breakthrough when concentrated and applied might bind to the gel. It was also observed that not all the bound activity could be eluted by substrate (maltose), at least in the cases where large amount of the enzyme was bound, when elution was carried out at cold room temperatures. This difficulty was overcome and almost complete elution with substrate was achieved when the column was brought to room temperature before substrate elution and this improved the overall yield to 60% from 40% achieved earlier [66]. To remove Triton from the Triton-solubilised enzyme, it was found that washing the column with about 25-bed volumes, of Triton free buffer alone was sufficient. The detergent was not detectable up to 40 µg in about one mg of the enzyme when tested by a sensitive colorimetric procedure [218] and it was observed that the signal due to Triton in FT-NMR was absent in the purified enzyme. However, a stoichiometric binding of Triton to the enzyme may not be detectable by



### Homogeneity of the enzyme preparation

The purified enzyme was homogeneous as judged by a variety of criteria for homogeneity. The enzyme eluted as a single peak during gel filtration on Sepharose-4B; it moved as a single band in all the electrophoretic systems both under acidic and basic conditions; focussed into a single sharp band during iso-electric focusing; sedimented and diffused as a single species during ultracentrifugation; formed a single sharp precipitin line with the antibody in Ouchterlony double diffusion experiment; showed no end-group other than the N-terminal amino acid, tyrosine, after dansylation and finally it appeared as a single species under the electron microscope.

## QUATERNARY STRUCTURE OF THE ENZYME

### Size and shape of the enzyme complex

It is mandatory to know about its structure before attempting to unravel the structure-function relationship of an enzyme and this is an essential prerequisite for the complete understanding of the system. To this date, the structure of many membrane proteins which are as a class vital to the living systems, has remained poorly understood

mainly because of the difficulty involved in their isolation in the native state and associated inability to crystallise them and to study by X-ray diffraction techniques [75]. Obviously, our knowledge at the molecular level about these systems is still lacking. What little is known about their structure from low resolution studies comes from those molecules which are soluble and easily purified. Electron microscopy and very recently, low angle X-ray scattering studies are potent techniques to study these macromolecules at a resolution close to  $20 \text{ \AA}$ , where one can study conveniently the size, shape and the subunit arrangement. Electronmicroscopic images are two dimensional projections of three dimensional objects and hence are associated with the problem of proper image reconstitution to gain an insight into these problems and electronmicroscopy cannot reveal the structural detail of smaller macromolecules ( $M_r < 60,000$ ). Hydrodynamic studies offer a powerful tool, in estimating the size and predicting the possible shape of macromolecules, which could range in size from a few thousand daltons (the range electronmicroscopy cannot handle) to a few million daltons, with the only limitation that the derived shape is only equivalent and must be compared with the shape obtained from techniques which record it directly. Hence, electronmicroscopy and hydrodynamic studies complement each other and this combination offers a very potent tool to unravel details about membrane proteins, and this approach was used in our study.

TABLE - I  
HYDRODYNAMIC PARAMETERS OF THE ENZYME

Hydrodynamic parameters	Values for glucoamylase	References
$S_{20,w}^0$	18.6 $\pm$ 0.6 S	Schachman, 1957
$D_{20,w}^0$	$2.17 \pm 0.02 \times 10^{-7}$ cm <sup>2</sup> sec <sup>-1</sup>	Kawahara, 1969
$[\eta]$	0.230 dl/g	Bradbury, 1970
$\bar{v}$	0.72 ml/g	Schachman, 1957
Molecular weight from $S_{20,w}^0$ and $D_{20,w}^0$	750,000 $\pm$ 30,000	Schachman, 1957
Archibald's approach to equilibrium	760,000 $\pm$ 10,000	Schachman, 1957
$K_s/[\eta]$	0.67	Creeth & Knight, 1965
$f/f_0$	1.65	Haschemeyer & Haschemeyer, 1973
$\beta$ , using $[\eta]$ and $S_{20,w}^0$ , and $[\eta]$ and $D_{20,w}^0$	$2.94 \times 10^6$	Yang, 1961
$\nu$ , viscosity factor	30.3	Yang, 1961
$V_e$ , hydrated volume	0.76 ml/g or $9.6 \times 10^{-19}$ ml/ molecule	Haschemeyer & Haschemeyer, 1973
$\phi$ , hydration factor	0.04 g of water/g of protein	Haschemeyer & Haschemeyer, 1973
Stokes' radius		
a) from $f$	10.0 nm	Siegel & Monty, 1966
b) from gel filtration on Sepharose 6B	12.0 nm	Siegel & Monty, 1966

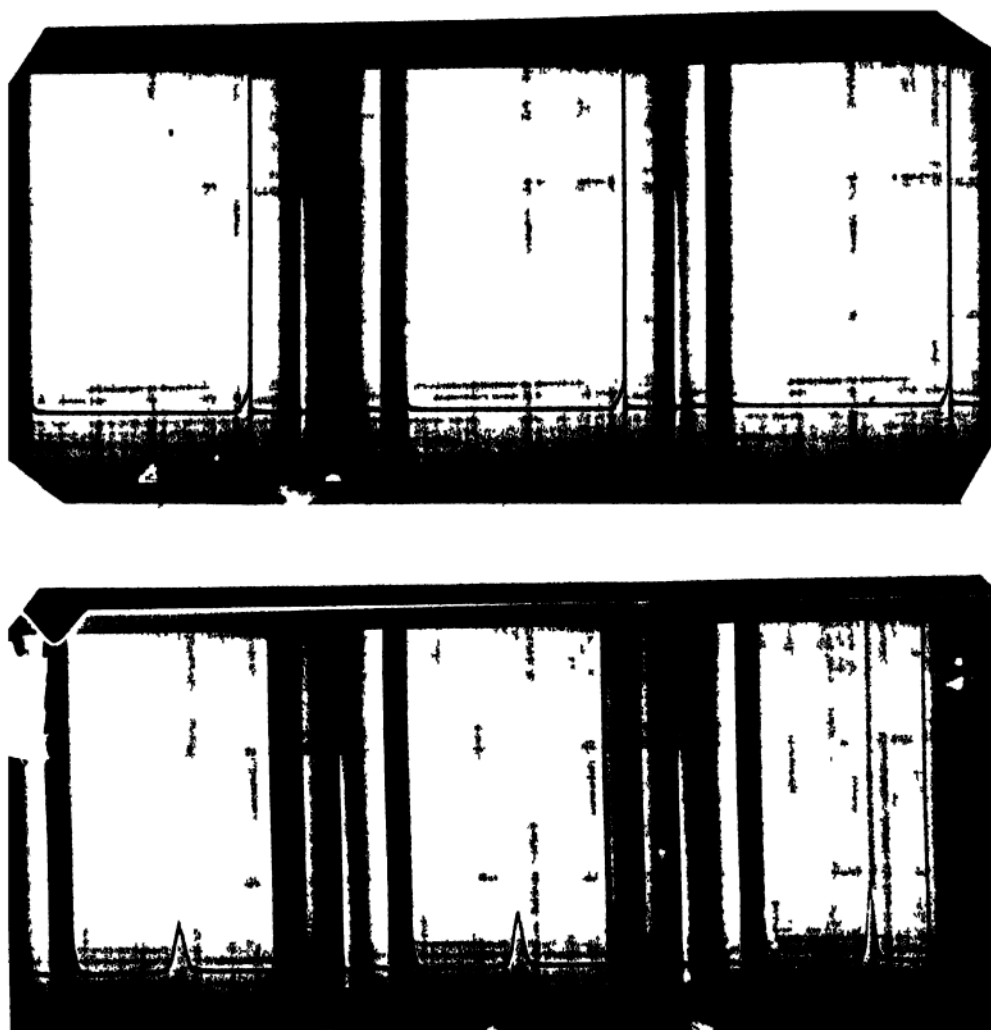


Fig.1 : Molecular weight determination by 'equilibrium-at-meniscus-only' method of Archibald.

- (a) Archibald's run in a single sector cell at 4,400 rpm showing the concentration gradient of papain solubilised enzyme (1.0%) The area under the curve is time invariant. Photographs were taken at 15 min intervals.
- (b) Synthetic boundary run of the sample used in Archibald's run, at 4,800 rpm. Photographs were taken at 10 min intervals.

Since hydrodynamic measurement should be made under conditions in which charge interactions between the solute molecules ~~should be~~<sup>are</sup> minimum<sup>al</sup> and individual molecules isolated, the parameters were measured, wherever necessary, at different concentrations and then extrapolated to zero concentration (infinite dilution) and at a pH 7.00 close to the isoelectric point, which is about 6.5 for the enzyme. This obviates the use of swamping amounts of KCl or NaCl to minimise charge interactions between solute molecules, and also helps to keep the system close to a two component system to which the various relationships used apply well.

Molecular weight: The values of various hydrodynamic parameters of the enzyme, measured and derived have been tabulated (Table 1). The Enzyme is a large protein as is evident from its large Mr of 760,000. The close agreement of molecular weight obtained from two different methods, S and D method using Svedberg's equation and sedimentation equilibrium method, not only increases the confidence in the measured value but also substantiates the homogeneity of the preparation. This is further confirmed by the invariance of the molecular weight with respect to time during approach to equilibrium run [148](Fig.1a). The large sedimentation rate and relatively smaller diffusion also justify the large molecular weight of the enzyme. The previous estimate on the molecular weight of the enzyme by Sivakami

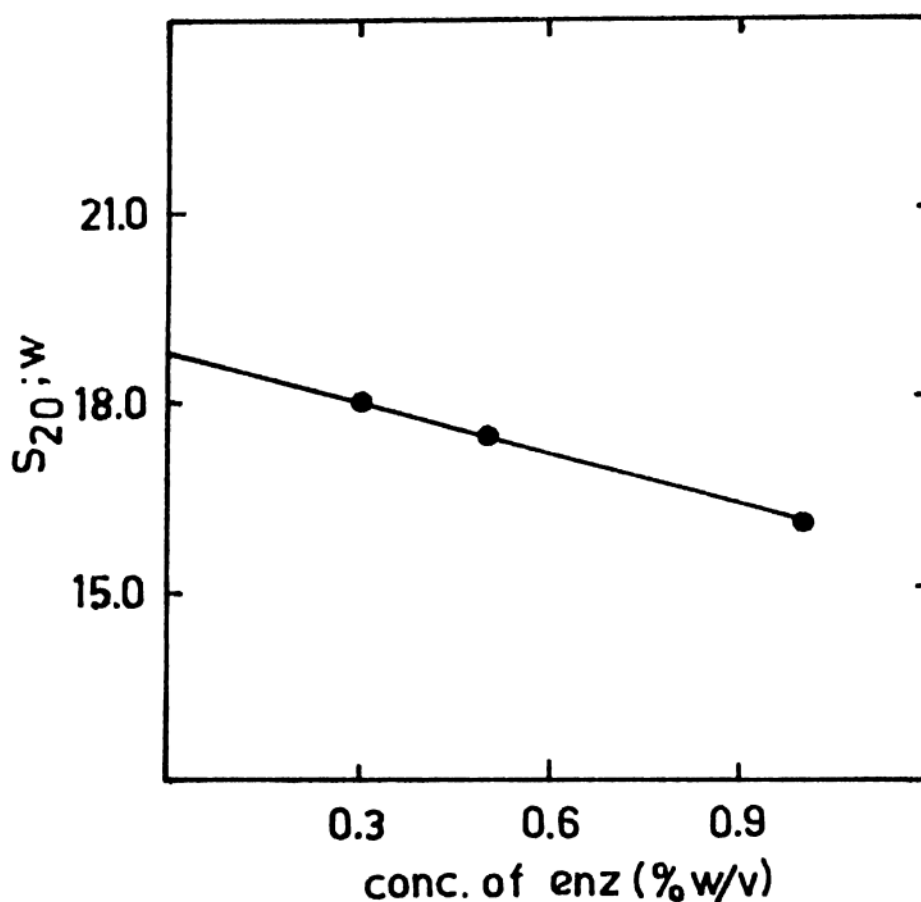
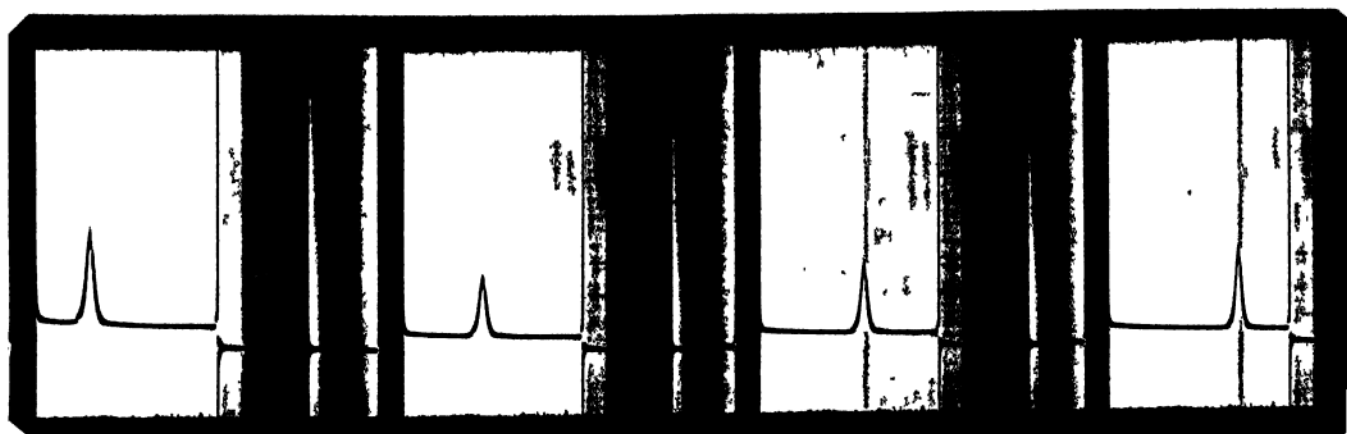


Fig.2a : Sedimentation behaviour of papain solubilised enzyme in a single sector cell. The hyper-sharp peak diffuses only slightly during the run suggestive of a large and asymmetric molecule. Run condition: 40,000 rpm; temperature, 24.2°C interval between photograph, 10 min; concentration of sample 0.5% (w/v), 10 min; concentration of sample 0.5% (w/v):  $S_{app}$ , 19S.

2b :  $S_{20,w}$  plotted against different concentration of papain solubilised enzyme. The intercept of the resulting straight line is  $S_{20,w}^0$  and equal to 18.6s.

and Radhakrishnan [116] would now appear to be an underestimate possibly owing to contamination by low molecular weight substance(s) which were most probably the substrate used for elution and the product. This is reflected in their synthetic boundary pattern, which appears as an overlap of two peaks, a broad one (due to fast diffusing small molecule) and a sharp one (due to the enzyme) unlike the pattern in our studies (Fig.1b). Since the area of the synthetic boundary appears in the denominator in the formula used for molecular weight calculation, the obvious consequence of an increase in the area of synthetic boundary is the reduction in  $M_r$ . To avoid such complications, especially when enzymes are eluted with small molecular weight substance( it is essential to dialyse the sample exhaustively prior to molecular weight determination and use the dialysate in the synthetic boundary cell. However, small amounts of such small molecular weight contaminants will not seriously alter the sedimentation behaviour of the enzyme and hence the reported sedimentation coefficient [116] is close to the value reported here.

#### Sedimentation, diffusion and gel filtration behaviour:

The Enzyme sediments with a characteristically large  $S_{20,w}^0$  of 18.6S (Fig.2b) showing no detectable diffusion of the peak even after 40 minutes (Fig.2a). The hyper-sharpness

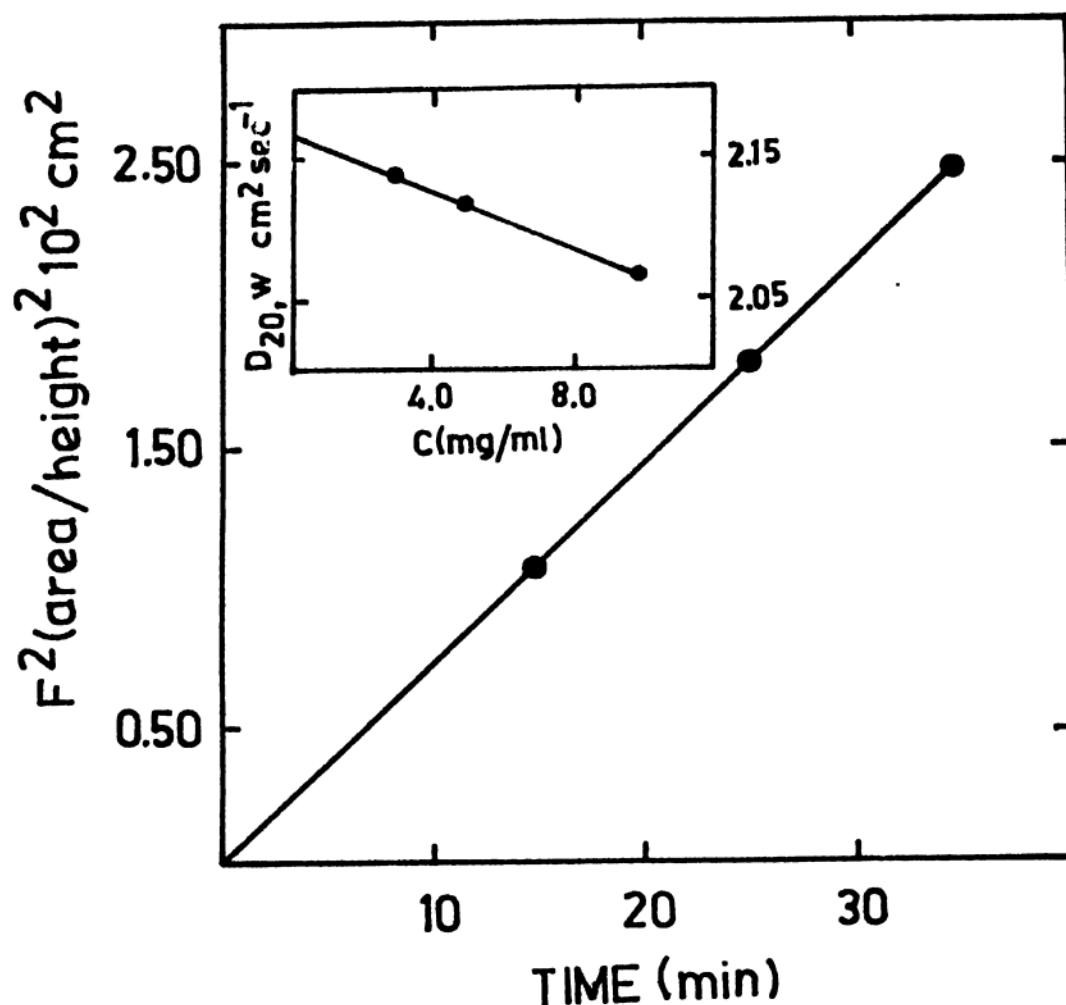


Fig.3a : Diffusion behaviour of papain solubilised enzyme in a synthetic boundary cell. Run conditions: 4,800 rpm; temperature, 22.6°C; time interval between photographs, 20 min: concentration of sample 0.5% (w/v).

$$D_{app} = 2.26 \times 10^{-7} \text{ cm}^2 \text{ sec}^{-1}.$$

3b :  $A^2/H^2$  vs time plot, to evaluate the diffusion coefficient of the enzyme, giving a straight line passing through the origin indicative of homogeneity of the preparation.

Insert:  $D_{20,w}$  plotted against different concentrations of papain solubilised enzyme. The intercept

$$\text{gives } D_{20,w}^0 \text{ as } 2.17 \times 10^{-7} \text{ cm}^2 \text{ sec}^{-1}$$



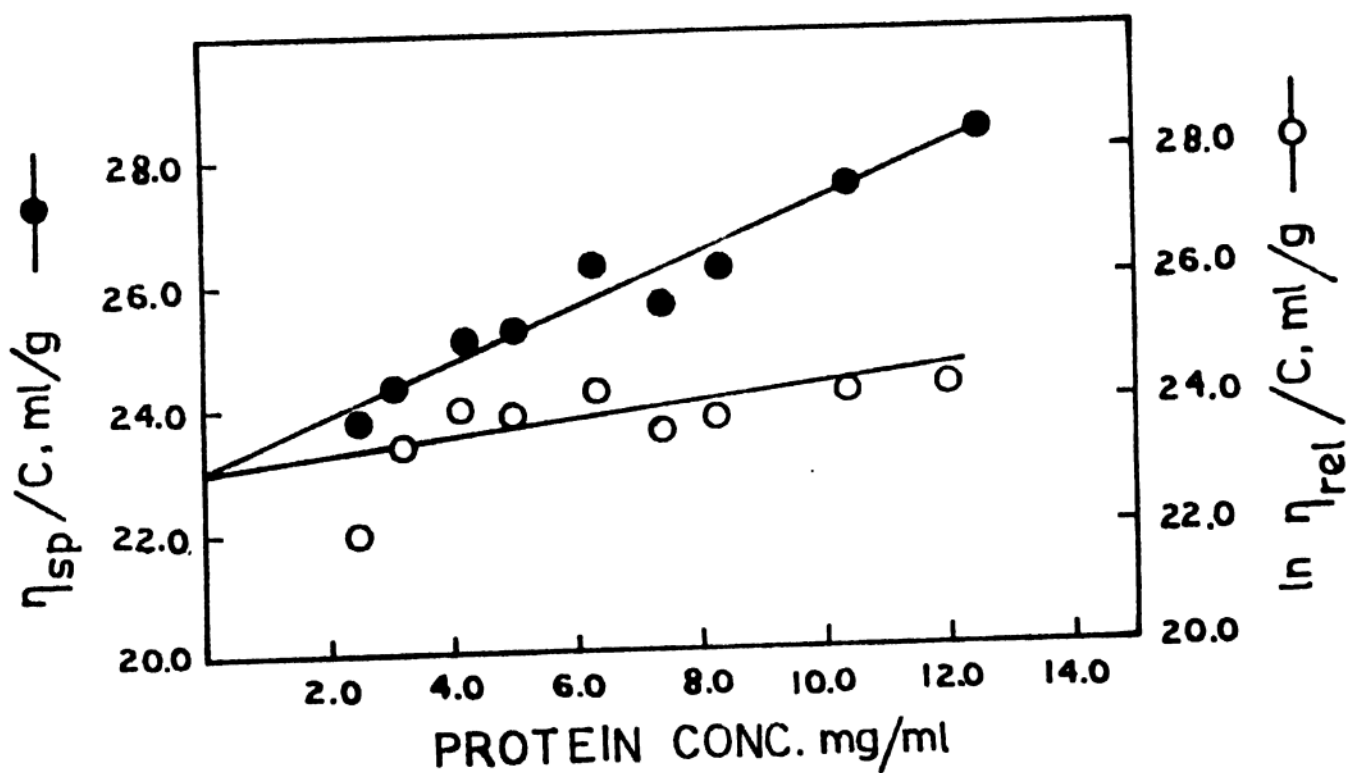


Fig.4 : Intrinsic viscosity from a plot as suggested by Yang (1961) :  
The plots of  $\eta_{sp}/c$  and  $(\ln \eta_{rel}/c)$  versus concentration converge towards the same point on the ordinate, giving a reliable intrinsic viscosity of 0.230 d /g and  $k'$  and  $k''$  (from slope) of 0.782 and 0.259 respectively.  $k' - k'' = 0.523$ . The plots were drawn by using the least-squares fit method.

of the peak results from the dependence of  $S$  on  $c$  and this indicates asymmetry in the molecule. The plot of  $A^2/H^2$  vs  $t$  is a straight line passing through the origin, a test for the behaviour of the molecule as a single species [152] (Fig.3a and 3b). The dependence of  $S_{2O,w}^0$  and  $D_{2O,w}^0$  on  $c$  is normal and the  $K_s$ , obtained from the slope of  $S$  vs  $c$  is not high. The value of  $D_{2O,w}^0$  ( $1.97 \times 10^{-7} \text{ cm}^2 \text{ sec}^{-1}$ ), which is less than that expected from its molecular weight and globular nature, is also an indication of asymmetry in the molecule. The high intrinsic viscosity of  $0.230 \text{ dl/g}$ , (Fig.4), large frictional ratio of 1.65 and  $K_s/[\eta]$  of 0.67 strongly suggest the asymmetric nature of the enzyme [219]. This is expressed or reflected in the reported behaviour of the enzyme during gel filtration on Sepharose 6B [116]. The molecule eluted ~~out~~ from the column at a position corresponding to a globular molecule in the molecular weight range greater than 900,000 daltons. The asymmetry in a molecule serves to increase its Stokes' radius and since the elution behaviour of the gel is more a function of Stokes' radius rather than the molecular weight, the expected consequence of the asymmetry is that the molecule should be eluted earlier than if it were globular. In fact, this is the case with the enzyme as seen by replotting the data of Sivakami and Radhakrishnan [116] as  $\sqrt{-\log K_{av}}$  vs Stokes' radius [220], which gives a value of  $120 \text{ \AA}$  for the Stokes' radius of the

molecule and this is comparable with the Stokes' radius ( $100 \text{ \AA}$ ) obtained from both sedimentation and diffusion coefficients. An equivalent sphere should have a Stokes' radius of only  $60 \text{ \AA}$ , which is almost half that of the experimental value and this sphere is about 8 times less in size or volume compared to the sphere with a Stokes' radius of  $120 \text{ \AA}$ .

Shape from hydrodynamic studies: The shape of the molecule which gives rise to this asymmetry was deduced from the shape factors, frictional coefficient and viscosity factor using model systems, based on well founded hydrodynamic theories.  $K_s/[\eta]$  value of 0.67, which is lower than 1.6 - 1.7, rules out the possibility of the enzyme being spherical or a random coil. It suggests an elongated shape [219], which is also evident from the high frictional ratio and viscosity factor, in the absence of excess hydration. Excess hydration is ruled out by a low hydration factor of 0.04 g of water/g. of protein calculated from  $\beta$  and  $[\eta]$ , and hence the asymmetry is probably related only to the shape. This rather low value of hydration which can be taken as evidence against excess hydration should not be treated as accurate, due to limitation laid on this method of determination. This lack of accuracy does not prevent or seriously alter the conclusions being derived regarding shape and

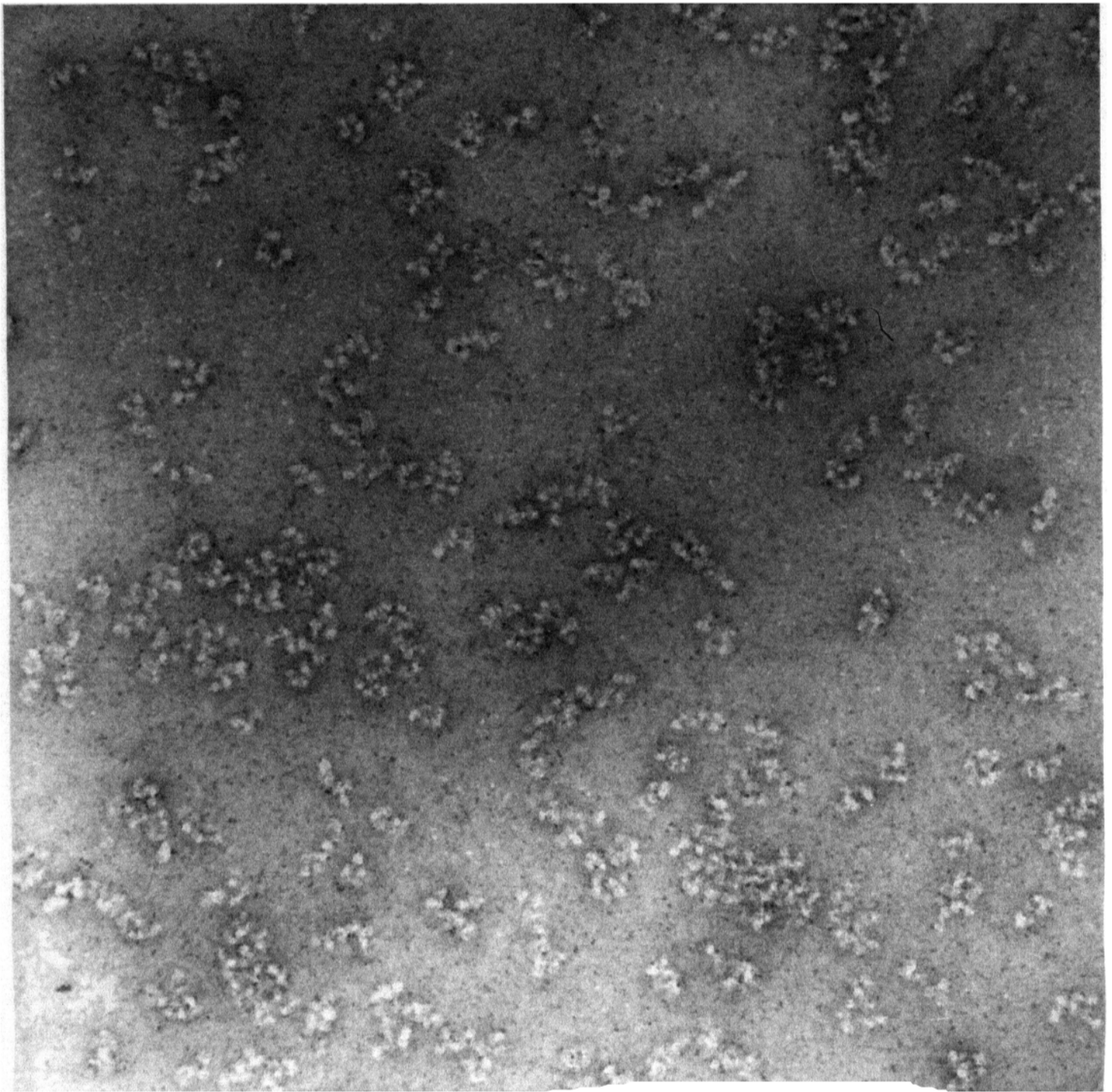


Fig.5 : Electron microscopic view of papain solubilised enzyme. Negative contrast staining with uranyl acetate was used; magnification  $\times 250,000$ . The beaded appearance of the enzyme is evident and there is no regular, repeating, geometrical pattern.

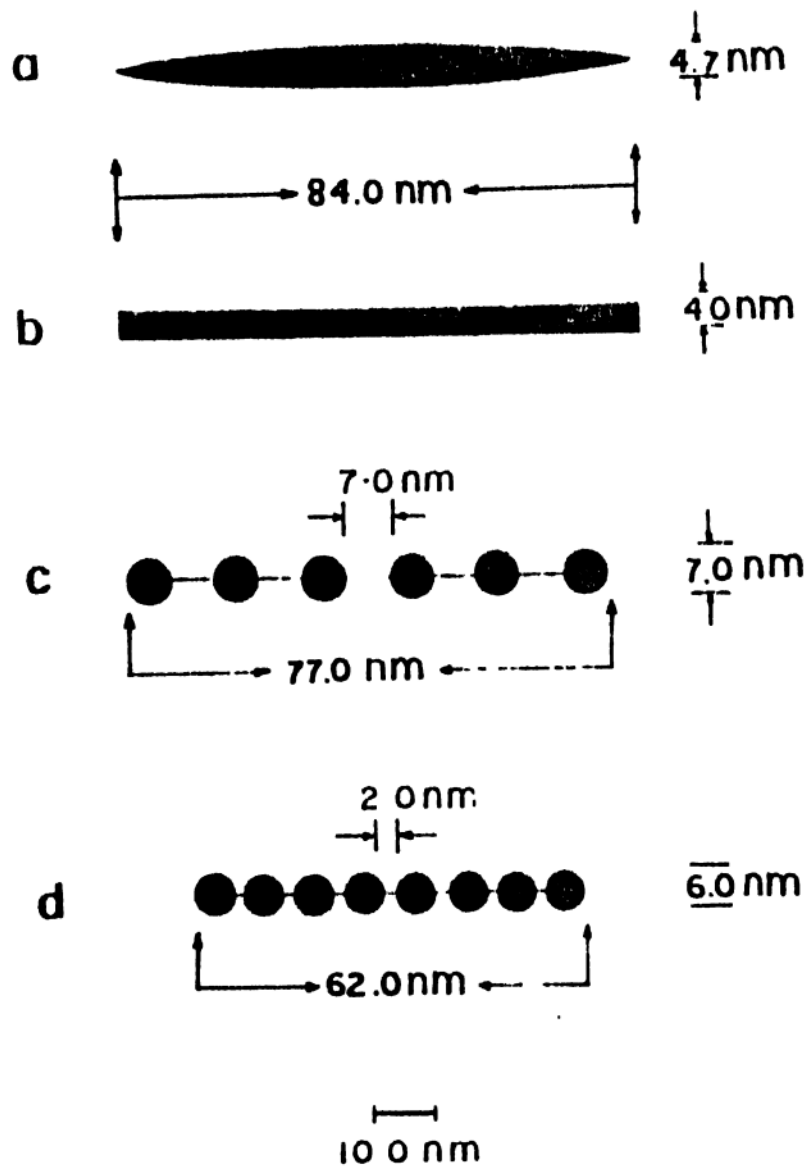


Fig.6 : Shape of the enzyme derived from the theoretical models by using viscosity factor and the electron-microscopic appearance (a) prolate ellipsoid (b) cylinder or rod (c) string of identical spherical beads (d) shape derived from electron microscopy; all shown in a fully extended form.

TABLE - 2

DIMENSIONS OF THE SHAPE OF THE ENZYME BASED ON THEORETICAL  
MODEL SYSTEMS AND ELECTRON MICROSCOPIC APPEARANCE

b, equatorial radius of the prolate ellipsoid; a, half the length of the prolate ellipsoid; l, length of the cylinder; L, length of the string; d, diameter of the bead.

Model system	Dimensions of the model	Hydrodynamic parameter used
Equivalent ellipsoid (Bradbury, 1970)	axial ratio $a/b = 18$ ; $2b = 4.7$ nm and $2a = 82.0$ nm	$\nu$
	axial ratio $a/b = 13$ ; $2b = 5.2$ nm and $2a = 68.0$ nm	$f/f_o$
Cylinder (Bradbury, 1970)	$l = 84.0$ nm $d = 4.0$ nm $l = 68.0$ nm $d = 4.2$ nm	$\nu$ $f/f_o$
String of spherical beads (Shulman, 1953)	$L = 77.0$ nm; $d = 7.0$ nm; $n=6$ interbead distance $7.0$ nm	$\nu$
	$L = 41.0$ nm; $d = 9.6$ nm; $n=2$ interbead distance $9.6$ nm	$f/f_o$
Electron-micrograph	$d = 6.0$ nm; $L = 62$ nm; $n=8$ interbead distance $2.0$ nm	

dimensions. A  $\beta$  value of  $2.15 \times 10^6$  is characteristic of spheres and ellipsoids of low axial ratios. Since the calculated  $\beta$  value was  $3.0 \times 10^6$  it indicated that the molecule could be a prolate ellipsoid [158]. From the contour of axial ratio vs hydration factor for various frictional ratios and viscosity increments, axial ratio of 13, using frictional ratio, and a value of 18 using viscosity increments were obtained. From the axial ratio and the volume of the molecule ( $9.6 \times 10^{-19}$  ml/molecule) the dimensions of the prolate ellipsoid i.e. equatorial diameter and length were calculated as 47 Å and 820 Å respectively for an axial ratio of 18, and 52 Å and 680 Å respectively for an axial ratio of 13. The corresponding cylinder will have a diameter of 40 Å and 42 Å respectively for the same length and volume (Table 2; Fig.6).

However, the electron microscopic appearance of the molecules did not resemble a rigid ellipsoid or a cylinder but was close to a string-of-beads structure (Fig.5). Hydrodynamic theory for the transport behaviour of such a structure was first formulated by Kuhn in 1932 [161] and later Shulman [162] applied a slightly modified version to derive the shape of fibrinogen and compare it with its actual electron microscopic appearance according to which the molecule appeared as a rigid string of three beads. This prompted us to follow Shulman's procedure and derive the shape using

viscosity increment as a  $770 \text{ \AA}$  long string containing six identical spherical beads each of diameter  $70 \text{ \AA}$ , arranged linearly with a uniform inter-bead (surface to surface) distance of  $70 \text{ \AA}$ , equal to the bead diameter (Fig.6).

However, as in the case of equivalent ellipsoid, Shulman's approach using frictional ratio as the shape factor gave an altogether different picture that of a string of two beads of diameter and inter-bead distance of  $96 \text{ \AA}$  and the total length being  $420 \text{ \AA}$  (Table 2).

Shape from electron microscopy: The enzyme appears as a string of beads under the electron microscope (Fig.5). The bead diameter, obtained as a modal value from about 200 images, is  $60 \text{ \AA}$  and they are arranged linearly with an inter-bead distance of about  $20 \text{ \AA}$ . The number of beads, corresponds to 8 per molecule according to the calculation from the molecular volume and the bead volume ( $V_M/V_{\text{bead}}$ ). The total length of the molecule is  $620 \text{ \AA}$  ( $8 \times 60 \text{ \AA} + 7 \times 20 \text{ \AA}$ ). The agreement of this with the model obtained from Shulman's approach using viscosity increment is fair. In fact, when axial ratio (10.3 and 11.0 respectively of the E.M. model and the theoretical model) alone is considered, the agreement is excellent. (Table 2 and Fig.6).

Flexibility in the molecule: A point of interest and possibly of considerable structural implication is the lack



of agreement in the dimensions of the shape obtained from frictional ratio or from viscosity increment irrespective of the model system chosen. Normally the agreement between the shapes derived from either of the two procedures should be very close. To reconcile this serious discrepancy, we have considered the possibility that it may be attributed to the flexibility in the links between the beads. We believe that this would allow the molecule to assume different overall shapes under different force-fields [146,147,221]. It is conceivable that in viscosity measurements the molecule might be in an extended form during its flow through a capillary owing to the operation of shearing forces, and during sedimentation which is a bulk motion under centrifugal field, the same molecule might be in a more compact form. In the electron micrographs the images are not repetitive in the overall geometrical shape and the molecule assumes various shapes owing to the different orientations of the beads with respect to one another (Fig.5 and 13). The freedom allowed by the flexibility in the links for the molecule to assume different shapes as seen in E.M. pictures may, therefore, be a reasonable assumption.

#### Subunit stoichiometry of the enzyme complex

It is rather unlikely that a large protein such as this ( $M_r = 760,000$ ) is a single polypeptide and normally

such large proteins are composed of subunits whose molecular weight ranges from about 30,000 daltons to about 50,000 daltons [222]. The upper limit in size, noted so far, for a single polypeptide is about 200,000 daltons [136]. An obvious conclusion, therefore, is that rabbit intestinal glucoamylase-maltase complex should have subunits arranged to give the overall shape described in the previous section. Hence, our immediate aim was to isolate these subunits and study their properties. It was already reported by Sivakami and Radhakrishnan [116] that the enzyme was not dissociable by the classical SDS-PAGE method, and that the enzyme lacked ~~totally~~ in sulphur amino acids. Treatment with 6M guanidinium chloride shifted the elution-volume of the enzyme in a Sepharose 4B column from the inner volume (native state) to the void volume (denatured) [116], which is owing to the transformation in the structure of the protein from compact to random coil structure, the latter having a higher Stokes' radius than the native structure eluted out earlier [223]. It is also clear from this observation that though denaturation by guanidinium chloride treatment was complete the molecule did not dissociate.

Evidence from SDS-PAGE: More drastic conditions, but not drastic enough to break covalent links were employed in this study to help in the isolation of the subunits. It has been shown that heating the proteins in 1% SDS at 100°C

for prolonged periods ( up to 1 hr) did not cause breakage of peptide backbone and such conditions were necessary for some proteins to dissociate them into subunits [224]. Similar treatments to our protein failed to dissociate it and even increasing the SDS concentration up to 2% was not successful. It is likely that SDS was not effective owing to poor binding, characteristic of many glycoproteins [225], but other denaturants like urea and guanidine hydrochloride might be effective as has been shown in a few cases [133-135]. It is relevant and of interest to mention here that the protein did not lose its enzyme activity in 5% SDS nor did it lose its ability to react with its antibody even in the presence of 2% SDS (page 149). These conditions are sufficient to destroy the activity of most of the enzymes. However, it lost its activity completely in 3M guanidinium chloride. Membrane bound intestinal hydrolases, have been found to be resistant to inactivation by SDS and other detergents used in their solubilisation and have been isolated in active form after electrophoresis in the presence of these detergents [57,81-84]. Denaturation by heating at 60°C for 1 hr with guanidine hydrochloride followed by SDS treatment after removal of guanidine hydrochloride and electrophoresis in the presence of SDS, failed to dissociate the molecule. Urea in place of guanidinium chloride was also not successful.

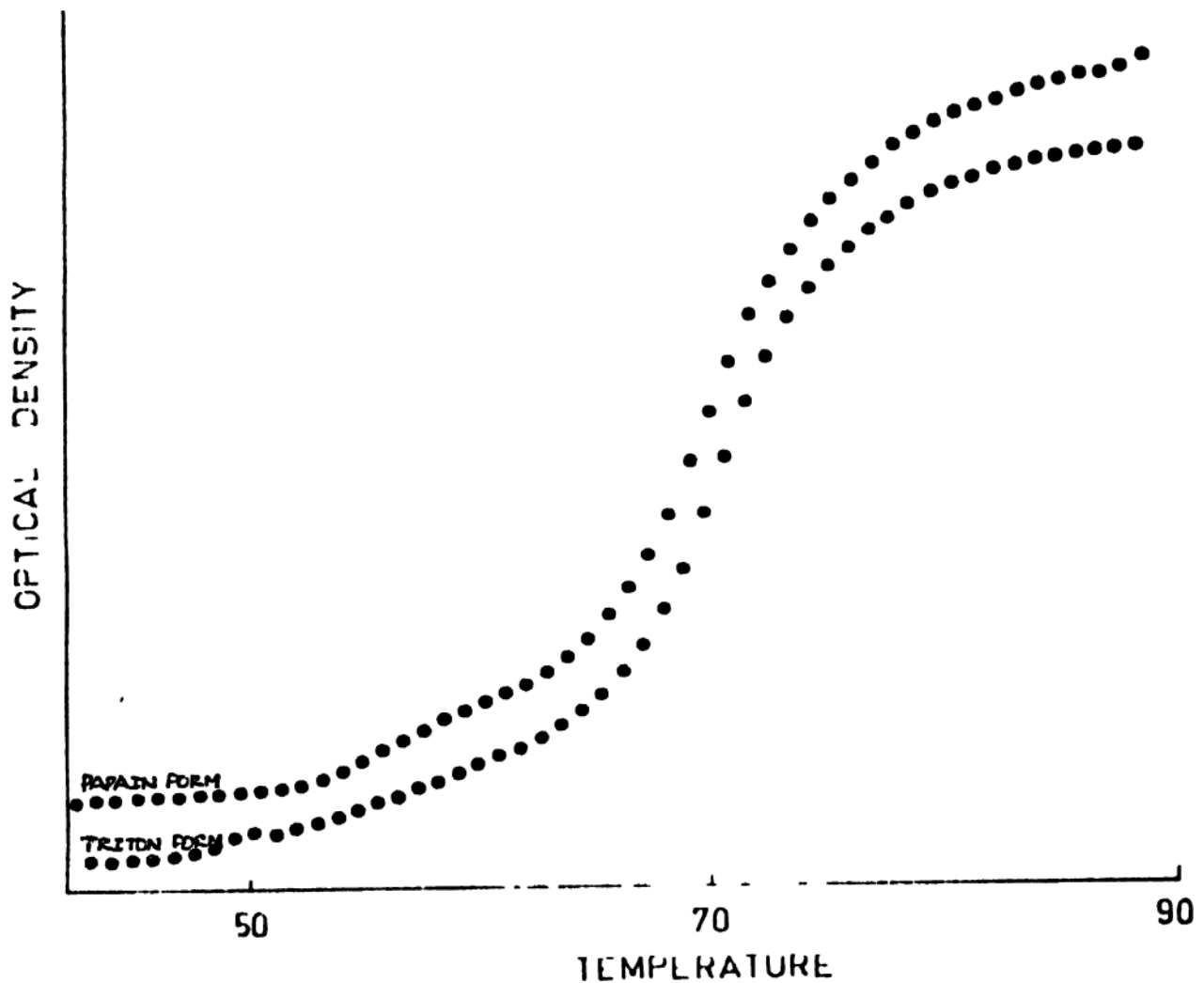


Fig.7 : The effect of heating the enzyme (both forms) at pH 4.0 from 30°C to 100°C at a rate of 1°C/min. The hyperchromic effect seen is due to turbidity caused by the precipitation of the enzyme. The enzyme at higher pH values did not exhibit hyperchromicity.

Evidence from acid PAGE: Owing to the reported success of acidic systems in the case of certain proteins which are otherwise difficult to dissociate, two such systems were tried [205,206]. In the acetic acid method, both untreated enzyme and the enzyme treated with 20% acetic acid, remained as a band at the top of 5% gel, while it was either partially or completely absent in the case of enzyme samples treated at 60°C for 15 min with higher concentration of acetic acid (60-100%) in a manner that was dependent on the severity of the treatment. However, no other bands were seen concomitant with the decrease in the intensity of the original band. Assuming that the fragments could be small peptides that might have escaped into the buffer in 5% gel, discontinuous gradient gel electrophoresis with 5% and 10% gels was performed without success. During thermal denaturation studies of the enzyme at various pH values for detecting a hyperchromic effect, it was observed that the enzyme precipitated when heated above 60°C at pH 4.0 (Fig.7). In the light of this observation it is possible that the enzyme aggregated and precipitated in the presence of acetic acid and hence failed to penetrate the gel and was removed during the washing and staining procedure. This aggregation must have been a function of the severity of the acetic acid treatment causing a progressive decrease of the band intensity and the final disappearance. Aggregation of proteins in this system has been noted earlier

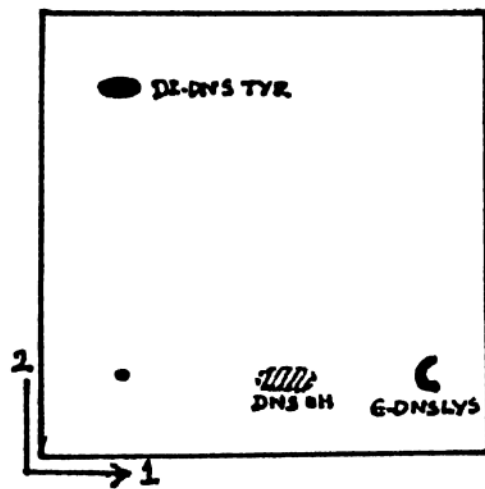


Fig.8 : Identification of the N-terminal amino acid of the papain form of the enzyme : The N-terminal amino acid, tyrosine, has been resolved by TLC on polymide sheets after dansylation, as didansyl derivative.

[205]. Evidence gathered from chemical studies also favoured the aggregation theory. When the dansylated enzyme was treated with acetic acid drastically and dialysed against 10% acetic acid, the fluorescent band remained on top of the 5% gel during electrophoresis. In the acetic acid-phenol-urea system, though acetic acid (37%) was present the enzyme did not behave in the same manner as in the acetic acid system. The enzyme remained a few mm below the top of the gel as a sharp band and did not disappear or lose its intensity even after heating it at 100°C for about 15 min in this system. The urea and phenol in this system, either did not allow aggregation or they had helped the aggregate to remain in the soluble state. Finally, it is to be concluded that the enzyme did not dissociate into subunits under any of the available methods and if subunits are present they must be linked covalently by unconventional bridges (disulfide bridges are excluded since S is absent in the protein).

Chemical studies-analysis of N-terminal: In view of the refractory nature of the protein to cleavage into subunits by conventional methods, it was considered that a quantitative end-group analysis and the end-group to protein stoichiometry might provide us with a lead. Using dansylation technique the only N-terminal amino acid that was detectable was tyrosine (Fig.8). Didansyl tyrosine, the dansyl deri-

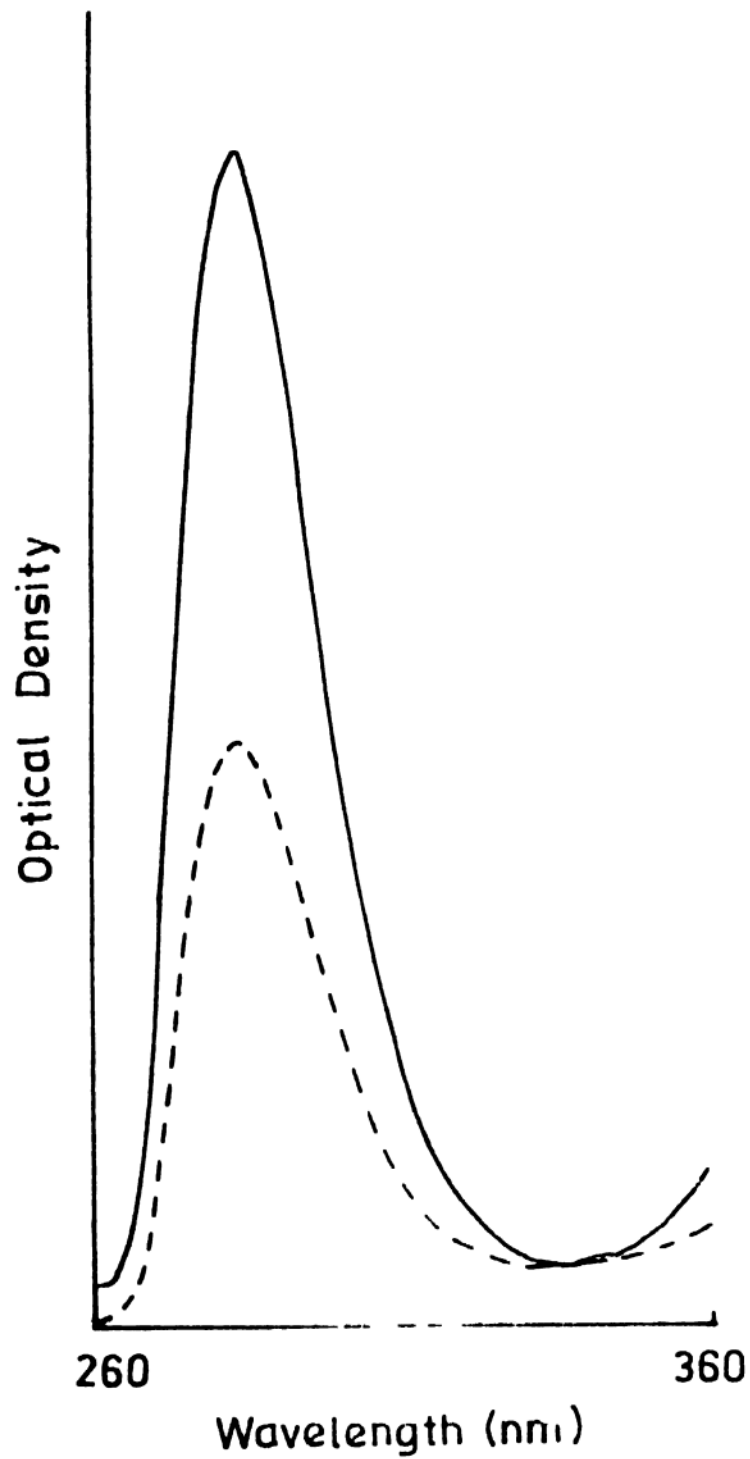


Fig.9 : Difference-spectrum (absorption) of authentic didansyl and isolated dansyl derivative of N-terminal against didansyl lysine as blank. —, spectrum of authentic sample (OD range 0-1) ---, spectrum of isolated didansyl derivative (OD range 0-2). For quantisation, OD at 280<sup>o</sup> nm was used.



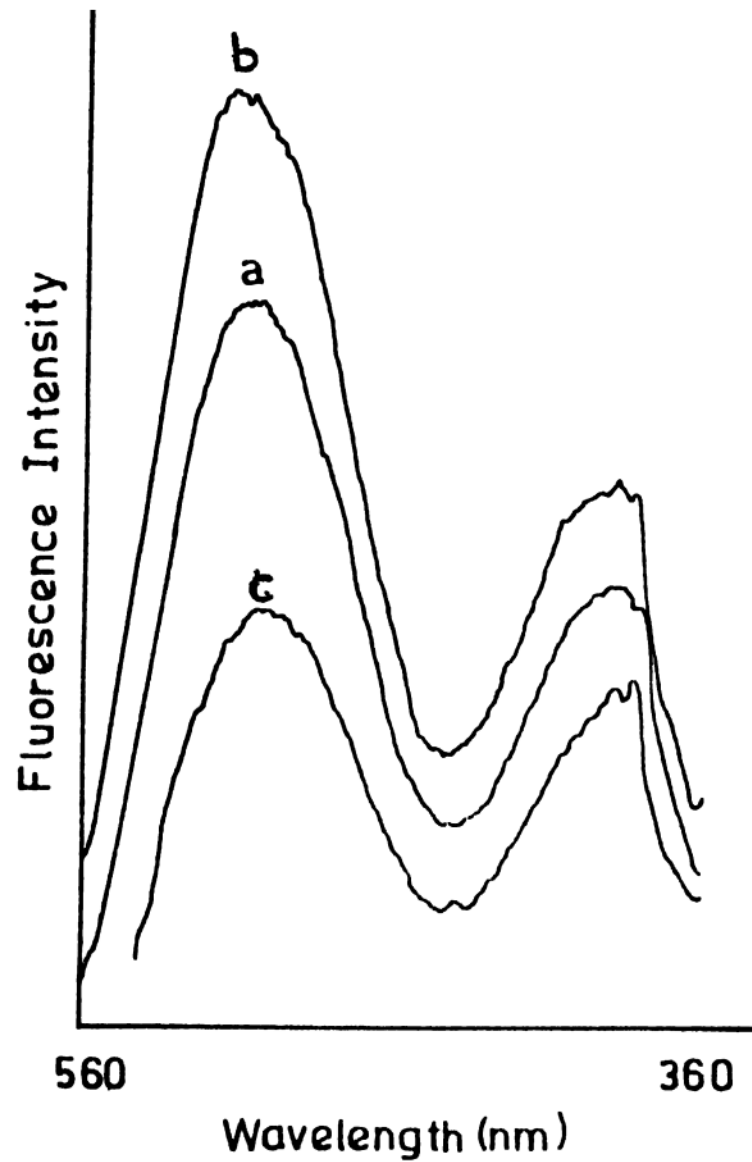


Fig.10 : Fluorescence spectrum of (a) authentic didansyl tyrosine, treated identically as the samples, (b) and (c) Dansyl derivative of N-terminal isolated from 360  $\mu$ g and 240  $\mu$ g of the enzyme respectively. Excitation wave length 280 nm.

vative of the N-terminal tyrosine has an  $R_f$  close to 1 in the solvent system benzene - acetic acid, 9 : 1 (v/v), employed to develop the TLC on polyamide sheets in the second direction. The other expected fluorescent products viz. dansic acid, O-dansyl tyrosine and  $\epsilon$ -dansyl lysine have a  $R_f$  close to 0 in this solvent system. It was, therefore, <sup>necessary</sup> ~~possible~~ to isolate the N-terminal derivative of the protein using a small column (bed volume 1 ml) of polyamide powder using the same solvent system. The difference spectrum of the isolated didansyl derivative of the N-terminal against didansyl lysine as blank, resulted in tyrosine spectrum as can be seen from Figure 9 and it matched well with the spectrum obtained in the same way using an identically treated authentic didansyl tyrosine from Sigma. The fluorescence spectra of the prepared derivative and the authentic sample also matched well (Fig.10). The stoichiometry of the purified end-group calculated using both tyrosine absorbance at 280 nm and fluorescence intensity was 40 moles and 70 moles respectively per mole of the enzyme. Since the absorbance methods are less susceptible to contributions by contaminants compared to fluorescence methods, the lower value of 40 moles/mole of enzyme is probably more reliable. Irrespective of the correctness of this estimate it served as the first direct evidence for the presence of multiple subunits.

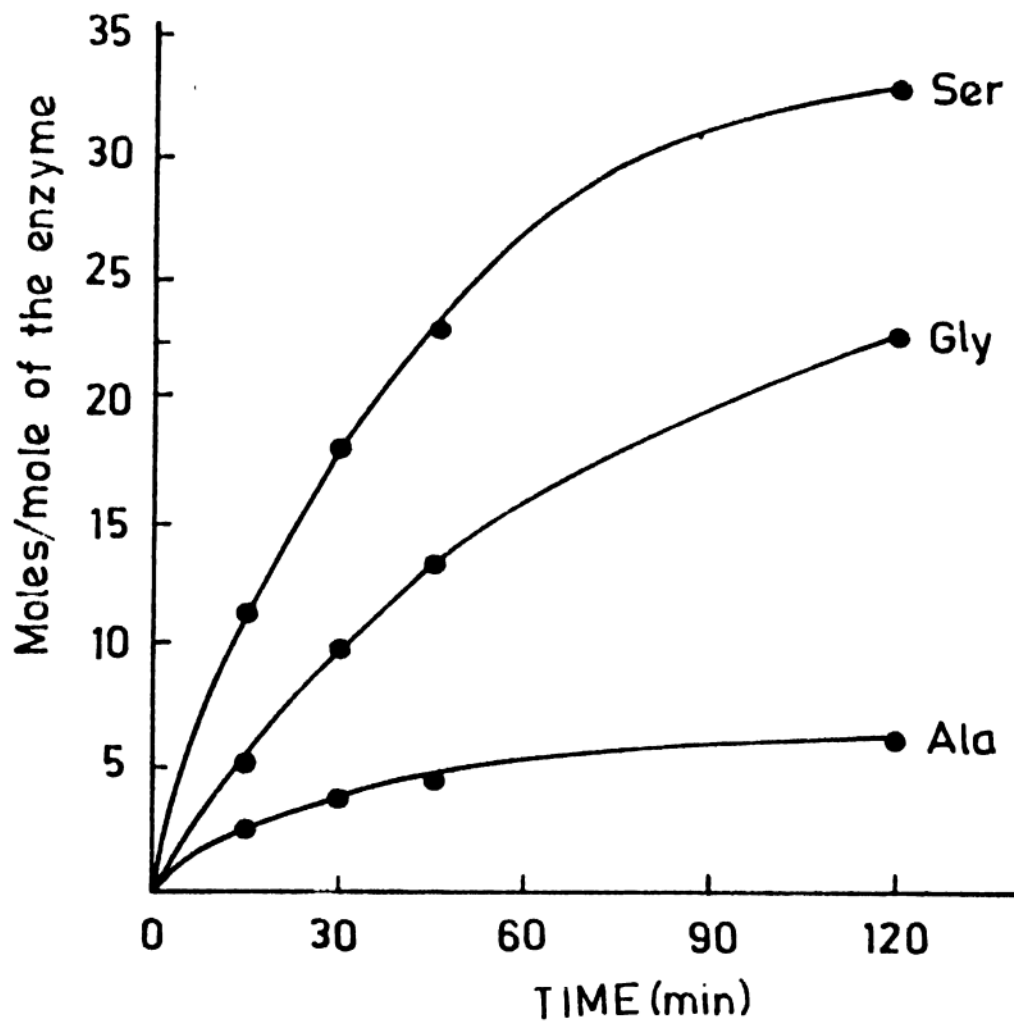


Fig.11 : Analysis of C-terminal amino acid. The amount of released amino acids by carboxy peptidase A vs time. At about 2 hours after the start of the digestion serine tends to plateau off a value of 32 C-terminal/molecule was deduced. Glycine and alanine are released at a lower rate corresponding to second and third residues. The graph suggests Ser-Gly-Ala--- as a possible partial sequence of the C-terminus.

Chemical studies - analysis of the C-terminal: The C-terminal was analysed using time-phased carboxypeptidase A digestion and subsequent quantization of the released amino acids by an automatic amino acid analyser. The results indicated that serine is the C-terminal amino acid and the second and the third residues are glycine and alanine respectively (Fig.11). The C-terminal to protein stoichiometry worked out from the amount of serine released at the end of 2 hours is 32 moles/mole of enzyme. The lower value of C-terminal stoichiometry compared to that of the N-terminal may be due to the incomplete release of all C-terminal serine, which is known to be released slowly by carboxypeptidase. Nevertheless, the procedure also confirmed existence of multiple subunits. Since tyrosine and serine respectively are the only N-terminal and C-terminal amino acids detectable it is most likely that the subunits are identical.

Chemical studies - peptide mapping: The enzyme denatured with guanidine hydrochloride was <sup>c. int. l. p. an.</sup> ~~subjected to tryptic action~~ (page 75 ). The tryptic peptides were dansylated and the dansyl peptides were resolved on polymide TLC, a technique which was found quite satisfactory for the separation of even closely related peptides as can be seen from Figure 12a. The tryptic peptide map of the enzyme contains only twelve

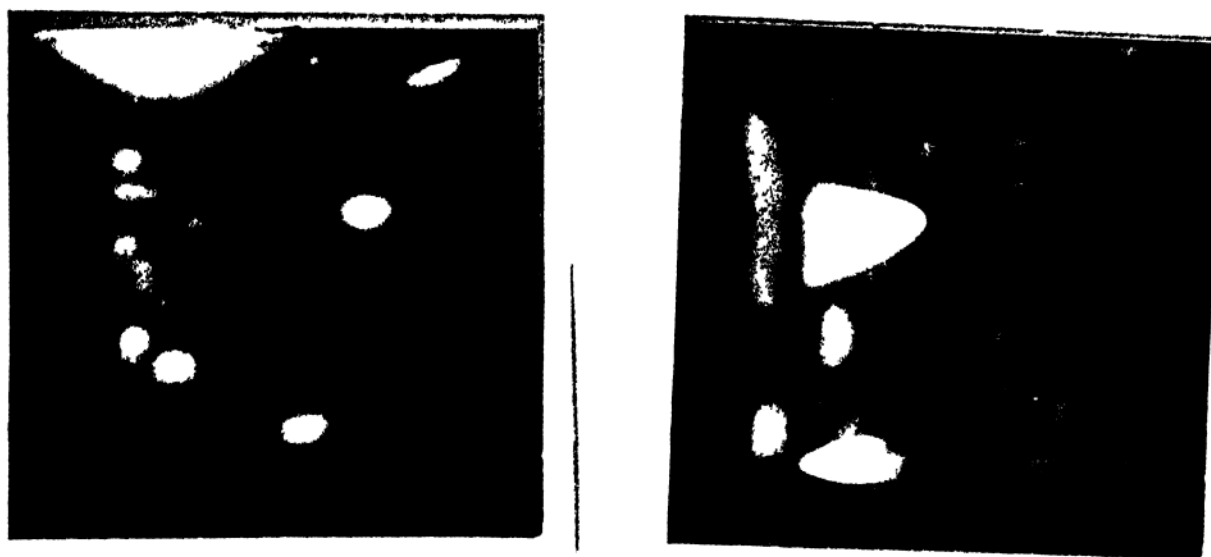


Fig.12a : Map of nearly 40 di- and tri-peptides after dansylation using the method described in the text under methods (page 75). Number of fluorescent spots correspond to about 35, close to the number of dansylated peptides. Some of the peptides had the same N-terminal or C-terminal. 1st direction formic acid water, 3:100(v/v); 2nd direction, benzene-acetic acid, 9:1(v/v).

12b : Map of the dansylated tryptic digest performed given under Fig.12a. There are only 12 fluorescent spots of the dansylated tryptic peptides, arising from 600 cleavage points (from the amino acid composition), thus suggesting the presence of about fifty subunits.

Table 3Amino acid analysis of the two forms

Amino acid	Papain form		Triton form	
	moles/mole of enzyme	resi-/sub- dues unit	moles/mole of enzyme	resi-/su dues ur
Asp	646	13	668	13
*Thr	287	6	293	6
*Ser	340	7	350	7
Glu	636	13	591	12
Gly	448	9	504	10
+Ala	396	8	400	8
+Val	394	8	395	8
+Ile	267	5	293	6
Leu	404	8	406	8
Tyr	263	5	248	5
Phe	263	5	256	5
His	100	2	100	2
Lys	392	8	356	7
Arg	202	4	228	4-5
Pro	380	8	380	8

\*Corrected to destruction during hydrolysis : 5% for Thr and 10% for Ser

+Values after 48 hr hydrolysis were given more weightage. Each value is an average of concordant values (within 5% variation) among at least four analyses. No. of subunits was taken as 48.

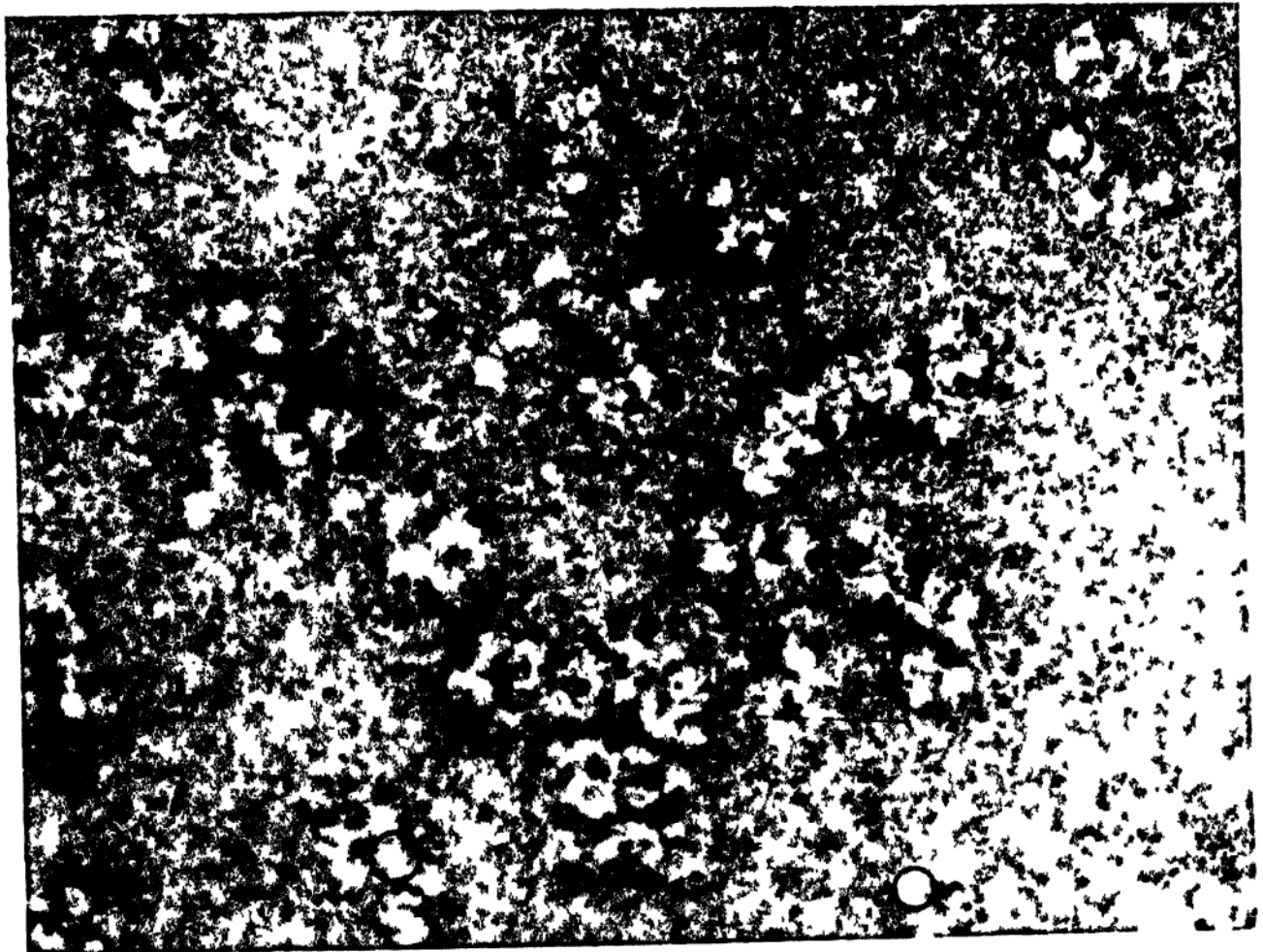


Fig.13 : Electron microscopic images of the enzyme at a higher magnification (x500,000) and a resolution of about 20 Å. The fine structure of beads is revealed. Each small bead measures approximately 35 Å in diameter and there are either 5 or 6 of them in each bead, in a octahedral geometry which is clearly seen in the images of some beads (circles).

fluorescent spots (Fig.12b) corresponding to the dansylated peptides. From the amino acid composition (Table 3 ) nearly 600 cleavage points (lys+arg) for trypsin can be expected and nearly as many peptides are theoretically possible if the enzyme were a single polypeptide or made up of many nonidentical subunits. Even allowing for resolution limitations in the technique and for the presence of overlapping peptides, the observed small number of peptides can not be explained unless it is assumed that the molecule is a multimer of about fifty identical subunits.

Fine-structure of a bead - Electron microscopic evidence.: The image of the enzyme at about  $20 \text{ \AA}$  resolution and at higher magnification reveals the presence of a fine structure of the beads (Fig.12). Each bead appears to consist of smaller beads, approximately  $35 \text{ \AA}$  in diameter. It is necessary that the diameter measurement should be accurate to  $\pm 1 \text{ \AA}$ , to work out the actual number of such smaller beads in a bead and obviously this is unpracticable in this case at least. The appearance, however, suggests that there could be either five or six such smaller beads within each main bead (Fig.13).

Geometry of the bead - Hydrodynamic study: Since it is a general observation that usually an even number of



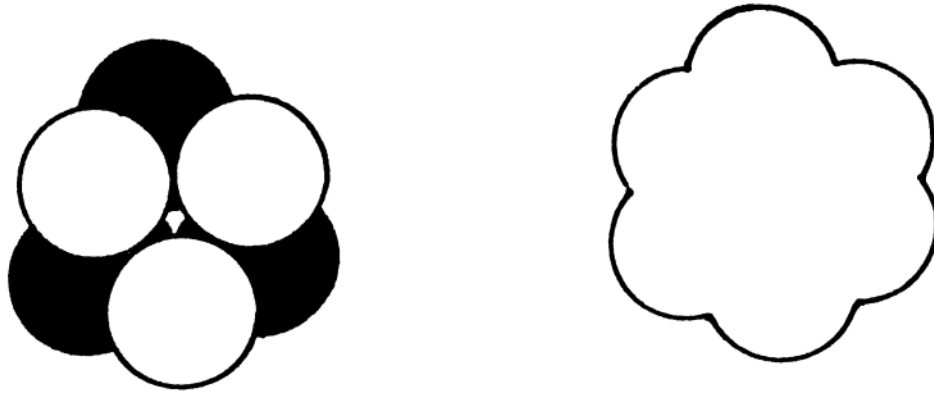


Fig.14 : The assumed geometry of the bead on the basis of electron-microscopic appearance. The two dimensional projection of the geometry shown at the right side has a striking resemblance to some of the images indicated in Fig.13. The geometrical factor of this geometry from hydrodynamics and that arrived at from purely theoretical grounds show good agreement (page 109).

polypeptides are seen to associate in a perfect symmetry around a central point to form oligomeric structures [136] and the chemical evidence suggests strongly that there are about fifty identical subunits, it is most likely that there are six subunits in each bead.

Recently, Teller et al [186] have laid down procedures for determination of the geometry of an oligomeric protein from its frictional coefficients and this prompted us to see if there is any correlation between the assumed geometry, based on the electromicroscopic appearance (Fig.13) and considering maximum symmetry possible to generate an approximate sphere, since in our earlier calculations we assumed the sphericity of each bead and worked out correct number of beads. Each bead according to our assumption is made up of two rows of three finer beads arranged in such a manner that their centres occupy three corners of an equilateral triangle and two of such triangles are placed one above the other with the corners of one in line with the centres of the sides of the other (Fig.14). In short the geometry is an octahedron with a  $D_3$  symmetry.

The geometrical factor,  $F_n$  of the enzyme (0.7148) calculated from  $S_n^0$ (18.6),  $M_r$ (760,000) and  $\bar{v}$ (0.72 ml/g) of the enzyme is considerably less than 1 suggesting a linear

arrangement of beads as has been already established. The geometrical factor, of the bead is 1.028, a value close to 1, suggestive of a compact structure with spherical symmetry. The geometrical factor calculated purely theoretically for the assumed geometry given above (Fig.14) is 1.06, apparently very close to the one derived from sedimentation coefficient. This close agreement is taken as a strong evidence for the assumed geometry to represent truly the actual appearance and geometry of the bead. The two dimensional projection of the assumed and verified geometry, compares well with some of the images of the beads in the electron micrographs (Fig. 13 ).

Quaternary structure of the enzyme complex: In summary, on the basis of various lines of evidence presented above, the following conclusions are drawn. The enzyme is made up of 48 identical subunits (ca.33 Å in diameter). The subunits are arranged in such a manner that groups of six associate as octahedrons with  $D_3$  symmetry, to form beads (60 Å in diameter each). Eight such beads are assembled linearly with a uniform interbead surface-to-surface distance of about 20 Å to generate the final shape of the enzyme. The flexibility in the links between the beads and the existence of the unusual covalent linkages between the subunits and between the beads, are unique and noteworthy.

## STUDIES ON THE ASSOCIATION OF THE ENZYME COMPLEX WITH THE BRUSH BORDER MEMBRANE

It is known for a long time intestinal hydrolases are membrane-bound and are not easily released from the membrane unless treated with a protease like papain or elastase [49] or with a detergent like Triton-X100. Detailed studies on sucrase-isomaltase and amino-peptidases have shown that these enzymes are anchored to the membrane by means of a very hydrophobic peptide present at the N-terminal end which often traverses the whole width of the membrane. Such a detailed information is not available for many other brush border membrane-bound enzymes. There is some evidence to indicate the presence of an anchor peptide at C-or N-terminal end in the case of pig intestinal glucoamylase-maltase complex [56].

The strategy employed in the above studies is to solubilise the enzymes by a protease (generally papain) or a detergent (generally Triton-X100), and to compare the molecular properties of the two forms to reveal the identity of the anchor peptide. It is assumed that the detergent removes the whole enzyme inclusive of the membrane-embedded portion and that the protease removes only that portion which is outside the membrane by cleavage of one or more susceptible peptide bonds.



Fig.15 : A close comparison of the sedimentation behaviour of Triton form (upper, Wedge shaped cell) and papain form (lower, ordinary cell) of the enzyme. Run condition: 60,000 rpm; temperature, 24.8°C; interval between photographs, 5 min; concentration, 0.5 w/v). Both the forms exhibit identical sedimentation behaviour.

Table - 4

Hydrodynamic parameters of the two forms of the enzyme.

HYDRODYNAMIC PARAMETER	VALUES FOR	
	TRITON FORM	PAPAIN FORM
$S_{20,w}^0$	18.42 S	18.6 S
$D_{20,w}$ (c=1% w/v)	$1.945 \times 10^{-7}$ cm <sup>2</sup> /sec.	$2.073 \times 10^{-7}$
Molecular weight by S and D method	800,000	770,000
Archibald's method	770,000	760,000

With a view to investigating the mode of attachment of rabbit intestinal glucoamylase-maltase complex, we adopted the strategy mentioned above. The enzyme was solubilised using papain or Triton-X100, purified to a state of homogeneity and a variety of molecular properties of the two forms compared. The results enumerated below indicate almost a monotonous identity of the two forms, thus differing significantly from sucrase-isomaltase.

#### Physical studies of the two forms

Aggregation phenomenon: Aggregation in the absence of detergent is a characteristic feature of the detergent form of membrane proteins [102], attributed to the presence of the hydrophobic anchor peptide and the protease form, as might be expected, is incapable of this aggregation. In fact, this difference is often taken as a primary evidence for the presence of an anchor peptide. As a consequence of this aggregation, the detergent form will be several fold bigger than the protease form in the absence of detergent and this will be reflected in the size and shape determinations. In the case of rabbit intestinal glucoamylase-maltose complex as can be seen from Table 4 both the forms have almost identical sedimentation (Fig.15) diffusion coefficients and molecular weight, and show identical gel

Gel filtration of papain and Triton-x100  
solubilised glucoamylase-maltase complex

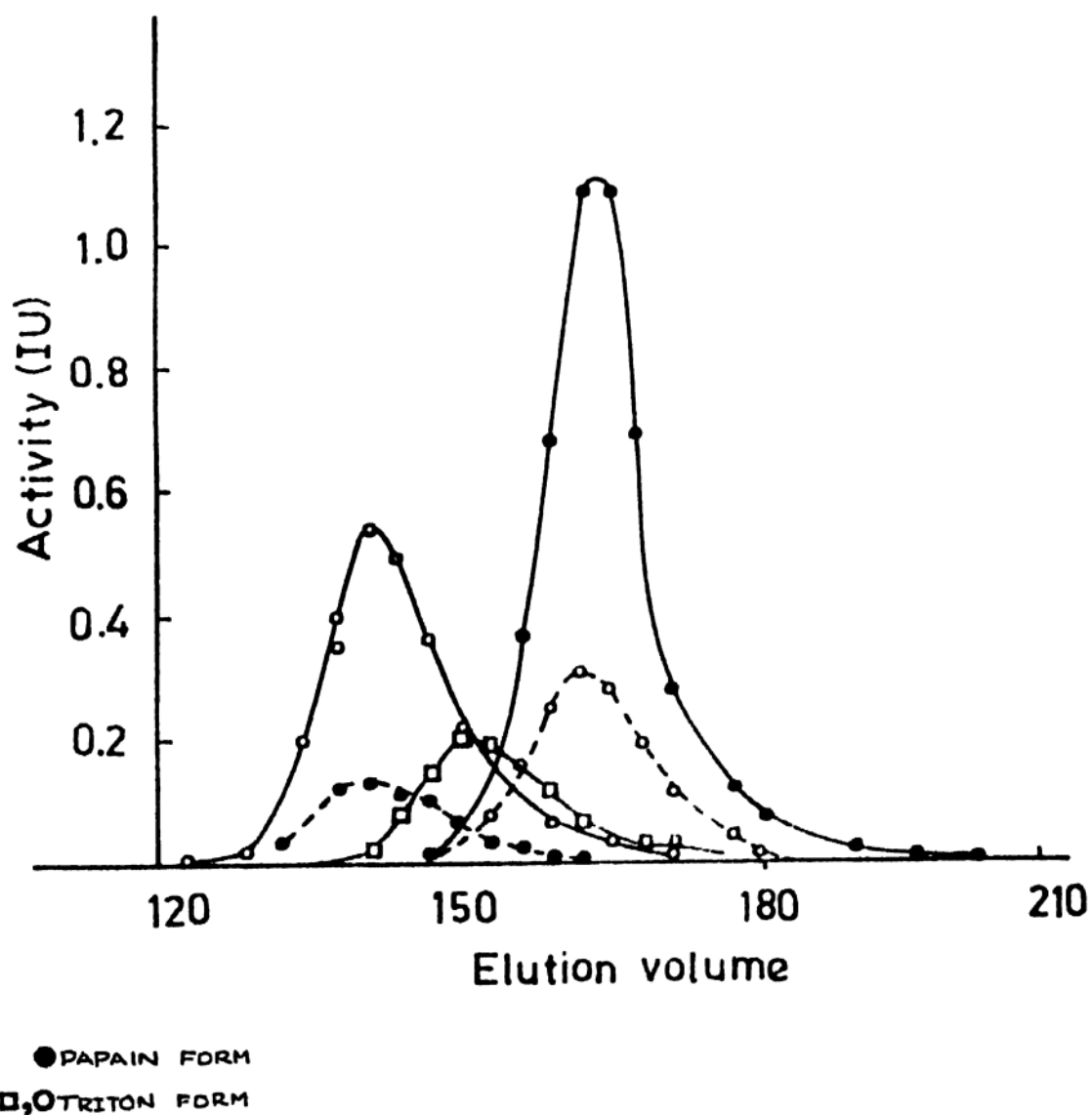


Fig.16 : Gel filtration behaviour of Triton and papain forms of the enzyme. There is a shift in the peak towards inner volume as a function of ionic strength of the elution buffer. Both the forms behave identically with respect to even this fine variation, suggesting identity.



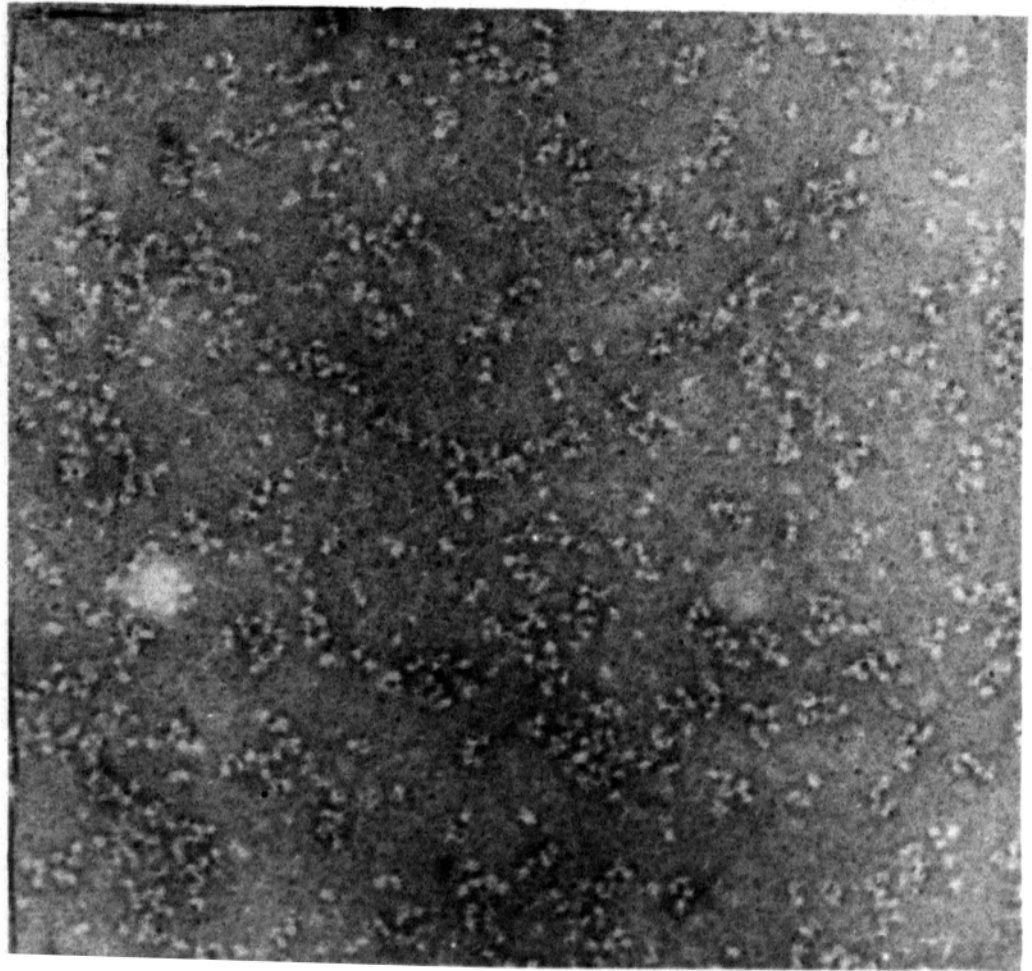


Fig.17 : Electron microscopic appearance of the aged-Triton form. Negative contrast by uranyl acetate on a Support - membrane, (Formvar). Absence of aggregation phenomenon and a close resemblance to the images of papain form (Fig.5) are evident.

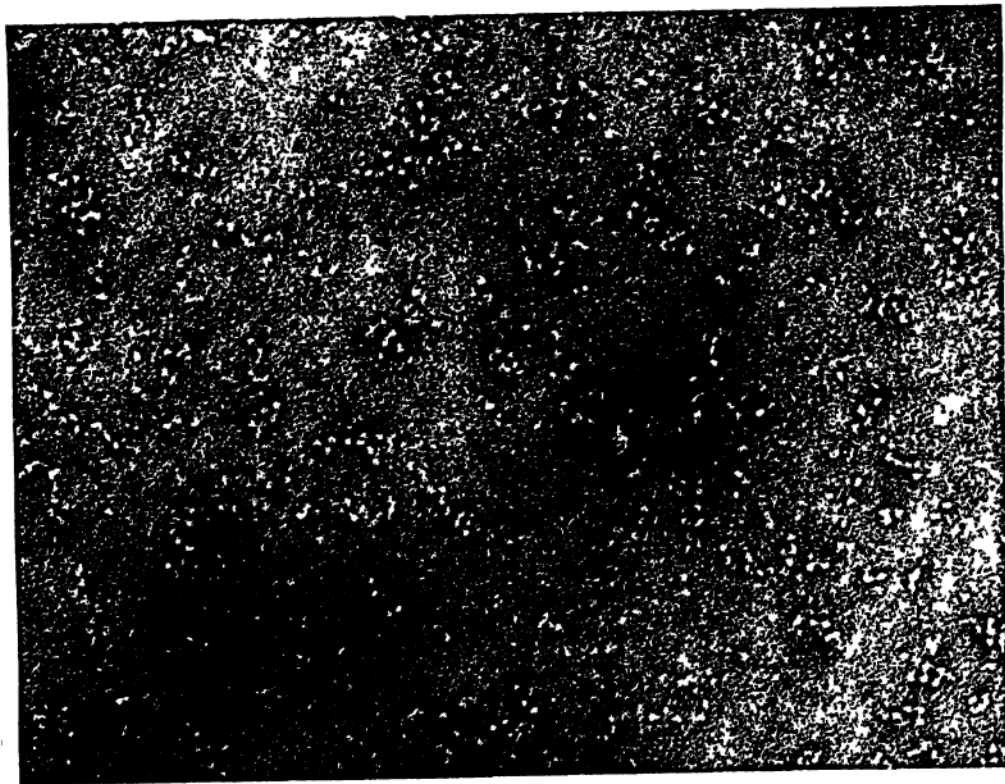
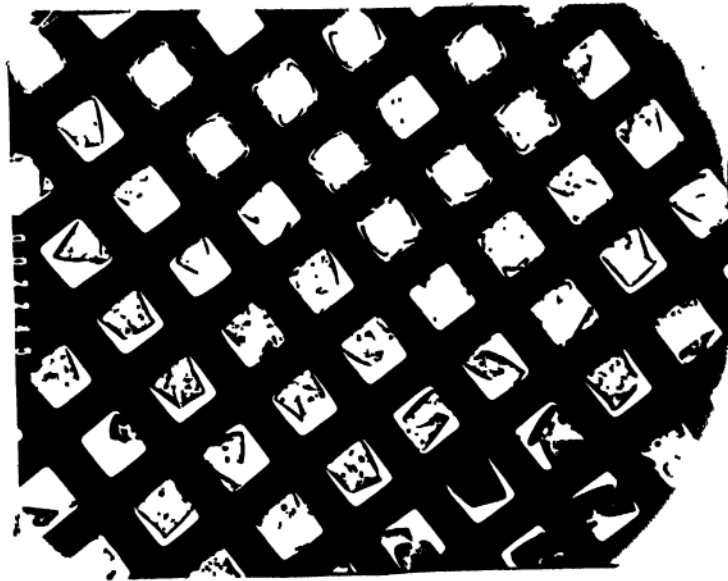


Fig.18 : Electron microscopic appearance of Triton form of the enzyme, negatively stained with uranyl acetate and pictured on naked grids. The membrane/film formed by the enzyme-uranyl acetate (2%) combination can be seen characteristically attached only to one of the edges of the windows. After an initial drift on exposure to the electron beam (80 Kv), the membranes stabilised and the images obtained were of high quality compared to what could be achieved under the performance of the E.M., with Formvar strengthened by thin carbon coating used as support film.

filtration behaviour (Fig.16). These results rule out the aggregation phenomenon and possibly also the presence of a prominent hydrophobic anchor peptide.

In the case of rat intestinal glucoamylase-maltase complex it was reported that though both the forms seemed identical with respect to the observed molecular properties, the detergent form exhibited an irreversible aggregation phenomenon on long storage and this was attributed to the possible presence Of a small hydrophobic peptide at the C-terminal (which was not further analysed) that might have escaped detection owing to its small size in a large protein ( $M_r$  500,000) [55]. However, the rabbit enzyme did not show any aggregation even after long storage (1 year) as can be seen from the electron micrographic images (Fig.17). The electron microscopic images of both the detergent form (Fig.18) and protease forms are strikingly identical.

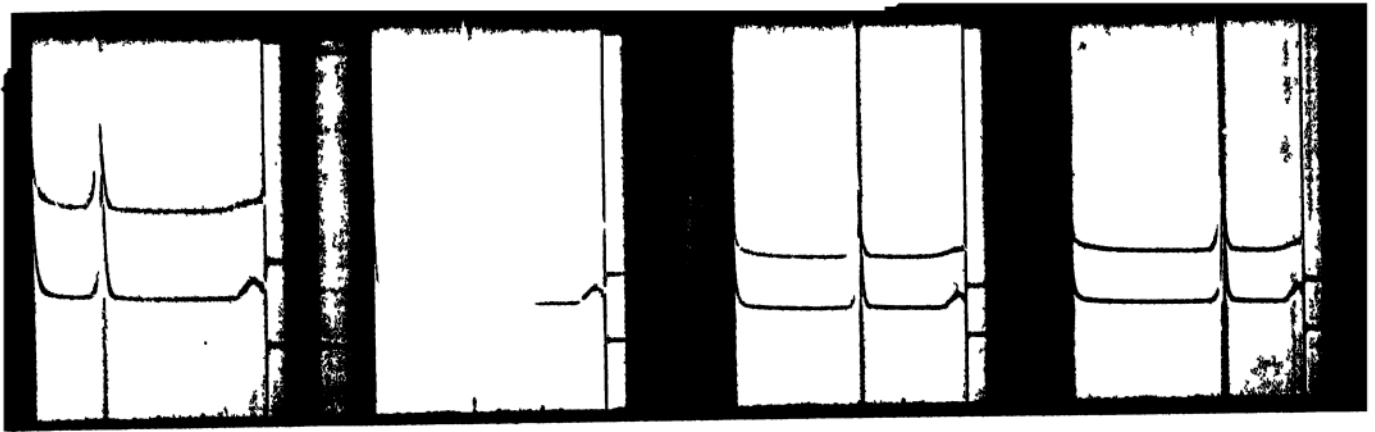


Fig.19 : A close comparison of the sedimentation behaviour of Triton form of the enzyme in presence of 0.5% Tritin-X100 (lower) and Triton form incubated with papain, activated by 0.01M  $\beta$ -mercaptoethanol for 1 hr at 37°C (upper). There is apparently no change in the sedimentation behaviour of the detergent form by both the treatments. This suggests lack of interaction with the detergent and also resistance to papain digestion.

Hydrophobic chromatographic  
elution pattern of papain from  
(●—●) and Triton form (■—■) of the  
Enzyme.

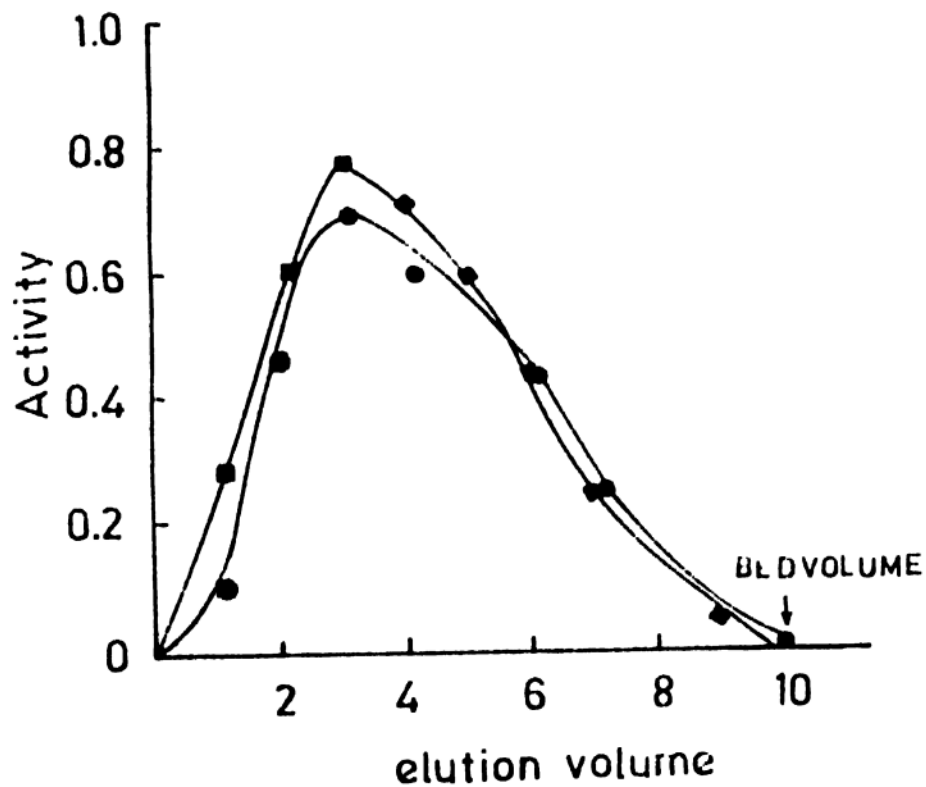


Fig.20 : Hydrophobic chromatography using Octyl-Sepharose CL-4B, of both papain (●—●) and Triton forms (■—■) of the enzyme. The forms are eluted completely with the equilibrating buffer (potassium phosphate buffer, 0.01M and pH 7.0) suggesting lack of hydrophobic interaction with the gel.

filtration behaviour (Fig.16). These results rule out the aggregation phenomenon and possibly also the presence of a prominent hydrophobic anchor peptide.

Stokes' radius: The above results suggest an identical Stokes' radius for both the forms. One of the major attribute of the detergent form and which can not be observed in the protease form is its ability to bind a miscelle of detergent owing to the interaction of the anchor peptide with the detergent [56]. Consequently, both molecular weight and Stokes' radius of the detergent form would be larger than the protease form e.g. in the case of  $\gamma$ -glutamyl transerase the Stokes' radius was larger by a factor of 2 and is readily reflected in the gel filtration behaviour [4]. There was no difference in this behaviour for the two forms of the rabbit enzyme even in the presence of 0.1% Triton-X100 (Fig.19).

An interesting observation made during our gel filtration studies was that the elution volume varied reversibly as a function of ionic strength of the buffer, (0.01 M potassium phosphate buffer, pH 7.0) with a pH close to its isoelectric point (Fig.20). Thus, the elution volume in the absence of NaCl was 140 ml. It increased to 150 ml with 0.01 M NaCl and to 140 ml with 0.1 M NaCl. This is possibly due to a decrease in Stokes' radius of the enzyme as a result

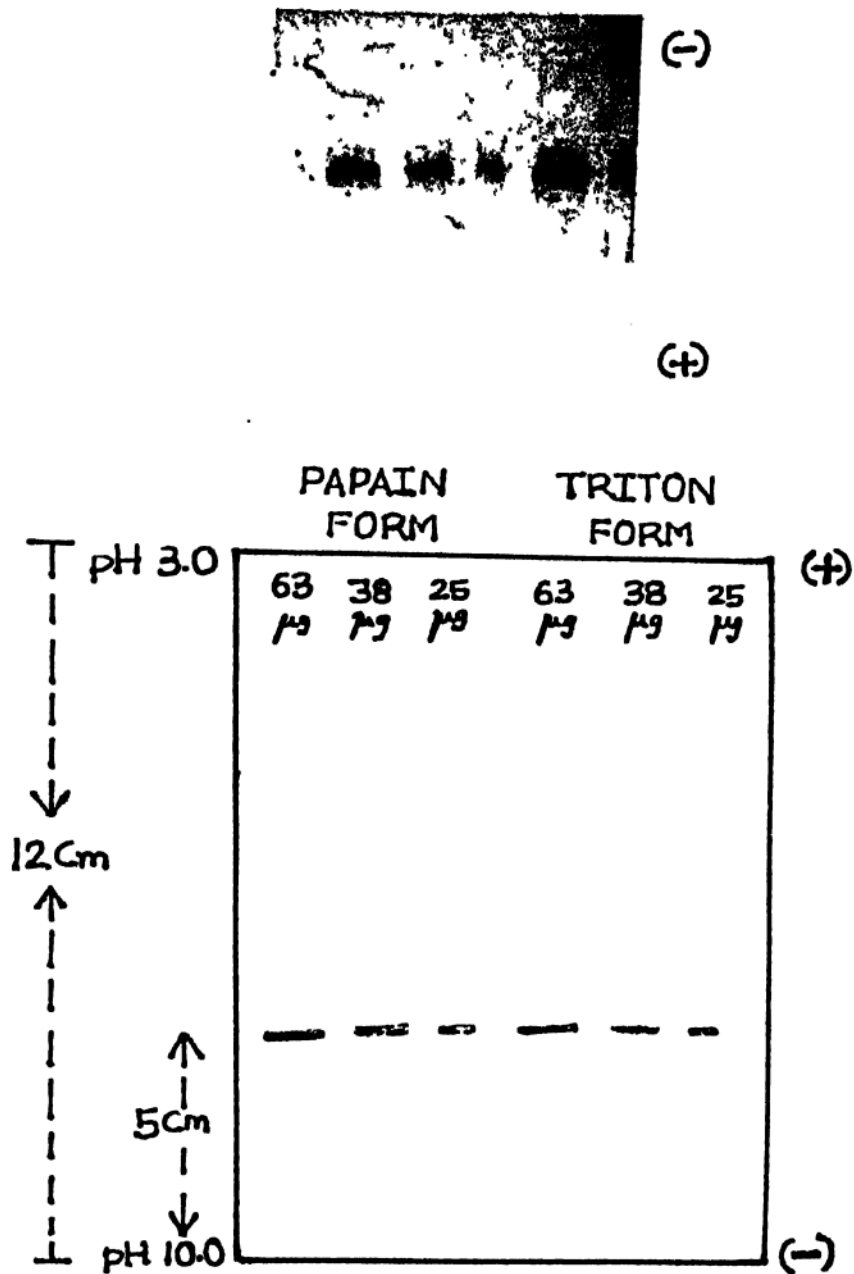


Fig.21 : Isoelectric focusing<sup>of</sup> papain and Triton forms of the enzyme. Both focus at the same isoelectric point which is about 7 ( $\pm 0.25$ ) as read from the position with respect to anode (3.0) and cathode (10.0). Focusing at a single point rules out micro-heterogeneity.

of interaction of salt with certain charged residues present in the links between the beads. The identical behaviour of both the forms of the enzyme even with respect to the subtle variation of elution behaviour with ionic strength is noteworthy.

Hydrophobic interactions: Owing to the presence of the hydrophobic peptide one of the properties expected of the detergent form is its ability to be severely retarded or bound by hydrophobic matrices like phenyl- or octyl-Sepharose. As can be seen from Figure 20, the two forms were not at all retarded or held ~~onto~~<sup>to</sup> these hydrophobic matrices, suggesting probable absence of (or lack of expression of the hydrophobic character of) an anchor peptide. Similarly it was reported by Lee et al [55], that the Triton-X100 solubilised glucoamylase-maltase complex of rat intestine, which was subsequently purified after the removal of the detergent, did not bind to freshly added Triton-X100 at all owing to the absence of hydrophobic interactions.

Ionic properties: Both the forms focus at the same isoelectric point (Fig.21) and exhibited identical electrophoretic mobility in various electrophoretic systems under both acidic and basic conditions. Since the anchor peptides as a rule lack charged amino acids [75], the ionic properties



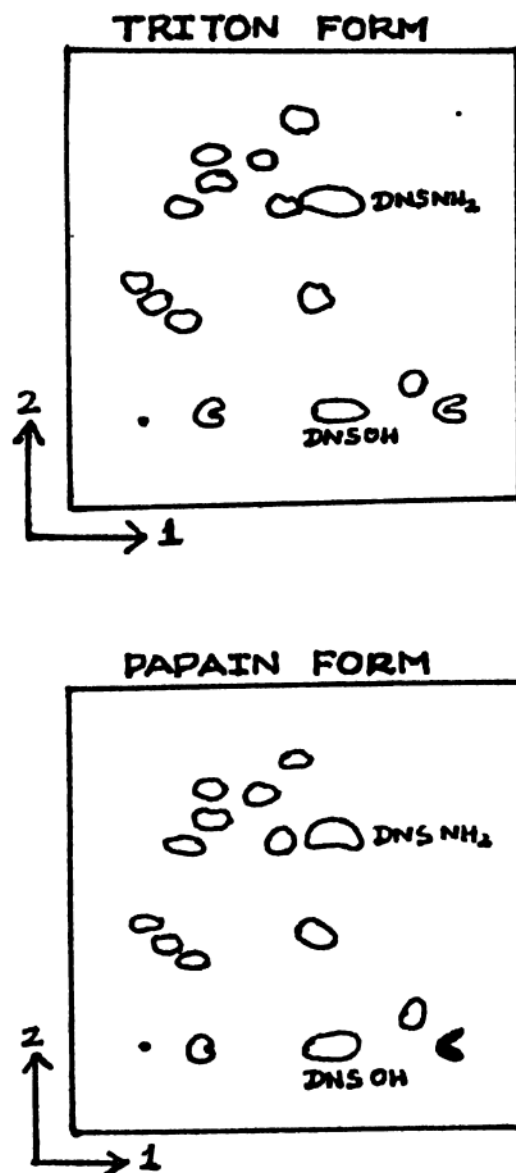


Fig.22 : Tryptic peptide maps of Triton and papain forms, of the enzyme (for details see under Methods section) (page 75) run under identical conditions. The striking resemblance of the maps is suggestive of identity of the two forms.

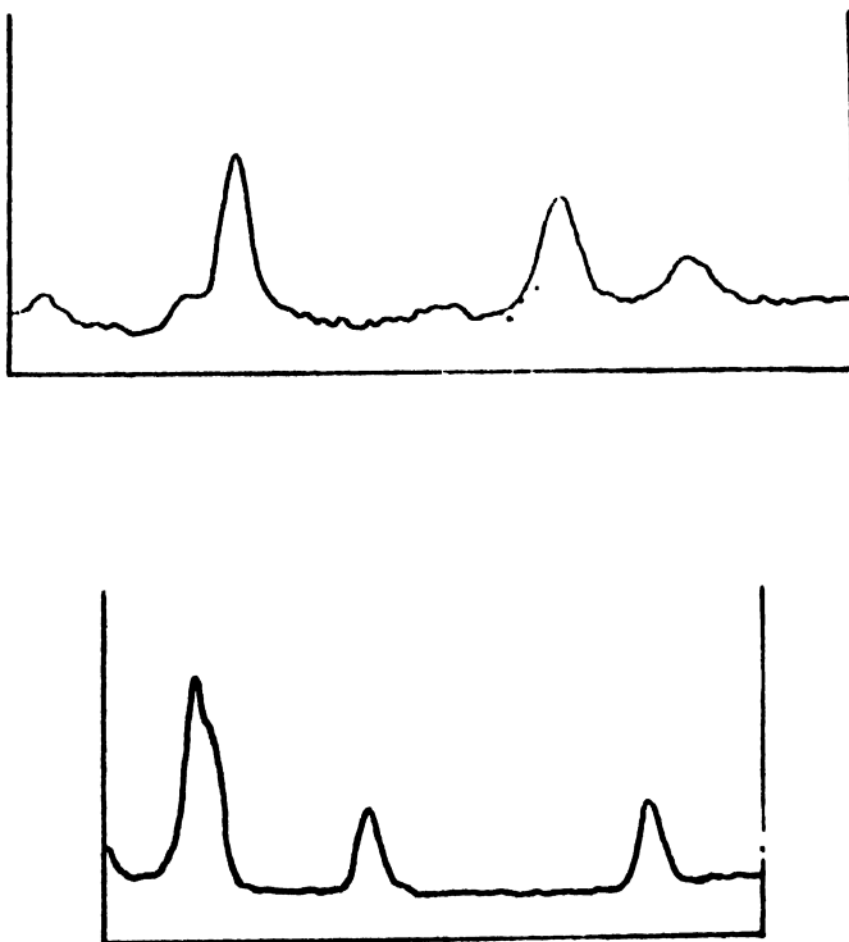


Fig.23 : Comparison of the C-terminal analysis of papain (upper) and detergent forms (lower). Both the forms show the same pattern of release in sequence of the C-terminal amino acids, serine, glycine and alanine, upon treatment with carboxypeptidase A.

of the two forms may be similar in isoelectric focusing and this procedure may not reveal the existence of an anchor peptide. It should, however, be pointed out that they are sensitive enough to pick up even microheterogeneity and the results rule out the presence of any microheterogeneity [226].

Chemical studies of the two forms: Assuming that the sensitivity of the physical method was inadequate for the detection of a rather inconspicuous (hidden or buried) hydrophobic peptide in a large sized molecule ( $M_r = 760,000$ ), we attempted to probe the primary structure of both the forms, which must have undergone a change in the case of protease solubilised form owing to the proteolytic action of papain during solubilisation.

The amino acid composition of both forms were the same within the limits of experimental error (Table 3). For such a large protein the presence of an extra length of peptide of about 25-30 amino acids, normally seen in anchor peptides [4], will not alter the amino acid composition confidently detectable within the error limits of the analysis. The identical tryptic peptide maps (Fig.22), the same partial C-terminal sequence (-Ala-Gly-Ser, Fig.23) and the same N-terminal amino acid (Tyr) for both the forms unequivocally establish the complete identity of both the forms and rules

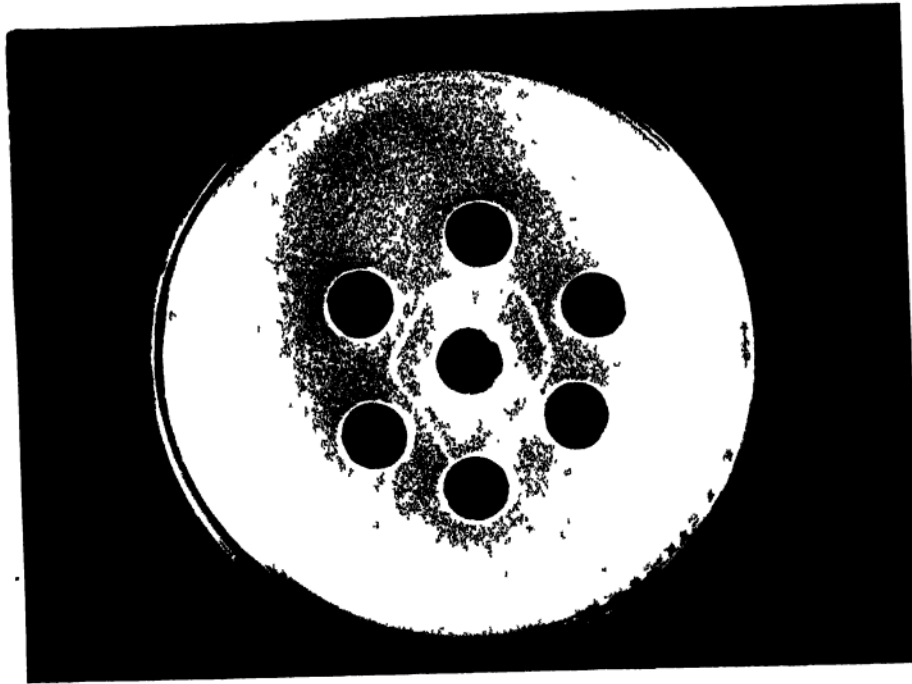


Fig.24 : Ouchterlony double diffusion technique. The pattern of precipitin lines around the antibody well indicate immunological identity. The samples were Triton form, aged-Triton form and papain form of the enzyme. The denatured enzyme (guanidinium chloride treated) did not show immuno precipitation.

out the presence of any anchor peptide. It is unlikely that the identity of both N- and C-terminals is fortuitous.

#### Immunological behaviour of the two forms

The difference in the immunological behaviour between two close related proteins arises because of extra antigenic determinants in one of them [227] or some of the antigenic determinants are different. Immunodiffusion offers a very sensitive and simple method to identify such small differences. The identity between papain and Triton (both fresh and aged) forms is apparent from the immunodiffusion pattern (Fig.24). Since the antigenic determinants are conformational, it would mean that the two forms are identical even at the conformational level.

#### Kinetic behaviour of the two forms

Kinetically both the forms behaved identically with respect to pH optimum (7.5), denaturation by SDS, urea and guanidinium chloride (Fig.19) and inactivation by various alcohols (Table 7 ).

Heat stability: The detergent form, however, was found to be more labile than the protease form to heat inactivation.

The Triton form lost all of its activity within 15 minutes at 60°C whereas the papain form lost only 50% of its activity. This is the only property in which a difference between the two forms was noted. It is possible that Triton is still bound in stoichiometric levels not easily detectable or removable at or near the active site, and aggravates the denaturation process in the presence of heat.

#### Studies on papain solubilisation

The identical nature of both detergent and protease forms of glucoamylase-maltase complex in the case of rat [55] and of rabbit raises serious doubts about the association of the enzyme to the membrane and about the mode of linkage of the protein to the membrane. Linkage by an anchor peptide which is cleaved off by the protease action is well-established at least in the case of sucrase-isomaltase [73], but there could be species differences and other modes of linkage. Papain is undoubtedly the most effective among the proteases tried in releasing the intestinal hydrolases from the brush border membrane. But, what is assumed rather tacitly is that the release of the intestinal hydrolases is due only to the proteolytic activity of papain completely overlooking the possibility of an esterase activity well-known to be associated with papain. After all, the intestinal hydrolases

are glycoproteins and some of them, if not all, might be associated with the membrane by an ester linkage between a glycon moiety of the hydrolase and the functional groups on the membrane. If the enzyme is released by an activity other than proteolytic activity, it would explain the identity of both the forms as far as the peptide backbone is concerned. Alternatively, after the release of the protein from the membrane by detergent the anchor peptide is cleaved off by a specific cellular protease, with a specificity <sup>the</sup> same as that of papain.

Proteolytic activity vs solubilisation activity - experimental details: The degree of solubilisation and the proteolytic activity have been concurrently monitored under a variety of conditions with a view to finding out whether there is a causal or direct relationship between the two processes. Proteolytic activity was measured with Azocoll as a general test substrate for protease and the degree of solubilisation was measured by the release of both glucoamylase-maltase and sucrase-isomaltase complexes. The release of the enzymes from the mucosal pellet fraction was measured under the following conditions: a) using heat inactivated papain b) using papain in the absence of added thiol compounds c) using papain in the absence of added thiol compounds and protease activity further inhibited by

iodoacetamide or p-hydroxy-mercuri-benzoate (10  $\mu$ M to 10 mM) and d) using papain activated by various concentrations of  $\beta$ -mercapto-ethanol (1  $\mu$ M to 10 mM). In all the above experiments the pellet protein to papain ratio was 50:1 (w/w) and incubation was at 37°C for 90 min (except in the experiments with  $\beta$ -mercapto-ethanol, when the incubation time was reduced to 10 minutes). During our experiments it was found that the solubilisation was completely arrested at high concentrations (10 mM, final) of p-hydroxy-mercuri-benzoate or iodoacetamide and this property was used with advantage in the above experiments. It should be mentioned that these are preliminary data and would require a more detailed study to come to definitive conclusions regarding the mode of attachment of glucoamylase-maltase to the brush border membrane, but are of sufficient interest as a starting point.

Solubilisation ability of papain not activated by thiol compound: Denatured papain was not able to release the enzyme at all and hence it was clear that an enzymatic process is involved in the solubilisation. In the absence of added thiols, papain exhibiting only 10% of the proteolytic activity compared to the fully activated papain, <sup>1</sup> <sup>1</sup> was effective in bringing about complete solubilisation of the enzyme complex. Assuming that this solubilisation was due to the presence of



## Proteolytic and solubilisation activities of papain

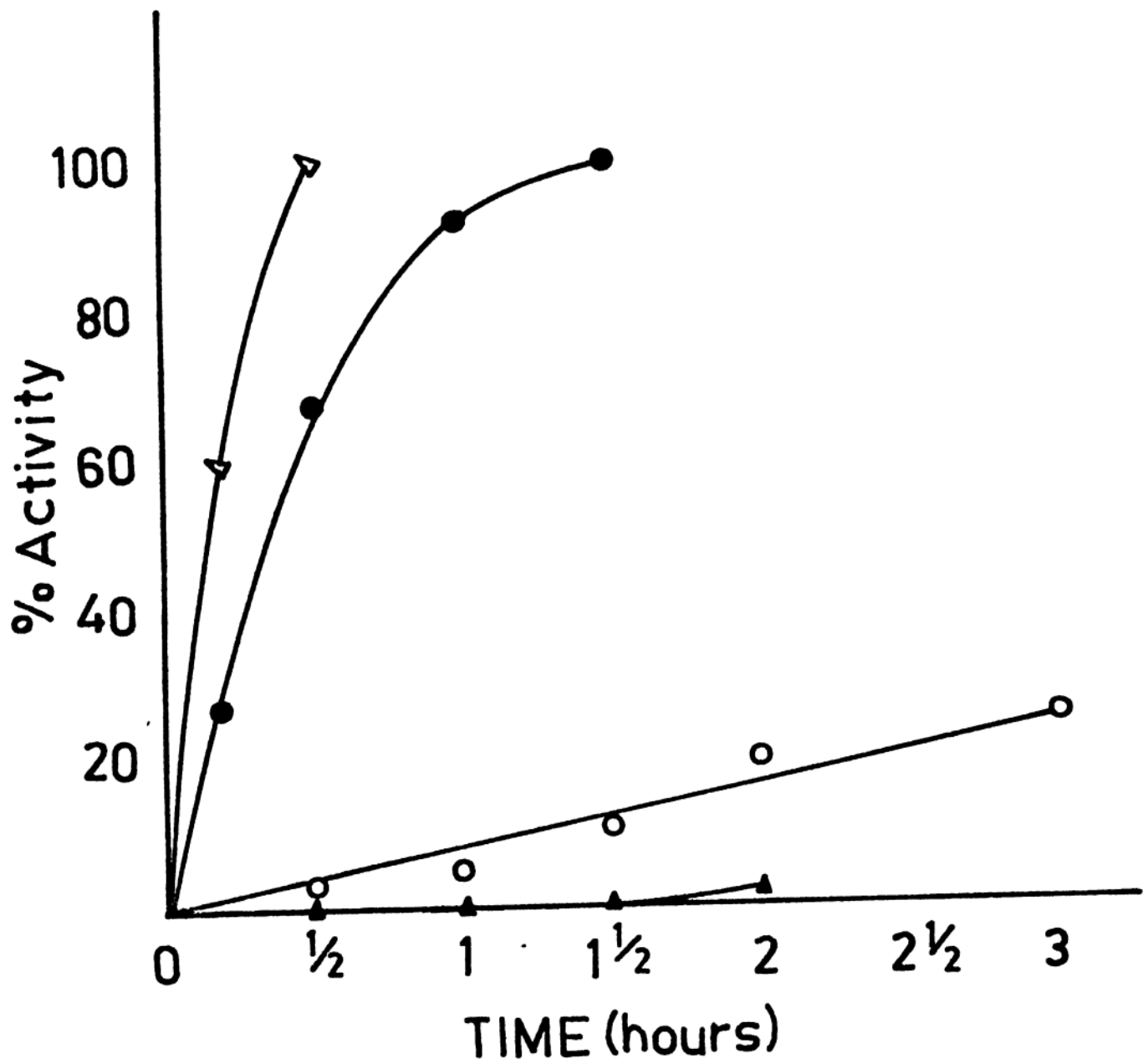


Fig.25 : Is protease activity of papain involved in the solubilisation process?; protease (○—○) and solubilisation (●—●) activities of papain not activated by  $\beta$ -mercapto-ethanol; protease (▲—▲) and solubilisation (●—●) activities of papain in the presence of 100  $\mu$ M p-hydroxy-mercury-benzoate; and (△—△) solubilisation in the presence of 1  $\mu$ M  $\beta$ -mercapto-ethanol. Complete solubilisation of the enzyme was effected using papain even in the absence of thiol compounds and in the presence of 100  $\mu$ M of p-hydroxy-merciribenzoate.

papain not activated by added thiol compounds. Even at very low concentrations (1  $\mu$ M) of  $\beta$ -mercapto ethanol, the proteolytic activity of papain was enhanced several fold, while the degree of solubilisation remained unaffected. At higher levels (1 mM and above) when the proteolytic activity of papain had already plateaued off, the degree of solubilisation was enhanced only 2 fold. From these experiments with thiol compounds and from the earlier experiments with sulphydryl reagents, it appears that there are two types of enzyme activities in papain vis-a-vis the degree of solubilisation. The protease activity is very sensitive to both activation and inhibition under conditions which do not severely affect the degree of solubilisation. The enzyme activity associated with solubilisation is also apparently involving -SH groups of papain, but it is insensitive to thiols and sulphydryl reagents at low concentrations, and is possibly an esterase type of activity long known to be inherent in papain.

Papain solubilisation in presence of azocollagen:

Supportive evidence for the above line of thinking was obtained by including azocollagen as a competitive substrate for the proteolytic activity in the solubilisation medium. The pellet protein-papain ratio was raised to 200:1 (w/w) so that only 50% solubilisation activity was exhibited by papain not activated by the addition of thiol compounds. If protease activity

of papain was involved in the mechanism of solubilisation one would expect an inhibition in the degree of solubilisation with azocollagen as a competitor for the membrane bound protein. Since solubilisation was unaffected under these conditions, it once again points to another enzyme activity in papain which enables solubilisation.

In all the above experiments, sucrase-isomaltase activity was also monitored and it is of interest to note that it closely followed the behaviour of glucoamylase-maltase complex suggestive of a common mechanism of papain solubilisation for both the complexes.

Concluding remarks on mode of attachment of the enzyme complex: Though all the foregoing evidences point to the possible involvement of an activity other than proteolytic activity during the solubilisation of the enzyme, they do not establish the actual nature of the activity or rule out the possibility of a very specific peptide bond being cleaved, since the sucrase-isomaltase complex in which an anchor peptide is presumably cleaved off by virtue of the proteolytic activity of papain, follows closely the release of glucoamylase-maltase complex in all the experiments mentioned above. Lack of competition by azocollagen, and higher concentrations of thiol reagents and thiol compounds needed respectively to

inhibit and activate the solubilisation process compared to the normal proteolytic activity (for example hydrolysis of azocollagen), would strongly suggest that the susceptible peptide bonds of the intestinal hydrolases have a very high affinity and specificity to papain. Such a peptide can serve as a 'signal' for a protease (like papain) involved in the turnover of these hydrolases. Though not commonly used, elastase, a pancreatic protease has been known to be as effective as papain in releasing the membrane bound hydrolases of intestine and has, therefore, been implicated in the rapid turnover of these hydrolases. A very recent observation by Lee and Forstner [77], was that the detergent form of rat intestinal glucoamylase-maltase complex could be isolated with a subunit susceptible to proteolytic activity, if the solubilisation and isolation were performed in media containing a proteolytic inhibitor. This would mean that subsequent to detergent solubilisation, the susceptible peptide is lost and the detergent form behaves identically as the protease form. Such a possibility also exists in the case of rabbit enzyme, especially when viewed from the point of susceptibility of the bond being broken, as revealed by the solubilisation experiments.

## STUDIES ON THE ENZYME ACTIVITY - A NEW MECHANISM OF ACTION AND DESIGN OF THE ACTIVE SITE

Glycosidic enzymes of intestinal brush border in general possess more than one activity and like other multi-enzyme complexes they are large proteins ( $M_r > 200,000$ ). They are not easily dissociated and are often made up of tightly associated subunits which are the actual sites of individual activity. Thus, sucrase-isomaltase of rabbit intestine has two large subunits ( $M_r = 100,000$ ) both exhibiting maltase activity but in addition one exhibiting sucrase activity and the other isomaltase activity. Lactase-phlorizin hydrolase complex is made up of two subunits one exhibiting lactase and the other phlorizin hydrolase activity. There is evidence for a third site for acid-phlorizin hydrolase activity which is activated by 4-carbon dicarboxylic acids with polar group, around the central carbons. The possible physiological role is ascribed to its yet another activity namely ceramidase which can be associated with either lactase activity as in rat and rabbit or phlorizin hydrolase as in monkey. The glucoamylase-maltase complex has glucoamylase, maltase and isomaltase activities. Owing to the complications in the understanding of its subunit structure and assembly, it is difficult to form a satisfactory kinetic model. Attempt to separate the molecule into subunits with any one of the

activities have proved to be unsuccessful and apparently they are tightly associated.

### Mechanism of action of intestinal glucoamylase - a hypothesis

On the analogy of the mechanism of action of fungal glucoamylase it has been assumed that the intestinal glucoamylase is an exo-enzyme and that it cleaves off glucose residues from the non-reducing end of the individual polymer chains of starch or glycogen. The work of Dahlqvist and Thomson [115] who found glucose as the major end product supported such a mechanism for the intestinal glucoamylase. However, there are a number of results in the literature which would cast doubt on such a mechanism and call for a new line of thinking and this section is an exercise in that direction. The results in the literature and some of our recent findings are given under appropriate headings. A new hypothesis for the mechanism of action for glucoamylase along with a possible design of the active site are given.

Action pattern of fungal glucoamylase and intestinal glucoamylase: If the mechanism of action of any two enzymes is the same, it is expected that both should show similar preference for various substrates. If fungal and intestinal glucoamylases share the same mechanism of action, then their preference for maltose and other oligosaccharides of various

degrees of polymerisation (DP) as substrates should be similar. While maltose is a poor substrate for fungal glucoamylase, it is one of the most preferred substrates for intestinal glucoamylase. Malto-triose, as well as higher oligosaccharides are good substrates for fungal glucoamylase. Maltotriose is a poor substrate for the intestinal enzyme compared to either maltose or higher oligosaccharides. There is a tremendous decrease in  $K_m$  and increase in  $V_{max}$  for maltotriose compared to maltose and this is a characteristic feature of the fungal glucoamylase action [118]. This characteristic feature is conspicuously missing in the action pattern of intestinal glucoamylase. On the other hand, there is an increase in  $K_m$  and a decrease in  $V_{max}$  for maltotriose compared to maltose and higher oligosaccharides (DP 4-6), in the case of intestinal glucoamylase [56,115]. This difference in the action pattern of the two enzymes towards maltose and various oligosaccharides clearly indicates that the two mechanisms deviate considerably.

Structural requirements of a substrate : From the detailed kinetic studies on substrate specificity, it is clear that the basic structural requirements for a disaccharide substrate are an unsubstituted glucose as glycon and an  $\alpha$ -linkage -which can be (1 $\rightarrow$ 4), (1 $\rightarrow$ 3), (1 $\rightarrow$ 2) or (1 $\rightarrow$ 6) in that order of preference [56]- between the glycon and aglycon

The aglycon part can be either a glucose moiety or a fructose moiety or even a phenyl-ring with or without substitutions [56,115]. Though there is a lack of specificity over aglycon part and the linkage (as long as it is  $\alpha$ ) the rate at which these substrates are acted upon is determined by the aglycon and the susceptibility of the linkage to hydrolysis. Non-reducing disacchases like sucrose and trehalose whose anomeric hydroxyl is involved in the glycosidic linkage are inhibitors inspite of their having an unsubstituted glucose as glycon and an  $\alpha$ -linkage between the glycon and aglycon moieties. If the anomeric hydroxyl of a disaccharide is involved in a glycosidic linkage with a neighbouring moiety, such as maltose is in maltotriose, then it appears to be a poor substrate [56,115]. However, in the case of panose, a triose, in which the additional glucose residue is attached to C<sub>6</sub>-OH instead of the anomeric hydroxyl of maltose, the rate at which it is hydrolysed is better than that of maltotriose [56]. This apparent importance of anomeric hydroxyl was also mentioned by Sorensen et al [56] in their work on pig intestinal glucoamylase-maltase complex. On the basis of the above findings, starch should be a poor substrate, (it is a substituted maltose, at the anomeric hydroxyl) but it is a preferred substrate hydrolysed at a rate comparable to that of maltose. This was one of the major reasons which prompted us to consider alternative



mechanisms such as cleavage of maltose from the non-reducing ends thus releasing the anomeric hydroxyl.

Appearance of maltose in the reaction - mechanistic implications: Dahlqvist and Thomson [112] while investigating the action of intestinal glucoamylase on starch, found that the enzyme hydrolysed starch by an exo-action, and produced only glucose upto first 40 min, and later along with glucose a small amount of maltose also appeared. Though the reduction power of the reaction mixture up to 10 minutes could be attributed solely to the glucose released, these two did not coincide, clearly indicating the presence or release of additional reducing compounds apart from glucose. The appearance of maltose (or additional reducing substances) was not considered seriously and they suggested that intestinal glucoamylase action corresponds to that of fungal glucoamylase.

The following experiments have been carried out with homogeneous rabbit intestinal glucoamylase-maltase complex: the disappearance of blue colour of starch-iodide complex as a test to distinguish an exo-action from an endo-action; correlation between the reduction power of the products of starch hydrolysis -measured by dinitro salicylate procedure [226] and expressed as equivalents of glucose- and that of the released glucose measured specifically by T.G.O. procedure [227], separation and identification of the reaction products by paper chromatography.

## BLUE VALUE DISAPPEARANCE OF STARCH HYDROLYSIS

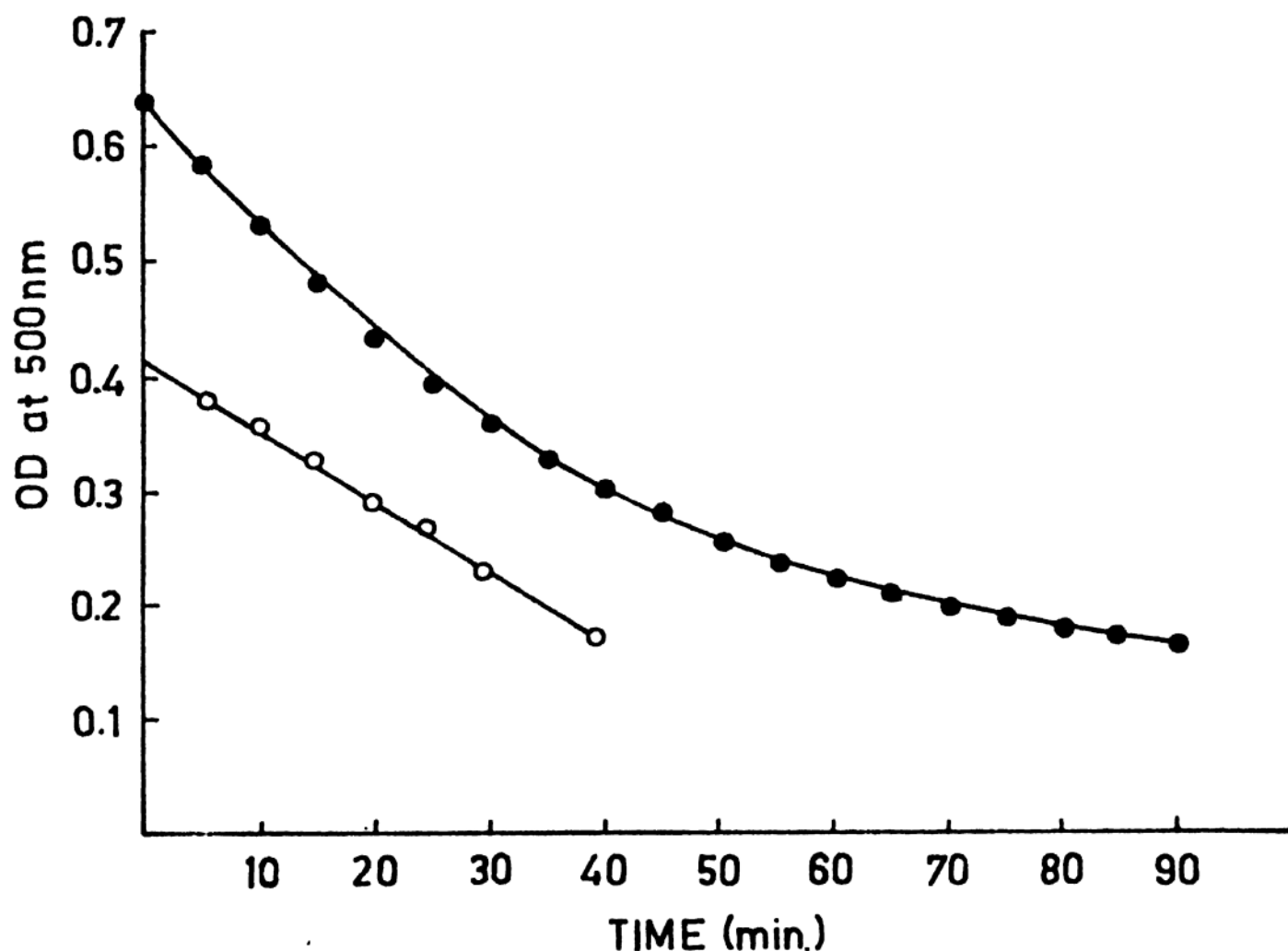


Fig.26 : The disappearance of blue colour of starch-iodide complex by the action of the enzyme. To about 500  $\mu\text{g/ml}$  of starch in 0.01M potassium phosphate buffer pH 7.0, enzyme (10  $\mu\text{g/ml}$ ) and 20  $\mu\text{l}$  appropriately diluted iodine reagent (0.4% w/v w.r.t. iodine) were added. The disappearance of blue colour was recorded at 500 nm using a spectrophotometer. In another experiment, (○—○) the iodine reagent was added after incubating starch with the enzyme for a stipulated time. The enzyme employed was at a concentration of 5  $\mu\text{g/ml}$ , the other conditions remaining the same. The 50% rate of hydrolysis of starch-iodide complex compared to starch is apparent.

Velocity of starch hydrolysis by DNS(o—o) and  
TGO(●—●) procedures

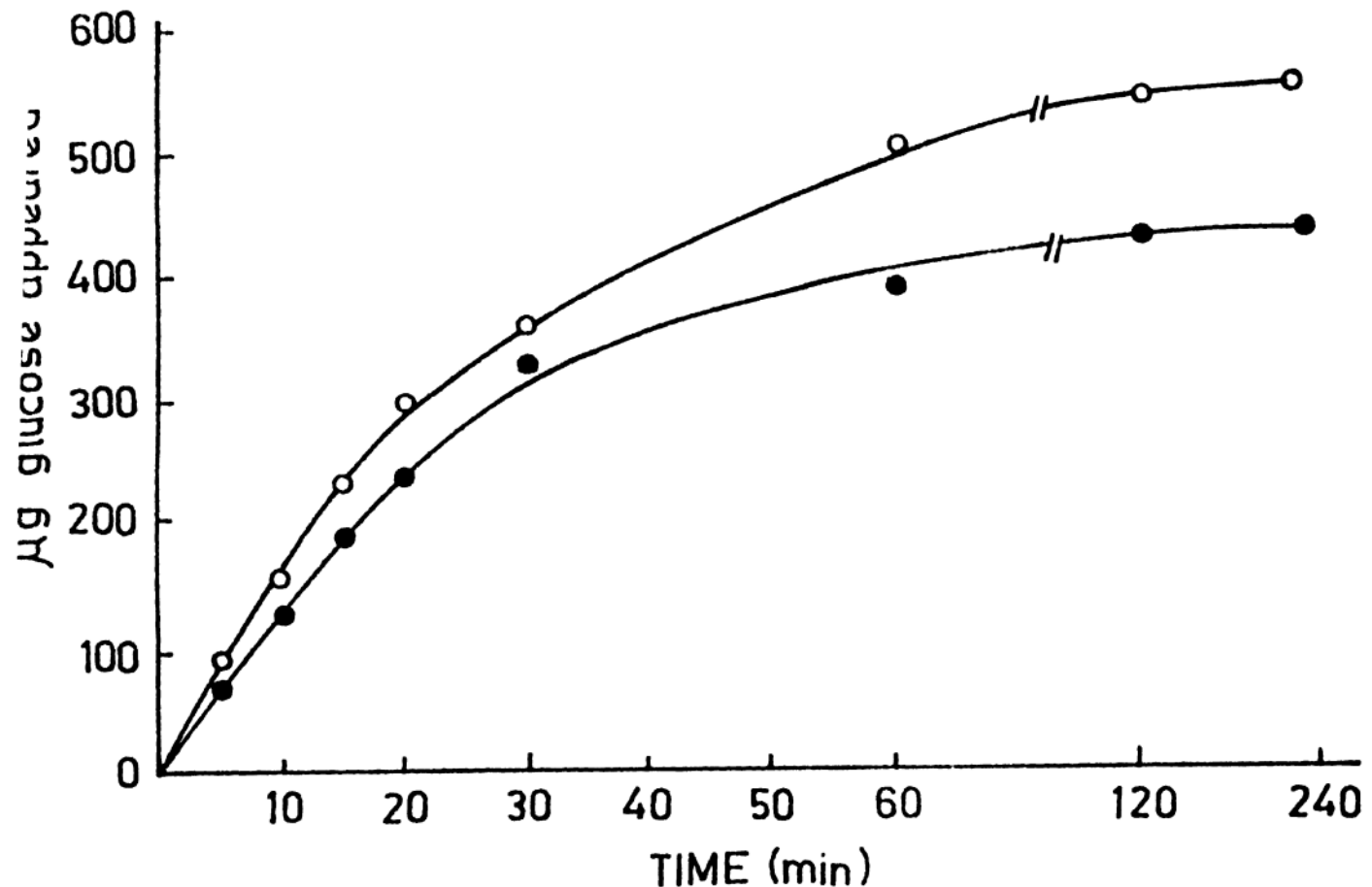


Fig.27 : The correlation between the amount of glucose released as measured by T.G.O. method (●—●) and reduction value measured by DNS method (o—o) (expressed as equivalent glucose released/starch hydrolysed) at various time intervals. Assay condition: starch (500  $\mu\text{g/ml}$ ) enzyme (4  $\mu\text{g/ml}$ ), buffer potassium phosphate buffer, 0.01M and pH 7.0, temperature 37°C. The lack of correlation from the beginning of the incubation is noteworthy.

Michaelis-Menten curve for starch hydrolysis  
by DNS (●—●) & TGO (○—○) procedures

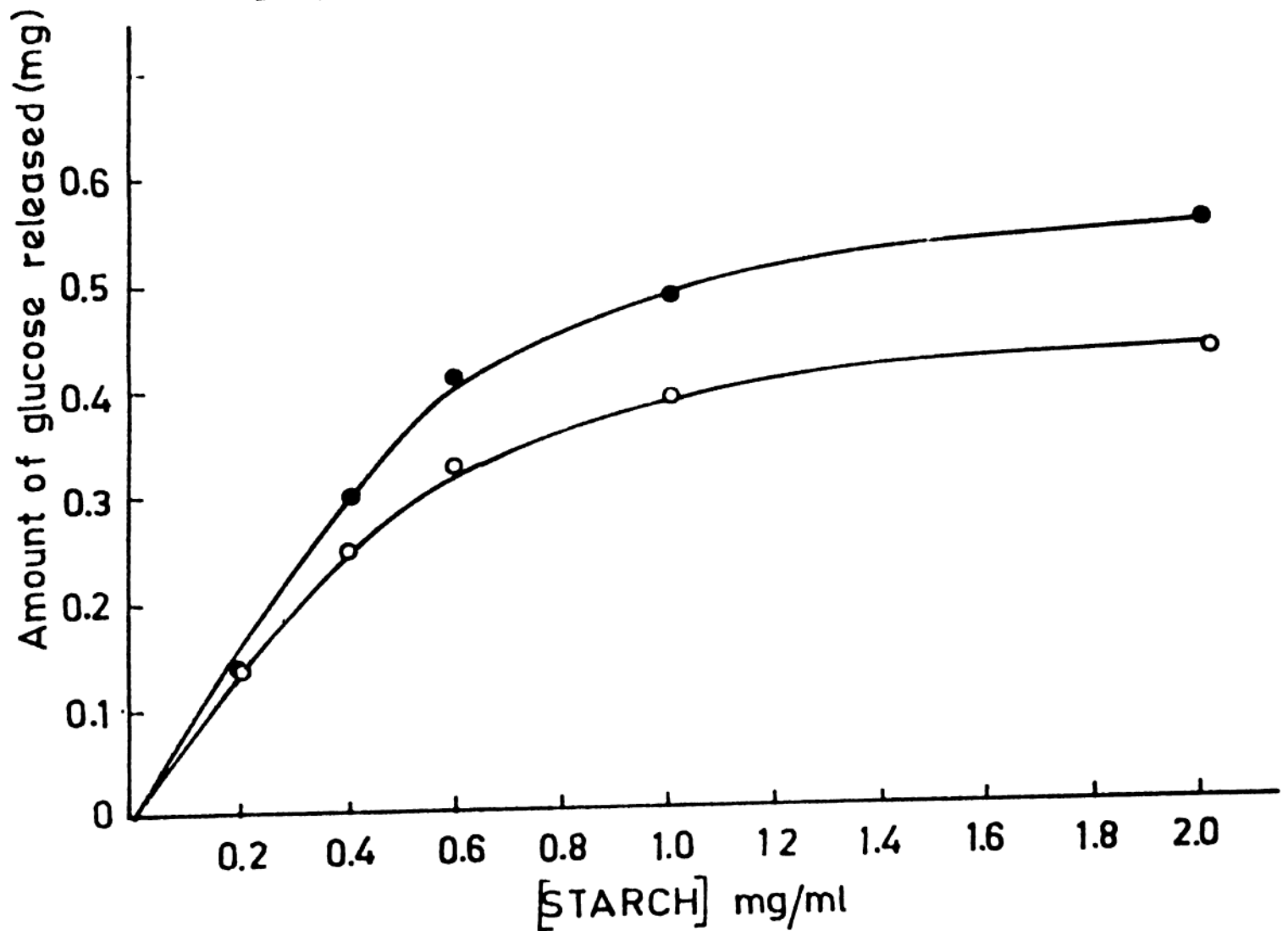


Fig.28 : The lack of correlation between the amount of glucose released as measured by T.G.O. method (○—○) and as measured by DNS method (●—●) at various concentrations of starch indicates the presence of additional reducing components in the reaction mixture. Assay conditions: Various concentrations of starch (as indicated) in 0.01M potassium phosph . buffer pH 7.0, enzyme concentration (5  $\mu$ g/ml) and incubation time, 1/2 hour.

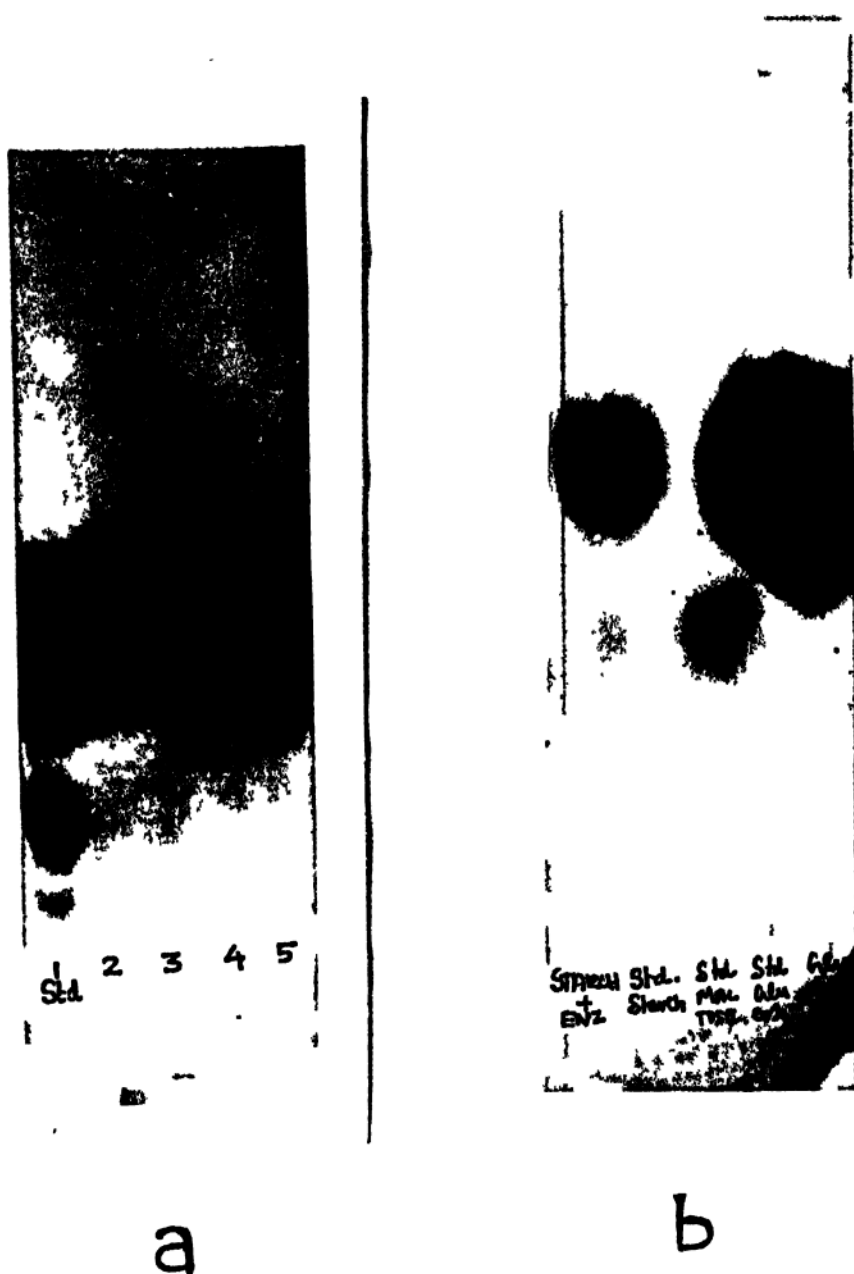


Fig.29 : (a) The paper chromatogram of the reaction mixture of starch hydrolysis by the enzyme, developed ascendingly using n-butanol-acetic acid-water (4:1:2) system. 2,3,4 and 5 correspond to respectively 10 min., 20 min., 30 min., 40 min., of incubation time. Assay condition: Starch (1 mg/ml) in 0.01M potassium phosphate buffer pH 7.0, enzyme 10 g/ml. At the end of the stipulated time aliquotes (100  $\mu$ l) of the reaction mixture were withdrawn; the reaction was arrested immediately by boiling; concentrated under vacuum and applied on to the paper. The faint spot of maltose is seen even within 10 min.

(b) Incubation of the enzyme did not produce maltose by trans-glycosylation or by synthesis. This indicates that maltose produce hydrolysis of starch by some other mechanism.

The disappearance of blue colour which was gradual and slow suggested an exo-type of action (Fig. 26). Moreover, at no stage during the hydrolysis of starch there was any indication of small limit dextrins like  $\alpha$ -limit dextrins obtained by the action of  $\alpha$ -amylase, an endo-enzyme. This rules out the presence of an endo-action of any of the activities in the enzyme, inherent or as a contaminant (as has been shown in apparently homogeneous preparations of fungal glucoamylase) [228]. The release of glucose from starch is thus a consequence of only an exo-action. Even at early stages of incubation there was lack of correlation between the reducing equivalents and glucose released (Figs. 27, 28). This indicated the presence of reducing compounds other than glucose. The chromatogram revealed a small amount of maltose as the only other reducing component within 10 min. after the start of the reaction [Fig. 29]. Glucose was the major product of starch hydrolysis. In a separate experiment it was shown that maltose is not formed by transglycosylation reaction, by checking the chromatograms of the reaction mixture containing the enzyme and an excess of glucose, 0.1 M (Fig. 29b).

The observations on rabbit intestinal glucoamylase are remarkably similar to those on rat intestinal glucoamylase [112], suggestive of a common mechanism of action of intestinal glucoamylases. It is not possible to account for the presence of maltose or other reducing substances in the reaction mixture of starch hydrolysis, on the basis of the mechanism of action of fungal glucoamylase. It has been clearly demons-

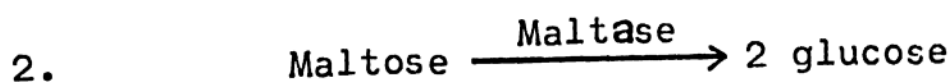
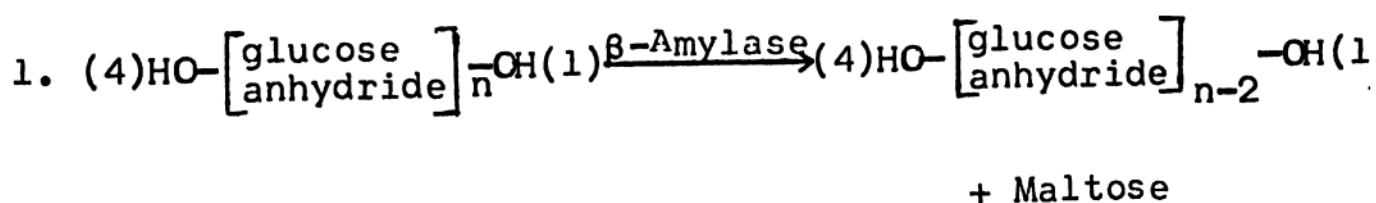
trated that fungal glucoamylase releases sequentially only glucose residues from the non-reducing ends of starch, by virtue of its  $\alpha(1-4)$  and  $\alpha(1-6)$  hydrolytic activities.

Maltase as an integral part of glucoamylase: In the case of the intestinal enzyme, apart from glucoamylase activity a very high maltase activity (compared to the feeble activity in fungal glycoamylase) has been noted for a long time. This maltase activity also accounts for a considerable proportion of the total intestinal maltase activity. The two activities have not been separated physically nor a differential inactivation or inhibition demonstrated, as in the case of sucrase-isomaltase complex. Kinetic evidence suggested that the maltase activity is an integral part of the glucoamylase site [115]. The nature and significance of this arrangement and its mechanistic implications during polymer hydrolysis have not been analysed carefully. From a teleological view-point, the presence of maltase activity as an integral part of the glucoamylase site points to a physiological function.

Possible mechanisms of action of intestinal glucoamylases: Any mechanism proposed should explain and take into account the following facts: the exo-action of the enzyme, the presence of other reducing substances (especially maltose) apart from glucose, the major product, the observed action pattern of the enzyme towards oligosaccharides of

various degrees of polymerisation, the inhibition pattern of various compounds and the nature and significance of the inherent presence of various activities implicated in the polymer hydrolysis.

We propose a possible mechanism of action of intestinal glucoamylase-maltase complex based on the arguments and experimental evidence provided above. The foremost proposal in this mechanism is a  $\beta$ -amylase type of action (referred to as  $\beta$ -amylase hereafter) which has been envisaged to precede the action by maltase, in the removal of glucose from the non-reducing ends of starch or any other polymer or oligomeric substrates. The polymer or oligomer hydrolysis by intestinal glucoamylase then becomes a two step process as given below



There are certain characteristic features of a two step mechanism as opposed to a single step mechanism. The rate of the overall reaction is determined by the rate of the slowest step. This in turn is dependent upon the affinity and catalytic efficiency of a particular step towards a



given substrate. The extent of inhibition and rate of inactivation are dependent on the step which is most affected. Accumulation of maltose a product of the postulated  $\beta$ -amylase activity can be expected by blocking maltase activity, which is the second step in the mechanism, unless, of course,  $\beta$ -amylase is not vulnerable to a feed-back inhibition by maltose. This phenomenon is known in multi-enzyme systems.

Action and inhibition patterns - Explanation based on the proposed mechanism: For maltotriose and possibly for maltotetrose, it appears that  $\beta$ -amylase is a rate limiting step because they are hydrolysed at rates smaller than that of maltose hydrolysis. For higher oligomers and polymers the rate limiting step is probably the maltase activity because their rates of hydrolysis approach that of maltose. When the hydrolysis of starch was performed in the presence of inhibitors like Tris, sucrose and glucono- $\delta$ -lactone, it was noted that the reduction power of the reaction mixture and the reduction in blue colour could be accounted for solely by the released glucose. In the presence of 6 mM maltose starch hydrolysis was completely inhibited as evidenced by the persistence of blue colour. During heat inactivation studies, the discrepancy between the reduction power of the reaction and the amount of released glucose, gradually ceased to exist as the inactivation progressed, suggestive of slightl

greater inactivation of  $\beta$ -amylase site by heat. Similar results were obtained with inhibitors like Tris and trehalose when  $\beta$ -amylase activity was affected more than the maltase activity ( $K_i$  values of these inhibitors are considerably smaller for starch hydrolysis compared to maltose hydrolysis [15]).

This mechanism can explain and account for the release of glucose by an exo-action from polymer substrates like starch on the analogy of plant  $\beta$ -amylase. There will be a small population of maltose at any time in the active site which survives maltase activity and this is possibly what is detected on the chromatograms. Like in the case of plant  $\beta$ -amylase maltose is an inhibitor of starch hydrolysis, maltotriose will be a poor substrate and oligosaccharides with intermediary DP(4-8) are the preferred substrates. This fits in excellently with the observed action pattern of the intestinal enzyme. Owing to the release of maltose prior to maltase action, the hydrolysis of starch and other polymer substrates will be at rates comparable to maltose hydrolysis. The mechanism of action accounts satisfactorily for inhibition pattern of various compounds. It also offers a possible explanation for the necessity of a tight association of maltase and glucoamylase activities. Maltase site is an integral part of intestinal glucoamylase as shown by kinetic studies

and this fits well with the proposed mechanism for which the proximity of the enzyme activities is a prerequisite.

Iodine .inactivation studies - evidence for two species of maltases and glucoamylases: During our studies, it was observed that the enzyme exhibited only 50% of its starch hydrolytic activity towards starch-iodide complex. Suspecting inactivation by iodine reagent the enzyme was pre-incubated with different concentrations of iodine reagent before assaying for glucoamylase, maltase and iso-maltase activities. It was found that all the activities are sensitive to iodine and are lost completely at a concentration of 0.3 mM (w.r.t. to iodine) of iodine reagent. When iodine reagent was added subsequent to the addition of respective substrates, 50% activities of glucoamylase and maltase were found to be protected against inactivation by the reagent. This apparently indicated two 'species' of glucoamylase and of maltase activities. In each case one activity is iodine inactivated substrate-protected and the other is iodine-inactivated-substrate unprotected.

Heat inactivation studies - evidence for heat labile and heat stable 'species' of activities: The enzyme was pre-incubated at 60°C for various intervals of time and the glucoamylase, maltase and isomaltase activities were assayed.

### Heat inactivation pattern of various activities

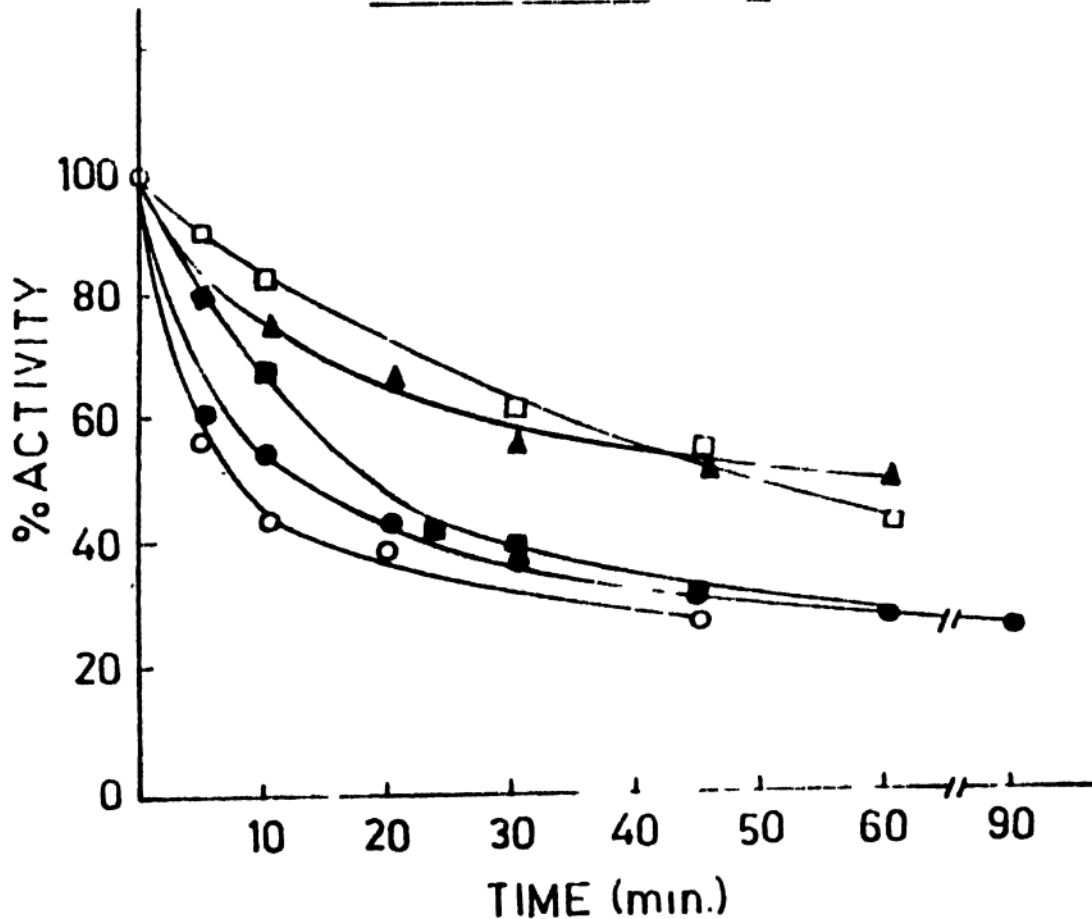


Fig.30 : The inactivation of the enzyme activities by heat (60°C). About half of the maltase (■—■) and glucoamylase (●—●) activities are lost within 15 min, and the remaining half is relatively heat stable, suggestive of two 'species' of activities for both glucoamylase and maltase. Estimation of the activity of iodine inactivated-substrate protected maltase (▲—▲) indicates that it is the stabler of the two maltase 'species'. Its loss of activity parallels that of isomaltase (□—□) suggestive of a close association between them. Isomaltase is relatively heat stable and it is a single species of activity. Glucoamylase activity measured by DNS (○—○) also parallels the profile of glucoamylase activity measured by T.G.O. (●—●).

The differential rates of inactivation indicated the presence of two species of both glucoamylase and maltase activities. Isomaltase activity was associated with the latter species of maltase (Fig.30).

Isomaltase and associated activity: From both heat and iodine inactivation studies it was found that there is only one 'species' of isomaltase activity. The loss of iodine-sensitive-substrate-protected-maltase activity during heat inactivation followed closely that of isomaltase and this suggested a close association of these two activities.

Inactivation studies - a possible support to the proposed mechanism: The results on the inactivation of the enzyme by heat and more especially iodine lend considerable support to the proposed mechanism of action. Both the studies indicated the apparent presence of two 'species' of glucoamylase and of two maltase activities. One is heat sensitive and iodine-inactivated-substrate unprotected while the other is relatively heat resistant and iodine sensitive but substrate protected. With the classical mechanism, two polymer binding sites have to be invoked, one for each 'species' of glucoamylase activity. Such a design of the active site involved in polymer hydrolysis will make it unwieldy and it may introduce other steric complications. Also, it is difficult

to conceive of an identical inhibition pattern by iodine of the two different and independent activities namely maltase and glucoamylase. The mechanism proposed in this thesis offers an elegant and perhaps more reasonable explanation for the apparent presence of two 'species' of glucoamylase activity, but with only one polymer binding site. Our mechanism invokes a combined action of  $\beta$ -amylase (primary polymer binding site) and of maltase mechanistically and sterically linked. The apparent presence of two species of glucoamylase then is a direct consequence of the actual existence of two species of maltase.

This would mean that the  $\beta$ -amylase need not be inhibited by iodine at all. The type of differential inactivation by iodine can be correlated with the earlier findings of Sivakami and Radhakrishnan [115]. They showed that a group with a  $pK_a$  of 5.7 was essential for the hydrolysis of both maltase and starch and that an additional group with a  $pK_a$  of 4.3 is responsible only for starch binding. Our hypothesis is that starch hydrolysis after the initial binding and  $\beta$ -amylase action, takes place with the involvement of the site where maltose is hydrolysed. We can assume that the group with a  $pK_a$  of 5.7 (presumably histidine, which has been implicated in the active sites of  $\alpha$ -glucosidases) is associated with the maltase site. Inactivation of this

group would affect both starch and maltose hydrolysis. On the other hand, if we assume that the  $\beta$ -amylase has the group with  $pK_a$  of 4.3 and that it is the only polymer binding site, inactivation of this group would affect only starch binding and starch hydrolysis. If iodine reagent reacts specifically with the group having  $pK_a$  of 5.7 it would affect only maltase but not  $\beta$ -amylase. Even if maltase is affected, starch hydrolysis cannot proceed because of the two step (linked) mechanism proposed. The fact that there is 50% of glucoamylase activity protected against iodine inactions would mean that starch binding offers protection to one of the maltases. This iodine sensitive-substrate protected-maltase seems to be associated with the isomaltase, as evidenced by their similar heat inactivation profile. Isomaltose (the substrate for isomaltase) inhibits only starch hydrolysis but not that of maltose. This specificity seen in its inhibition behaviour is an indication of a specific interaction between isomaltose binding and starch binding or hydrolysis. Since maltase is not inhibited, the inhibition effect of isomaltase can be attributed to the inhibition of binding of starch to  $\beta$ -amylase or its subsequent hydrolysis to maltose. In any case, it is evident that starch binding can influence isomaltase and vice versa. Thus not only is there an evidence for the observed protection of isomaltase by starch binding, but it can also be expected to be

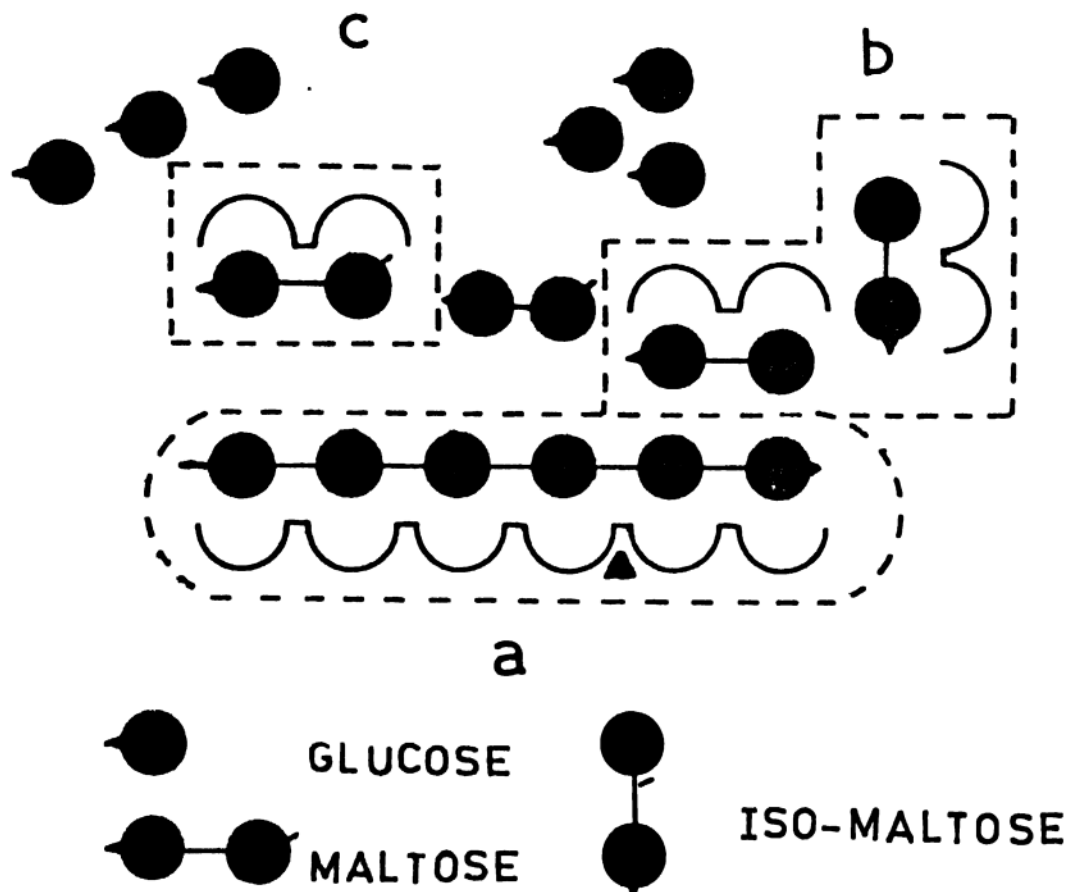


Fig.31 : The proposed design of the active site. The entities a, b and c respectively represent  $\beta$ -amylase (polymer binding site), iso-maltase-maltase unit ( $\alpha$ - &  $\beta$ -limit dextrin binding site) and maltase (which is iodine inactivated and not protected by substrate against inactivation). It appears that (see text for details) the isomaltase and the associated maltase (iodine sensitive-substrate protected) have a more intimate connection with the  $\beta$ -amylase and hence depicted as being close to the 'hydrolysing centre' (indicated by the triangle). Mode of action on a polymer has also been indicated. See text for further details.



since complete hydrolysis of starch to glucose requires isomaltase activity.

### Design of the active site of the enzyme complex

Based on the results of inactivation studies and the proposed mechanism of action of the enzyme, a possible design of the enzyme active site has been conceived. According to this design illustrated in Fig.31, it consists of three entities designated as a)  $\beta$ -amylase site b) isomaltase-maltase site and c) a maltase site, explained in greater detail below.

$\beta$ -amylase site: This is the primary polymer binding site. It can bind to six glucose residues from the non-reducing end of a polymer (branch) or it can conveniently accommodate the oligosaccharides with a degree of polymerization of 5-6. This will be keeping in with the preference the enzyme exhibits in hydrolysing these oligosaccharides compared to maltotriose or maltotetrose. It catalyses the sequential release of maltose from polymers like starch or glycogen.

Isomaltase-maltase site: This is involved in the binding of the  $\alpha$ - or  $\beta$ -limit dextrins. There are two activities

associated with this unit. One is relatively heat stable and iodine inactivated-substrate protected-maltase activity and the other is isomaltase activity. This unit takes part in polymer hydrolysis and can catalyse the hydrolysis of maltose,  $\alpha$ - and  $\beta$ -limit dextrins.

Maltase site: This is yet another binding site for maltose and its hydrolysis. This is heat labile and iodine-inactivated and does not get protection by substrate binding.

The isomaltase-maltase site rather than maltase site seems to be more intimately associated with the starch hydrolysis. This is depicted by placing the isomaltase-maltase close to the 'hydrolysing centre' of  $\beta$  amylase site. Maltase site is depicted away from the hydrolysing centre. Nevertheless, this site is important for the hydrolysis of starch and maltose. From the inactivation studies it was inferred that this site accounts for nearly 50% of each of the activities. While isomaltase-maltase site gets protection by binding of starch, maltase site is not protected and hence is inactivated in presence of iodine reagent. The glucoamylase activity seen under these conditions is, therefore due to the maltase activity of isomaltase-maltase site subsequent to  $\beta$ -amylase action. This probably represents the iodine sensitive-substrate protected glucoamylase activity (one of the two observed 'species').

### Mode of action on starch:

The complete hydrolysis of starch takes place according to a sequence discussed below.

Starch binding and  $\beta$ -amylase action: Six residues from the non-reducing end of a branch of starch bind to  $\beta$ -amylase site. Maltose is cleaved off one after the other from the non-reducing end, till the branch point is reached.

Maltase activity subsequent to the  $\beta$ -amylase action. The maltose resulting from  $\beta$ -amylase action is acted upon by both the maltases (isomaltase-maltase and maltase sites) and glucose is released into the medium. It is considered that maltose arising from  $\beta$ -amylase action is not an enzyme-bound intermediate, since maltose is detectable in the reaction mixture. On the other hand, it is likely that the concentration of the released maltose in the active site builds up to such an extent that is effectively hydrolysed by maltases. This will result in a steady-state concentration of maltose, which seems to play an important role in the regulation of  $\beta$ -amylase activity by a feed back inhibition by the product.

Attack on the branch points: When starch is reduced to  $\beta$ -limit dextrin (the core structure left after the complete

action of  $\beta$ -amylase on starch, with all the branch points exposed), the isomaltase with its associated maltase activity takes over and leads to further degradation to glucose.

The hydrolysis profile of starch indicates an initial fast reaction for about 20 min. at which time about 50% of the starch is hydrolysed, followed by a slow rate of release of glucose. The 50% of starch hydrolysed initially also correlates with the 50% of mass distributed between the first branch points and the non-reducing ends. Presumably, the initial fast reaction is due to the hydrolysis of  $\alpha(1\rightarrow4)$  linkages in the branches catalysed by the combined action of  $\beta$ -amylase and maltases and the subsequent hydrolysis at a slower rate is due to isomaltase-maltase action on the resulting  $\beta$ -limit dextrin. This would require that the functional unit of the enzyme should detach itself when the hydrolysis of a branch is completed and attach itself to another branch. This process will continue till a  $\beta$ -limit dextrin results, and which will be acted up on at the isomaltase-maltase site to release glucose sequentially. The mechanism of action of isomaltase is probably analogous to that of the isomaltase unit (dextrinase) of sucrase-isomaltase with  $\alpha$ -limit dextrans.

## Number of binding sites for various substrates

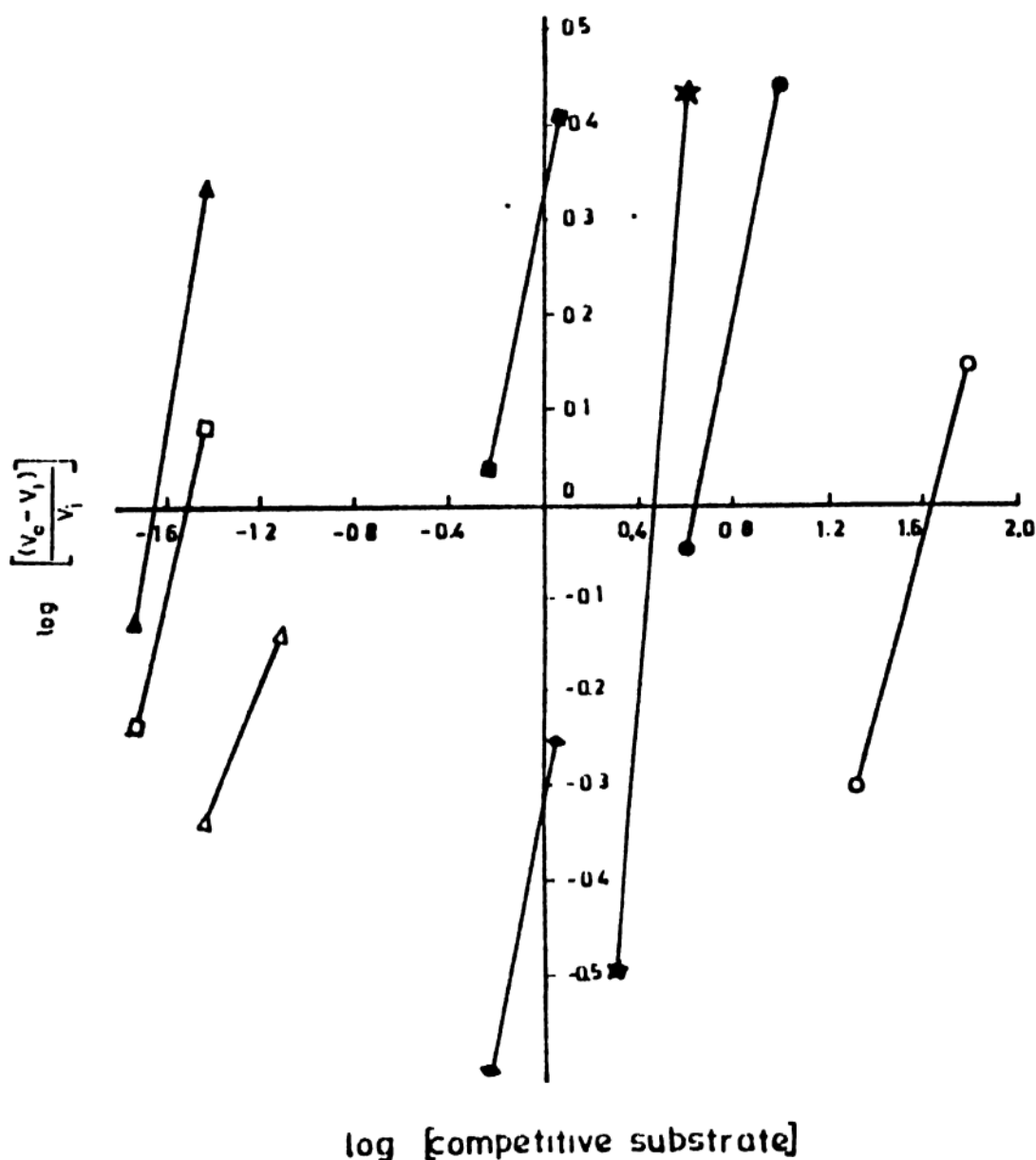


Fig.32 : The evaluation of number of binding sites for various competitive substrates during the hydrolysis of starch, glycogen or maltose. The slope of the straight line resulting from the plot of  $\log[(V_o - V_i)/V_i]$  vs  $\log [i]$  (where  $V_i$  and  $V_o$  are respectively velocities of the reaction in the presence and in the absence of the competitive substrate) yields the number of binding sites available for a competitive substrate. The straight lines ( $\star-\star$ ) ( $\circ-\circ$ ) and ( $\square-\square$ ) were obtained from the data on the inhibition of hydrolysis of starch by maltose, palatinose and glycogen respectively. The straight lines ( $\diamond-\diamond$ ), ( $\circ-\circ$ ), ( $\triangle-\triangle$ ) and ( $\square-\square$ ) resulted from the inhibition of hydrolysis of maltose, by starch, palatinose, maltotriose and malto pentose respectively. ( $\blacktriangle-\blacktriangle$ ) is from the data on the inhibition of glycogen hydrolysis by maltopentose. The number of sites have been tabulated (table 5).

# Number of binding sites for various inhibitors

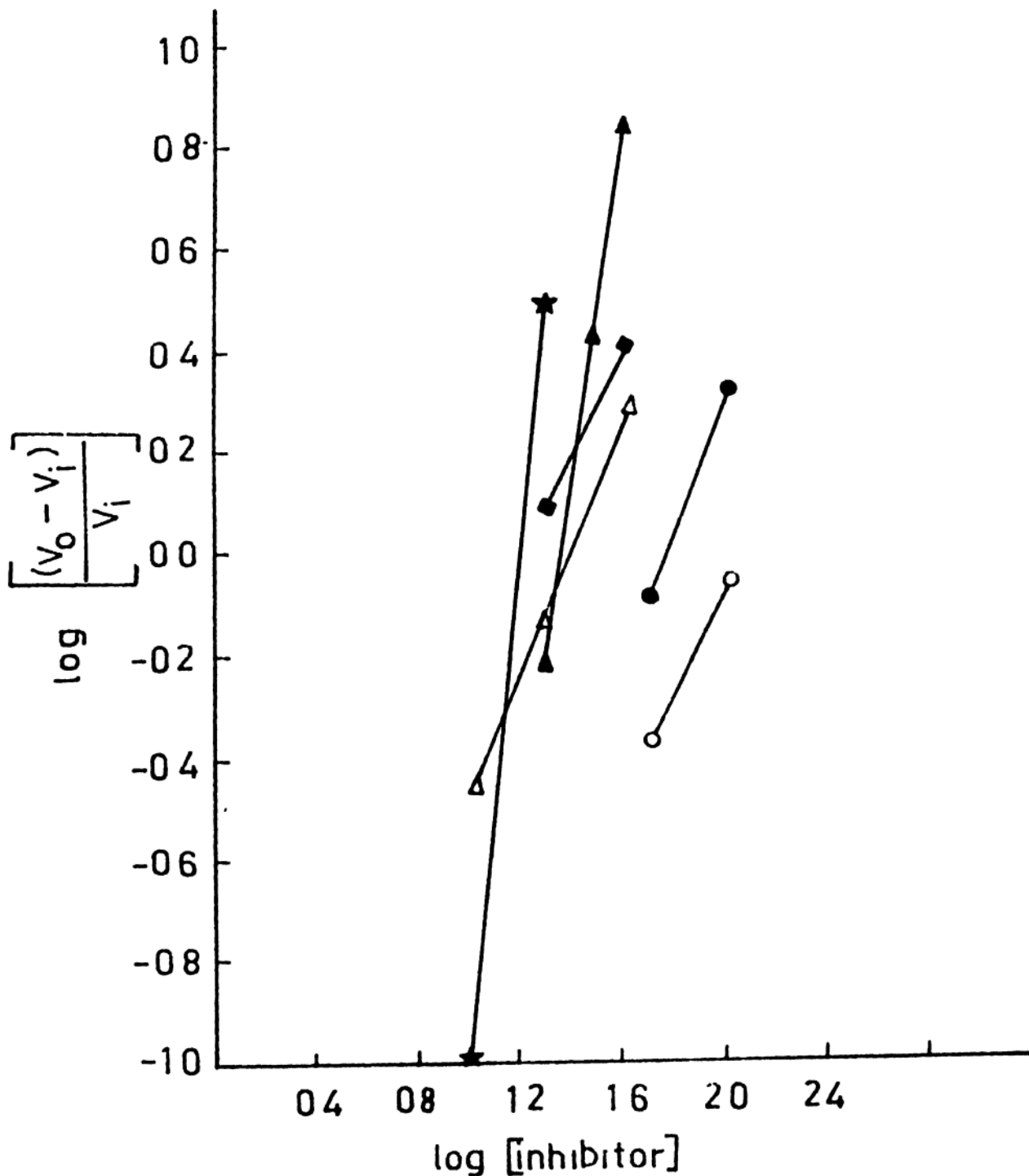


Fig.33 : The evaluation of the number of binding sites available for various competitive inhibitors during inhibition of hydrolysis of starch or maltose according to the method detailed under Fig.32. The straight lines (▲—▲), (●—●) (■—■) and (★—★) respectively, correspond to the inhibition of starch hydrolysis by sucrose, Tris, trehalose and glucono-δ-lactone. The number of binding sites for Tris and sucrose during inhibition of maltose hydrolysis were obtained from the straight lines (○—○) and (△—△). For the number of sites see Table 5.

Table 5

Number of binding sites for various competitive  
substrates and inhibitors

Type of hydrolysis	Competitive substrate	Competitive inhibitor	No. of sites per active site*
Starch hydrolysis	Maltose		3.25 (3)
	Palatinose		1.25 (1)
	Glycogen		1.25 (1)
		Surcose	3.2 (3)
		Trehalose	1.0 (1)
		Tris	1.35 (1)
		Glucono lactone	5.0 (5)
Maltose hydrolysis	Starch		1.25 (1)
	Palatinose		0.95 (1)
	Maltotriose		0.7 (1)
	Maltopentose		1.0 (1)
		Sucrose	1.25 (1)
		Tris	1.0 (1)
Glycogen hydrolysis	Maltopentose		1.7 (2)

Figures in the paranthesis refer to the numbers of binding sites expressed as the nearest integer.

### Number of sites for various substrates and inhibitors

With the presence of three activities viz.  $\beta$ -amylase, maltase and isomaltase and two species of maltase activities the proposed active site design of intestinal glucoamylase maltase complex is rather complicated. It was desirable at this stage to have a quantitative picture regarding the number of binding sites for various substrates and inhibitors to verify whether the proposed model can provide the expected number of binding sites for various compounds. This was achieved by plotting the data from inhibition and competitive substrate incubation studies of Sivakami [229], and some of our own as shown in Figures 32 and 33. The number of binding sites for a substrate or inhibitor obtained from the slopes of the resultant straight lines have been tabulated (Table 5 ).

In the case of starch hydrolysis there are, according to this procedure, three sites each for disaccharides maltose and sucrose; two sites each for oligosaccharides like maltotriose and maltopentose (the data on glycogen hydrolysis has been adapted on the assumption that the mechanism of hydrolysis for both starch and glycogen are essentially the same); one site for polymers like starch and glycogen, and one site each for TRIS, trehalose, and palatinose; and as many as five sites for glucono- $\delta$ -lactone. In the case of maltose hydrolysis it can be seen that the various substrates and inhibitors



have only one binding site. Sucrose is an inhibitor of both maltase and glucoamylase activities. It would resemble the conformation of maltose especially in the strained state (half chair conformation of the aglycon part) which it has to assume prior to binding. On this basis, sucrose can be expected to bind to the same three sites to which maltose can bind. Glucono- $\delta$ -lactone has a half chair conformation corresponding to the glucose moiety in a substrate molecule which has to undergo a conformational transition (from chair to half chair) prior to hydrolysis by the enzyme. It has 5 binding sites accommodated in this fashion: two in isomaltase-maltase (one for each) and one each in maltase,  $\beta$ -amylase, and the last one can bind to any other site available. Trehalose, Tris and palatinose each bind to only one site to effect inhibition by preventing either the binding or subsequent hydrolysis of starch. Though the available data are inadequate to pin-point the actual location of their binding, we are only suggesting their probable binding sites. Palatinose, owing to its structural resemblance to isomaltose, binds at the isomaltase. Trehalose, being not an inhibitor of maltase, will not bind to both the maltases but can bind to either  $\beta$ -amylase or isomaltase site. Tris has been shown to bind specifically at the glycon portion in sucrase-isomaltase [103] and on analogy, Tris probably binds to  $\beta$ -amylase at the glycon site and prevents the

hydrolysis of starch. Since trehalose and TRIS can bind to different sites at the same time, there will not be any mutual interaction between them during inhibition of starch hydrolysis. This has been observed and reported by Sivakami and Radhakrishnan [115].

Based on this model and the proposed mechanism there is a possible explanation for the observed substrate inhibition phenomenon, in the case of hydrolysis of maltotriose and maltopentose. This was not observed in the case of either maltose or starch during their hydrolysis. According to Dahlqvist [230] the substrate inhibition is due to transglycosylation, a process in which the glucose cleaved off from one of the substrate molecule is transferred to another molecule of the substrate instead of water. So, there should be two sites in the active site for the oligosaccharides, one which binds the acceptor and the other the donor. There are two sites available for these disaccharides according to the results from graphical method mentioned above. An alternative explanation can also be offered based on the proposed mechanism of action of the enzyme. Maltotriose and maltopentose are substrates for  $\beta$ -amylase. Hence they naturally bind to  $\beta$ -amylase site. This accounts for one of their binding sites. Since they are inhibitors for maltase activities, the second binding site is the maltase site. It is not clear if both the

maltases or only one of them is involved in this binding. According to the proposed mechanism of action, maltase activity (the second step) is essential for the hydrolysis of these oligosaccharides. A consequence of their binding to the maltase site will be inhibition of their own hydrolysis, somewhat <sup>like</sup> suicidal inhibition which appears as substrate inhibition. This phenomenon is not seen in the case of maltose because it is a substrate for maltase and an inhibitor for  $\beta$ -amylase. Substrate inhibition as a consequence of transglycosylation, has been found even in maltose hydrolysis, catalysed by other  $\alpha$ -glucosidases [230]. So based on transglycosylation hypothesis it is not possible to account for the absence of substrate inhibition in maltose hydrolysis in the case of the intestinal enzyme. Hence it appears that the alternative explanation provided above based on the proposed mechanism of action appears to be a more reasonable explanation.

The ability of the model to account satisfactorily for the number of binding sites available for various substrates and inhibitors is indicative of the correctness of the approach. The ability of the proposed design to explain other observed phenomena, especially substrate inhibition and lack of interaction between Tris and trehalose, is in support of the mechanism of action also.

A suggested method for calculating the  $K_m$  for branched polymers with an exo-enzyme

It is not out of place to include a comment on the logic of calculating the  $K_m$  for a polymer substrate of an exo-amylase based on the anhydride glucose concentration, in the medium, instead of the polymer concentration. Unlike endo-amylases, the exo-amylases are very specific to the non-reducing end and hence the concentration of this end group should determine the effective concentration of the substrate species rather than the internal moieties. It is apparent, therefore, that the  $K_m$  should be expressed in terms of this end group concentration. For a linear polymer like amylose, this can be conveniently calculated from the amount (in gms) and its approximate molecular weight, since each molecule has only one non-reducing end. The evaluation of the concentration of non-reducing end in the case of branched homopolymers like amylopectin and glycogen is not straight-forward. Apart from the  $M_r$  a detailed knowledge about its structure, especially with regard to the number of glucose moieties between the first branch point and the end group of a branch (called branch length) and the mass of the polymer distributed between the first branch point and the end group are required. Fortunately, this information is available for the amylopectin portion of potato starch. For those cases where this information is not available the same can be easily

Table 6

$K_{cat}$  and  $K_{cat}/K_m$  values for various substrates

Substrate	$K_m$ ( $\mu$ M)	$V_{max}$	Turnover No.	
			$K_{cat} = \frac{V_{max}}{E_o}$ per molecules	$\frac{K_{cat}}{K_m}$ or $\frac{V_{max}}{E_o \cdot K_m}$ *per site
Maltose	1.43	25	320	40 $2.23 \times 10^5$
Maltotriose	8.3	16	200	25 $2.4 \times 10^4$
Maltopentose	4.0	25	320	40 $8 \times 10^4$
Amylopectin.	0.078	19.6	245	31 $3.14 \times 10^6$
Starch	0.039	16	200	25 $5 \times 10^6$

\* eight protomers/enzyme molecule was assumed.

obtained by  $\beta$ -amylosis of the branched polymer. Since the action of  $\beta$ -amylase can not proceed beyond the branch point, the mass of starch hydrolysed by  $\beta$ -amylase will correspond to the mass distributed between the first branch points and end groups (denoted as  $M_b$ ). The molecular weight of the polymer ( $M_p$ ) can be approximately calculated from gel filtration. Finding out the number of glucose residues ( $n$ ) in a branch is not simple. From the data available in the literature on the structures of these polymers, a typical value of 25 for amylopectin like polymers and 14 for glycogen like polymers can be assumed. The concentration of the non-reducing ends can then be obtained by the following relationship:

$$[\text{Non-reducing end}] = \frac{M_b}{n \times M_g} \frac{\text{amount of polymer (g)}}{M_p}$$

( $M_g$  is the molecular weight of glucose anhydride)

Even such an approximation would be more reliable in the determination of  $K_m$  than the conventional method. It can be seen from Table 6 that calculations based on this method suggest that starch is a better substrate compared to maltose or oligosaccharides since its  $K_m$  ( $39 \mu\text{M}$ ) is about two orders less than that of maltose and oligosaccharides. Consequently  $K_{cat}/K_m$  also is in favour of starch or amylopectin compared to either maltose or oligosaccharides. By the conventional method, using an equivalent glucose anhydride

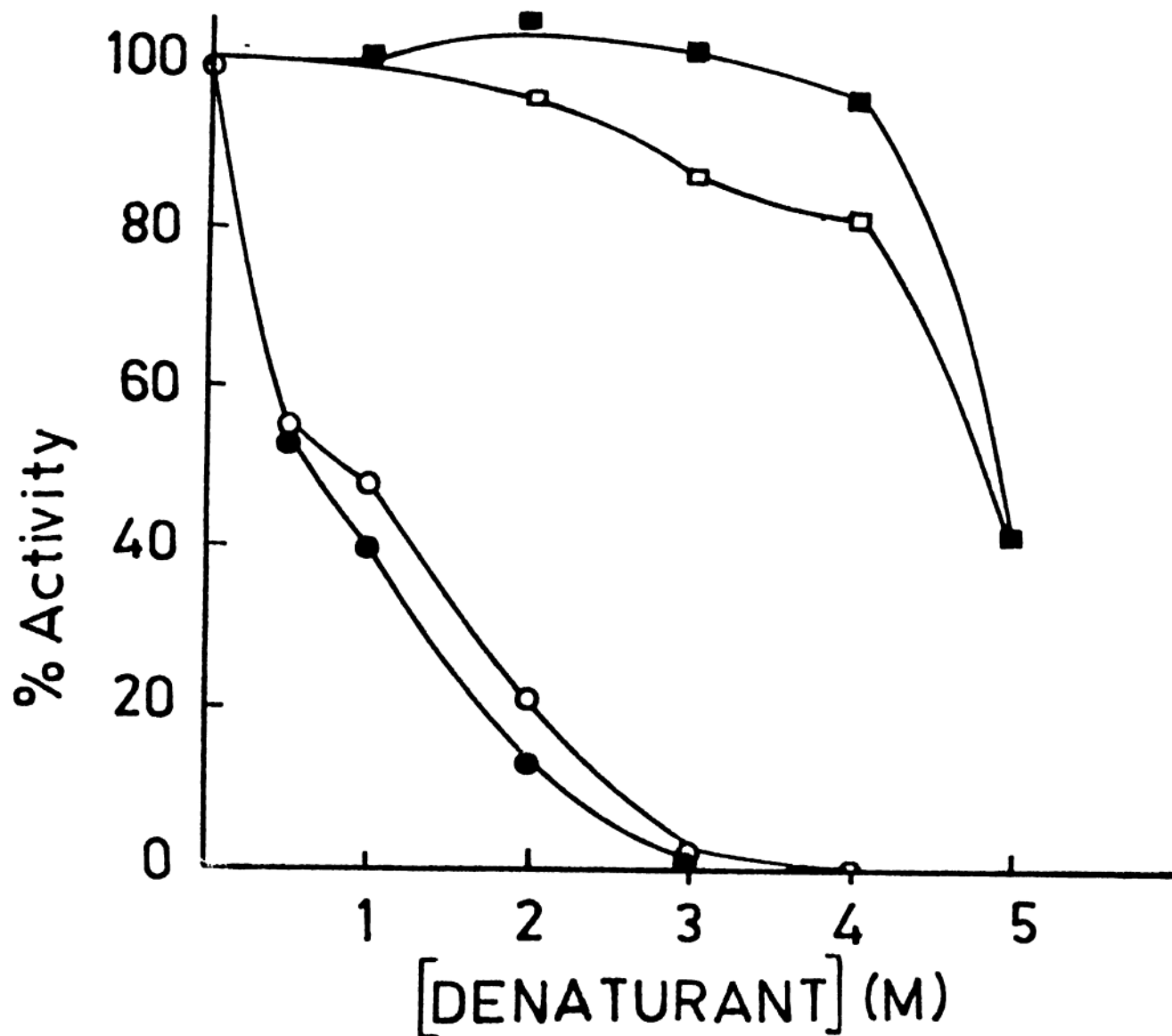


Fig.34 : The denaturation pattern of glucoamylase (■,●) and maltase (■,○) in the presence of different concentrations of guanidinium chloride (●—●) and urea (■—■). The presence of appreciable enzyme activity even in presence of 5M urea is indicative of the stability of the active site against denaturation.

mass, starch was found to be a substrate only as good as maltose, ( $K_m$  for maltose, 1.43 mM;  $K_m$  for starch, 2.0 mM). This method can also explain why amylose and amylopectin give very different rates when they are at the same concentration in mg/ml. For a given amount of amylose the number of non-reducing ends will be much smaller  $\frac{\text{amount}}{50,000}$  than that of amylopectin. Yet another advantage of amylopectin is the proximity of branches which may compliment the known structure of rabbit intestinal glucomylase-maltase complex (Fig.6 ).

#### Stability of the enzyme active site - studies with detergents denaturants and alcohols

In spite of the intricate design of the active site, the stability of the enzyme against denaturation is quite remarkable. It retains partial activity at the end of 2 hours at 60°C and in the presence of 8 M urea at 37°C and exhibits total activity even after incubation for 1 hour with 5% SDS (in fact, at lower concentrations SDS slightly activates the enzyme activity). However, the enzyme loses all the activity in 3 M guanidium chloride. The stability of the membrane enzymes in general and intestinal hydrolases especially against denaturation by SDS is well-known [58 ]. This not surprising since the membrane-bound enzyme is associated with long chain fatty acids.



Table 7

Extent of inhibition by various alcohols (10% w/v)

Alcohol	10%(v/v)		10%(v/v)	
	% activity p.enz		%activity T.enz	
	Maltase	G.A.	Maltase	G.A.
Methanol	91	78	97	65
Ethanol	60	58	59	58
n-Propanol	0	0	0	0
Isopropanol	30	32	36	32
n-Butanol	52	56	59	50
Sec. Butanol	36	42	38	51
Tert Butanol	21	22	25	30
Ethane Diol	84	70	87	76
Propane Diol	71	66	89	71

G.A. = glucoamylase

The enzyme is rather sensitive to several alcohols. Among the alcohols tested, n-propanol is the most potent inhibitor followed by t-butanol and iso-propanol. Ethanol, methanol, ethane-diol and propane-diol are poor inactivators at 10% (v/v) concentration (Table 7). This pattern of inhibition suggests that n-propanol satisfies the steric requirement, for the alcoholic hydroxyl to interact specifically with a particular group, essential for catalytic action of the enzyme. Since the substrate is a poly-hydroxyl compound, it is quite possible that alcohol interaction, especially that of n-propanol mimicks the interaction of one of the essential hydroxyl groups of the substrate (for example, the 4-OH of the glycon moiety or the anomeric hydroxyl), with some essential groups in the active site. Since propane-diol is not a good inactivator at all and iso-propanol is not as good an inactivator as n-propanol, the actual structural requirement for this interaction would be that of n-propanol.

The enzyme does not lose its activity on immuno-precipitation, with both starch and maltose as substrates. This indicates that the active site and the antigenic determinants are spatially well-separated.

## IMMUNOCHEMISTRY OF THE ENZYME

The enzyme elicited a good antibody response in rat as can be seen from the titre value of 2.4 mg/ml plasma. The antibody reacts avidly with the enzyme forming a visible precipitate within one hour of their mixing. The antigenic determinants are conformational, since the enzyme when converted to the open chain conformation by reacting with 6 M guanidinium chloride and subsequent removal by dialysis, failed to complex with the antibody of the native enzyme. It is not clear if these conformational determinants are at the level of quaternary structure of the protein or at the tertiary level of individual subunits. The antigen-antibody complex formation leading to a precipitin line in immunodiffusion experiments did not take place when the enzyme was heat denatured at 60°C or incubated with 5% SDS at 37°C for 1 hr or treated with 10% ethanol. On the other hand it retained partial enzyme activity at 60°C and in 10% ethanol and in fact, fully active in 5% SDS. This observation and the fact that the enzyme does not lose its enzyme activity after antibody binding lead to the conclusion that the active site and the antigenic determinants are placed well apart on the molecule. Since rat also has a similar intestinal glucosyl- $\alpha$ -D-glucanase-maltase complex, the active site conformation may be similar and hence not considered as 'non-self',

Quantitative immuno-precipitation Ag-Ab stoichiometry

Amount of antigen added ( $\mu\text{g}$ )	Amount of precipitate formed ( $\mu\text{g}$ )	Amount of antigen ( $\mu\text{g}$ )		Amount of antibody in precipitate ( $\mu\text{g}$ )	Ab/Ag (w/w) in the precipitate	moles of Ab in one mole of Ag	Number of antigenic sites per mole of enzyme
		in supernatant	in precipitate				
5	54	0.0	5.0	49	9.8	50	50
20	104	0.0	20	84	4.2	21	21-42
40	144	0.0	40	104	2.6	13	26
50	160	0.0	50	110	2.2	11	22
60	180	0.0	60	120	2.0	10	20
80	171	13.5	66.5	104.5	1.57	8	16
120	104	79	41	63	1.54	8	16
160	86	120	40	46	1.15	5.8	12
240	36	220	20	16	0.8	4	8

Antibody : 50  $\mu\text{l}$  of anti serum is equivalent to 120  $\mu\text{g}$  of antibody

The presence of full activity in the (antigen-antibody) complex, either in the soluble form or in the precipitate form, helped us to work out the stoichiometry of antibody binding to an antigen molecule (Table 8 ) in quantitative precipitation analysis (page 79 ). In the antibody excess zone there are at least 50 antibodies and presumably as many binding sites per antigen molecule. This will include both specific and non-specific sites. This value drops, to about 25 in the near equivalence zone on the antibody excess side. At equivalence zone only 10 antibodies are bound to the antigen. Assuming that all the antibody valencies are saturated, it could be inferred that the antigen has about 20 antigenic determinants, on it. In the excess antigen zone, this figure drops to 16 and in the far excess antigen zone there are only half as many sites as in the equivalent zone. In the supernatant, i.e. in soluble complexes of the far-excess-antigen-zone, there are about 2 antibodies/antigen, on an average. Thus, this multivalent nature of the antigen is in line with the large size of the molecule and from the value of the equivalent zone for the valency, it can be seen that there are about 2 determinants/bead. It is likely that the determinants are placed one on the bead and another in the linkage portion between the beads. It has been observed that, at equivalence zone, the ratio of antibody to antigen correlates with the molecular weight of an antigen [231]. From the

## QUANTITATIVE PRECIPITIN ANALYSIS

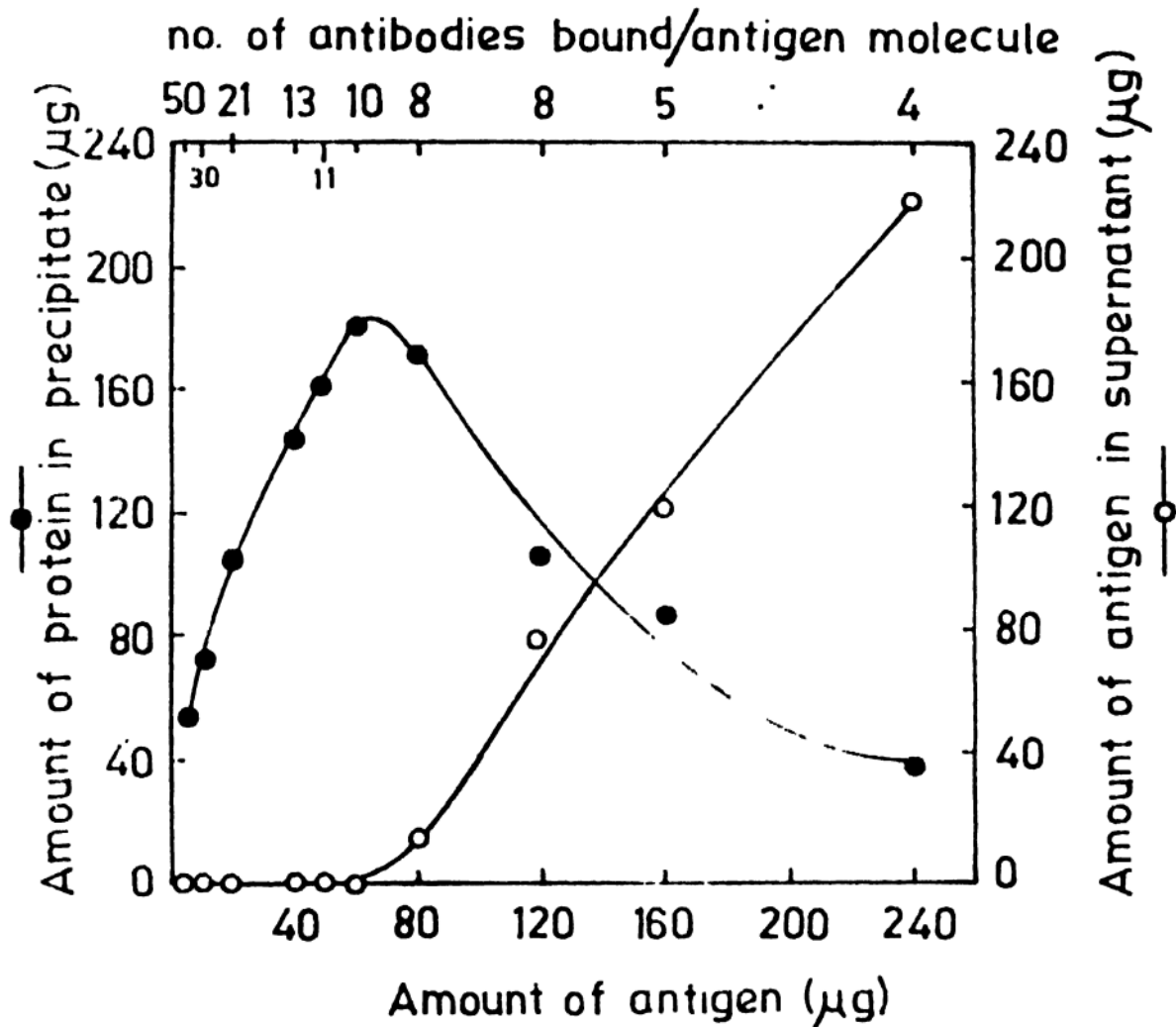


Fig.35 : The profile of the quantitative immuno precipitin analysis, obtained employing varied concentrations of the enzyme to react with a fixed amount of (50 μl) the antibody. The full presence of enzyme activity (○—○) in both the soluble complexes and the precipitates enabled us to evaluate the antibody-antigen stoichiometry at various points in the profile. (see also Table 8).

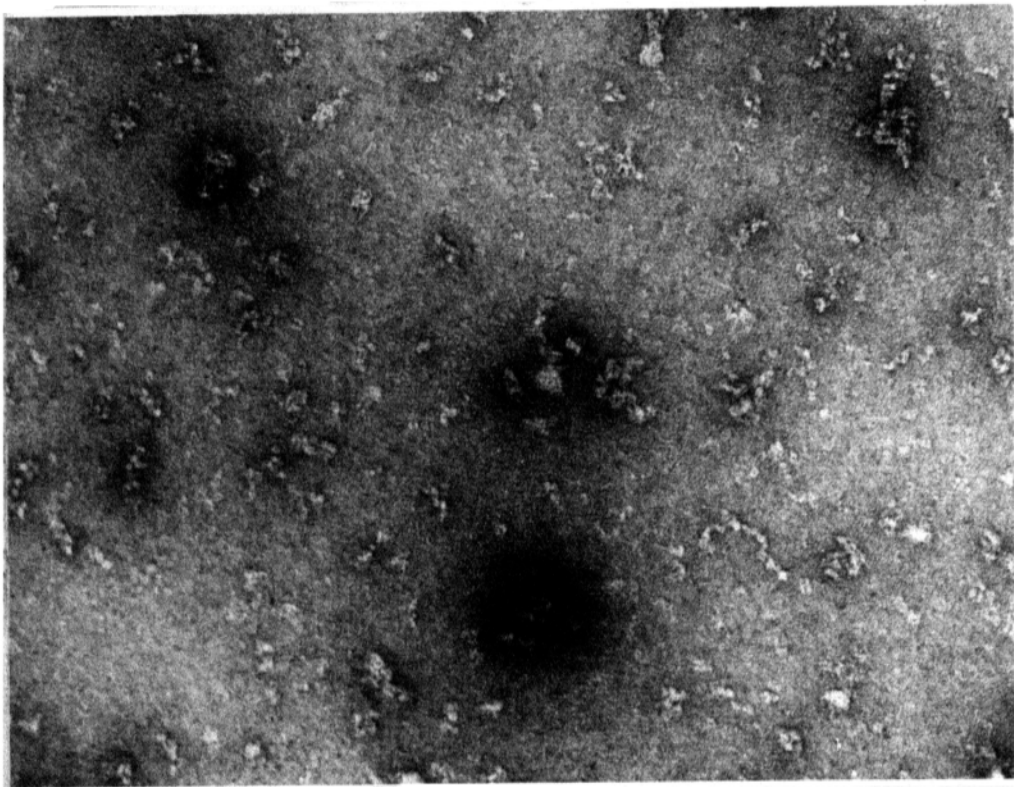


Fig. 36.

weight ratio of antigen to antibody at equivalent zone, the molecular weight of the enzyme was calculated as 800,000 a value close to that obtained by sedimentation methods.

#### Immuno-electron microscopy

With a view to investigating the mode of association of the antibody with the enzyme, especially from the consideration of the interesting supra-quaternary structure, the soluble antigen-antibody complex was purified and subjected to electron microscopy. But, unfortunately no useful information was obtained owing to the matching of the size of the bead with that of the antibody, which gave a confusing picture. One observation made during this study was that the antigen-antibody complex formed membrane/film in the presence of uranyl acetate, on naked grids (Fig.36) just like the enzyme complex.



## STRUCTURE-FUNCTION CORRELATIONS - A SPECULATIVE EXERCISE

Among the proteins studied in detail, the rabbit intestinal glucomylase-maltase complex represents a very unusual protein with respect to the size, shape, subunit and protomer assembly, supra-quaternary structure and presence of unusual linkages. It is probably the only enzyme which is so intricate in its structure. In some functional proteins commonly there are quaternary structures in which protomers/subunits assemble around a central point, exhibiting cubic, dihydedral, tetrahedral, or spherical symmetries, because of the requirement that all the contact points in the units are saturated and the individual units are equivalent [136]. In the rabbit intestinal glucoamylase-maltase complex there are about fifty identical subunits. Six of them combine in a compact spherical symmetry and constitute a functional unit or protomer ('bead') and eight such protomers are in turn connected by flexible covalent links of 20 Å length, to form a linear array. This linear arrangement of protomers is an open structure which distinguishes the end units from the rest, at least physically. The open ended supra-quaternary structures have not received adequate attention and it has been indicated that this type of arrangement is unlikely in proteins [136]. However, such an arrangement is found in nature and has been clearly suggested by the

## STRUCTURE-FUNCTION CORRELATIONS - A SPECULATIVE EXERCISE

Among the proteins studied in detail, the rabbit intestinal glucomylase-maltase complex represents a very unusual protein with respect to the size, shape, subunit and protomer assembly, supra-quaternary structure and presence of unusual linkages. It is probably the only enzyme which is so intricate in its structure. In some functional proteins commonly there are quaternary structures in which protomers/subunits assemble around a central point, exhibiting cubic, dihyedral, tetrahedral, or spherical symmetries, because of the requirement that all the contact points in the units are saturated and the individual units are equivalent [136]. In the rabbit intestinal glucoamylase-maltase complex there are about fifty identical subunits. Six of them combine in a compact spherical symmetry and constitute a functional unit or protomer ('bead') and eight such protomers are in turn connected by flexible covalent links of 20 Å length, to form a linear array. This linear arrangement of protomers is an open structure which distinguishes the end units from the rest, at least physically. The open ended supra-quaternary structures have not received adequate attention and it has been indicated that this type of arrangement is unlikely in proteins [136]. However, such an arrangement is found in nature and has been clearly suggested by the

structures of natural polymer of urease [221] and that of haemocyanin [232]. Just as the majority of the proteins with multi-subunits, our enzyme is also built up of identical subunits, but the presence of unusual and very stable covalent linkages between the subunits is unique. Although disulphydryl bridges are the most common linkages between the polypeptides, it is remarkable that the presence of other unconventional bridges were recognised several years ago by Edsall [233]. There is no a priori reason why bridges like phosphodiester, glycosidic or iso-peptide bonds between polypeptides should not be present in proteins especially in those which lack sulfur amino acids. Indeed, such linkages are beginning to be seen in proteins. It is conceived that the animal fatty acid synthetase, a multi-functional enzyme which is not dissociated by SDS, must be composed of identical subunits held by covalent linkages and the covalently linked enzymes obviate the need for specific non-covalent interactions to maintain a multi-functional structure [234]. It is evident, especially from the recent work [236] that ( $\gamma$ -Glu)-Lys cross-linking by the associated enzyme systems may play a vital role in linking protein polypeptide chains.

The evolution of such a complicated supra-quaternary structure may become meaningful when the function of glucoamylase is considered as an example. An apparent advantage the enzyme might have while acting on

branched polymer subunits like starch/amylopectin is that when one of the protomers attaches to the non-reducing end of one of the branches, the remaining protomers are brought into proximity with other branches. The protomers can assume different orientations allowed by the flexibility in the links between them, and they can attach to other branch ends and catalyse the hydrolysis almost simultaneously. This advantage is reflected in the  $K_m$  for starch ( $39 \mu\text{M}$ ), which is lower by about two orders of magnitude compared to that of maltopentose ( $4 \text{ mM}$ ). Consequently  $K_{\text{cat}}/K_m$  (a lower limit for second order rate constant for the association of an enzyme and its substrate), for starch and malto pentose are  $5 \times 10^6$  and  $8 \times 10^4 \text{ M}^{-1}\text{sec}^{-1}$  respectively. Both have almost the same  $K_{\text{cat}}$  (saturating substrate condition) expected from the common mechanism operative during their hydrolysis. A decrease in  $K_m$ , however, has a decisive influence when the hydrolytic conditions are such that  $[S]$  is not much greater, equal to or less than  $K_m$ .

Since starch, being a polymer made up of only one type of monomer i.e. glucose, the enzyme has to recognise only this particular molecule in a particular conformation and for this purpose identical subunits, each with a recognition site for glucose would suffice. But, because the glucose in starch molecule is involved in two types of linkages  $\alpha$ -(1-4)

and  $\alpha$ -(1-6) and because the enzyme has to hydrolyse both for effecting complete hydrolysis, there is a necessity that the subunits are oriented in a particular way to suit the overall geometry of their structure. Presumably, this fixing is done by the covalent linkages between the subunits. The iso-maltase unit of surcase-isomaltase is capable of catalysing the hydrolysis of both  $\alpha$ -(1-4) and  $\alpha$ -(1-6) bonds but it can not hydrolyse starch. It is apparent especially in view of this, that for polymer hydrolysis apart from the two activities mentioned there must be a polymer binding site (and an associated degradation). This would require more sub-sites than what are available with iso-maltase and maltase and so there is a need for at least a few subunits (six in the case of glucoamylase-maltase complex) to be associated into a protomer. The covalent linkages seem to be necessary to keep these subunits and their associated activities sterically and mechanistically close (page no.137), - even under adverse conditions -, as demanded by the proposed mechanism of action. It is not clear why there are two maltases and consequent glucoamylase activities, in the enzyme complex, one being more stable than the other. This is probably a measure of abundant caution to enable the enzyme to function even in unfavourable conditions.

Glucoamylase-maltase complex with its unusual covalent linkages between subunits is very stable against denaturation and proteolytic damage, an environment present in the intestine with a variety of proteases and bile salts (natural detergents). An enzyme of this size and its stability may have an additional role in the stability and integrity of the membrane, which after all is mostly a lipid-protein barrier between two aqueous compartments.

Though the present study implies the intrinsic association of the enzyme with the membrane, it has not been possible to identify the exact nature of such association. The recent study on rat glucoamylase maltase complex [77] indicates that a peptide portion of the enzyme associated with the membrane was cleaved by intestinal proteases during solubilisation with Triton X100 and presumably this could be so in our case, especially in view of the reported lability of the linkage (see page 121). Rings of particle of diameter  $60 \text{ \AA}$  associated with 'maltase' activities have been observed in glycocalyx, under E.M. Though these are thought to be sucrase-isomaltase in aggregated state at high concentration, some of them could be glucoamylase-maltase complex also, since the diameter or beads in the enzyme structure are of  $60 \text{ \AA}$  diameter and it could take up a ring structure in membrane associated form. This possibility is compatible with

the view expressed by Ulev [1], that the close association of  $\alpha$ -amylase and glucoamylase-maltase complex will be a great advantage in terminal digestion in the brush border. The association with the glycocalyx, in that case, can be covalent and would require the action of papain by virtue of its protease or esterase activities, depending on the type of covalent linkage. During detergent solubilisation, this susceptible linkage is specifically severed by intestinal proteases.

The biosynthesis of glucoamylase with all its complexity must also be a complicated process. Perhaps the subunits are the first to be synthesized from the genetic information of a small stretch of a genome and the synthetic machinery may be 'polycistronic' yielding a protomer or the 'bead'. There must be extensive post-translational modifications in this process and in the subsequent assembly of the protomer to yield the supra-quaternary structure of eight beads. It is highly unlikely that this assembly is an uncontrolled or random process. For example, in a string of beads, addition or deletion of a bead would be possible from either or both ends resulting in a population of molecules with a number of beads greater or less than 8 beads. Such a heterogeneity of molecules can be easily detected, if it existed. On the other hand, at no stage of purification (which fortunately is based essentially on a single step affinity system) was there evidence for

heterogeneity and indeed the various criteria for homogeneity that the enzyme satisfied is suggestive of a single population of molecules. Since all these processes are envisaged as post-translational, it is possible that they are controlled by the specificity of the required enzymes. Alternately, a string of beads of the size and shape demonstrated for glucoamylase may exhibit a geometry, hitherto unrecognised, which is restrictive in its nature and which can recognise the first bead (initial signal) and the last bead (termination signal) and hence impart a 'direction' to the final assembly process.

We believe that intestinal glucoamylase can handle the total load of dietary starch and glycogen. Salivary amylase although quite active plays essentially no role in starch hydrolysis. Pancreatic  $\alpha$ -amylase being an endo-enzyme possibly plays a complimentary role to glucoamylase, an exo-enzyme. It is of interest to note that even under conditions of severe pancreatic deficiency affecting the levels of  $\alpha$ -amylase, there are no reports of defective starch hydrolysis, nor are there reports of a genetic deficiency of  $\alpha$ -amylase which would have been detected if starch hydrolysis was defective. McGeachin and coworkers [110,111] have reported that removal of pancreas and salivary glands in the rat, does not severely affect the hydrolysis of starch in the intestine. In nature it is not



uncommon to have a surplus of certain related enzyme activities. Absence of pepsin as in total gastrectomy does not severely affect the hydrolysis of dietary proteins. It is thus conceivable that glucoamylase alone and  $\alpha$ -amylase along with intestinal isomaltase, are both designed for the total hydrolysis of starch/glycogen, a major dietary component.

## GENERAL SUMMARY AND CONCLUDING REMARKS

The microvillus machinery of the small intestine plays an invaluable role in the digestion and absorption of dietary components. Unfortunately, the structure-function relationship of this intricate structure is not adequately understood owing to the lack of molecular details regarding the components of which hydrolases are preeminent. In view of this lacuna in the understanding of this system and since the earlier studies emanating from this laboratory on the various microvillous enzymes for more than two decades provided the required background and confidence, we ventured to study the molecular structure of one of these enzymes in depth. Intestinal glucoamylase-maltase complex was chosen for the reasons that it is an important enzyme in the terminal digestion of starch, a major component of the diet. The rabbit enzyme was prepared in relatively large amounts and in a state of homogeneity by a simple and elegant affinity procedure developed by Sivakami and Radhakrishnan [ 66 ]. The structure and function relationships have not been adequately studied as in the case of sucrase-isomaltase, and an attempt has been made in this direction.

Since our efforts to crystallise homogeneous preparations of the enzyme were not successful, we resorted to the

next best alternative of combining inferences from the hydrodynamic data with the structural details available from electron microscopic studies at 20 Å resolution, to unravel the quaternary structure of the enzyme complex.

From the detailed hydrodynamic studies, we could establish not only the correct molecular size of the enzyme ( $M_r = 760,000$ ) but also ascertain the suspected asymmetry of the enzyme using a variety of criteria which included the frictional ratio, intrinsic viscosity,  $\beta$  and  $k_o/[\eta]$  values. The equivalent shape of the enzyme derived from its viscosity factor, using theoretical model systems, especially that of Kuhn agreed reasonably well with the actual appearance of the molecule under the electron microscope. Our conclusion on the shape and molecular dimensions of the molecule is that it is a 660 Å long string containing eight linearly arranged 'beads' each of diameter 60 Å, with a surface-to-surface inter-bead distance of about 20 Å.

Since it is unlikely that such a large protein is a single polypeptide, we were prompted to probe into its quaternary structure. Earlier studies of Sivakami and Radhakrishnan [116] showed that this enzyme was not dissociable by SDS or guanidinium chloride and that it is lacking in sulphur amino acids. Our investigations using a variety of dissociating

conditions not only supported the finding of Sivakami and Radhakrishnan but also ruled out the presence of only non-covalent linkages between the subunits. Direct evidence for the presence of several subunits in the enzyme came from chemical studies such as quantitation of the N- and C-terminal amino acids, tryptic peptide mapping, and from direct visualisation under the electron microscope. The enzyme was shown to have only one N-terminal amino acid, tyrosine, by dansylation techniques and the partial amino acid sequence at the C-terminal is ---Ala-Gly-Ser. The results of quantitation of the N-terminal and C-terminal amino acids and tryptic peptide maps suggested the presence of nearly fifty identical polypeptide chains. This idea was supported by the electron-microscopic view, in which each 'bead' appeared as an assembly of six smaller beads with a diameter of about 35 Å. The geometry of the beads, on the basis of its electron microscopic appearance, is assumed to be a octahedron with a  $D_3$  symmetry formed by six spherical subunits.

The observed frictional properties of the enzyme and the theoretical considerations lent support to this model. The inability to dissociate this assembly strongly suggests the presence of unusual covalent linkages such as an isopeptide linkage ~~OR~~ a similar type, seen only in some structural proteins. Since this enzyme is a glycoprotein, a

linkage involving carbohydrate moieties is also a possibility worth considering. In brief, it is considered that six subunits assemble into an octahedron and form a protomer which in turn linearly associates with covalent linkages in between, with seven others to generate a supra-quaternary structure. The flexibility between the protomers was indicated by the lack of correlation between the shapes derived hydrodynamically from various model systems using viscosity factor and frictional ratio, and also by the overall shape of the enzyme as seen in the electronmicrographs.

The classical mechanism of action of this enzyme was found to be inadequate to account for certain aspects of its action on polymer substrates. Analysis of the available data in the literature indicated a need to consider an alternative more plausible mechanism of action. Detailed information is available in the literature on: The action pattern on oligosaccharides with different degrees of polymerisation, structural specificity of its disaccharide substrates, inability to isolate or separate glucoamylase and maltase activities, appearance of more reduction power in the assay mixture than can be accounted for by glucose alone and the appearance of maltose as a minor component during starch hydrolysis apart from glucose. Based on these observations and on some of our recent findings, we propose an alternative mechanism

which invokes the presence of a  $\beta$ -amylase-like action to precede the maltase activity, for explaining the mode of hydrolysis of polymer substrates and oligosaccharides. It has been shown that the proposed mechanism is superior to the classical one in offering an explanation for a variety of experimental observations. Iodine and heat inactivation studies showed the presence of two 'species' each of glucoamylase and maltase activities but only one of isomaltase. These studies not only provided experimental support to the proposed mechanism but helped us to conceive of a possible design of the active site of the enzyme. According to this design, the active site has three separate but sterically and mechanistically interacting entities: (a)  $\beta$ -amylase, (b) isomaltase-maltase unit in which maltase is associated with isomaltase and is relatively heat resistant and which exhibits substrate protectable iodine inactivation, and (c) a maltase which is heat labile and which exhibits iodine inactivation not protected by substrate. The presence of two 'species' of glucoamylase activity is merely a direct consequence of two kinds of maltases, according to the proposed mechanism. The isomaltase-maltase unit seems to be associated more closely with the  $\beta$ -amylase rather than with maltase. In support of the proposed design of the active site is its ability to account for the number of sites available for various substrates (maltose, 3; oligosaccharides 2; and polymers, 1) and inhibitors (sucrose, 3; glucono- $\delta$ -lactone, 5;

Tris, trehalose, and palatinose, 1 each) calculated from the data available from literature by a graphical method.

In spite of the intricate structure of the active site the enzyme is very stable towards denaturation. It is quite active in the presence of 5% SDS, but is inactivated by certain alcohols of which n-propanol is very effective. It is suggested that n-propanol mimicks an essential hydroxyl interaction with the active site and probably satisfies the necessary or minimal structural requirements in this regard.

The immunochemical studies also suggest that the enzyme is large [ $M_r = 800,000$ ]. It is multivalent with about 20 antigenic determinants which are conformational. The active site is not an antigenic determinant in the rat, since the enzyme is fully active in the presence of the antibody.

We have also attempted a speculative exercise to correlate the supra-quaternary structure with the function of the enzyme which is the hydrolysis of glucose polymers, but we have considered it more from the point of view of branched polymers. The proposed structure of the enzyme and the intricate design of the active site would call for an equally complicated mode of biosynthesis with extensive

post translational events.

The postulated  $\beta$ -amylase activity of the enzyme has not been experimentally demonstrated and there are also technical difficulties in this regard. Nevertheless, it is hoped that the work presented in this thesis would stimulate further research which would close the gaps in our understanding of the mechanism of action of this enzyme, by kinetic and physico-chemical studies.





# BIBLIOGRAPHY

1. Ugolev, A.M. (1974) in Biomembranes Vol 4A (Smyth, D.H., Ed.) pp.285-362 Plenum press, London and New York.
2. Brunner, J., Houser, H. and Semenza, G. (1978) J. Biol. Chem. 253, 7538.
3. Creamer, B (1974) in Biomembranes Vol 4A (Smyth, D.H., Ed.) pp 1-42 Plenum press, London and New York.
4. Kenny, A.J. and Booth, A.G. (1978) Essays in Biochemistry Vol 14, (Campbell, P.N. and Aldrige, A.W.N., Ed.) pp 1-44, Academic Press, London, New York.
5. Tinley, L.G. and Mooseker, M. (1971) Proc. Natl. Acad. Sci. U.S. 68, 2611.
6. Mukherjee, T.M. and Stachelin, L.A. (1971) J. Cell Sci. 8, 573.
7. School Mayer, J.V., Goll, D.E., Tinley, L., Mooseker, M., Robson, R. and Stromer, M. (1974) J. Cell. Biol. 63, 304a (abstract).
8. Cajori, F.A. (1933) Am. J. Physiol. 104, 659.
9. Dahlqvist, A. and Borgstrom, B. (1961) Biochem. J. 81, 411.
10. Miller, D. and Crane, R.K. (1961) Anal Biochem. 2, 284.
11. Miller D. and Crane R.K. (1961) Biochim. Biophys. Acta 52, 2
12. Forstner, G.G., Sabesin, S.M. and Isselbacher, K.J. (1968) Biochem. J. 106, 381.
13. Eicholz, A. and Crane R.K. (1965) J. cell. Biol. 26, 687.
14. Louvard, D., Maroux, S., Barratt<sup>i</sup>, J., Desnuelle, P. and Mutaftschiev, S. (1973) Biochim. Biophys. Acta 291, 747.

15. Nachlas, M.M., Morrin, B., Rasenblatt, D. and Seligman, A.M. (1959) J. Biophys. Biochem. Cytol 7, 261.
16. Dahlqvist, A. and Brun, A. (1962) J. Histochem. Cytochem. 10, 294.
17. Lojda, Z. Histochemie (1965) 5, 339.
18. Doell, R.G., Rosen, G. and Kretschmer, N. (1965) Proc. Natl. Acad. Sci. 54, 1268.
19. Lojda, Z. (1974) in Biological membranes Vol.4A (Smyth, D.H., Ed.) pp 43-122.
20. Ernst, S.A. (1975) J. Cell. Biol. 66, 586.
21. Cohen, R.B., Ruttenberg, S.H., Tsou, K.C., Woodburg, M.A. and Seligman, A.M. (1952) J. Biol. Chem. 195, 607.
22. Dahlqvist, A. and Nordstrom, C. (1966) Biochim. Biophys. Acta 113, 624.
23. Lojda, Z. (1970) Histochemie 22, 347.
24. Eicholz, A. (1968) Biochim. Biophys. Acta 163, 101.
25. Eicholz, A. (1969) Fed. Proc. 28, 30.
26. Tsubou, K.K., Kwong, L.K., Burvil, P.H. and Sunshine, P. (1979) J. Memb. Biol. 50, 101.
27. Oda, T. and Seki, S. (1965) J. Electron Microscopy 14, 310.
28. Johnson, Ch. F. (1967) Science 155, 1670.
29. Johnson, Ch. F. (1969) Fedn. Proc. 28, 26.

30. Nishi, Y., Yoshida, T.D. and Takesue, Y. (1968) J. Mol. Biol. 37, 441.
31. Gitzelmann, R., Bachi, Th., Binz, H., Lindemann, J. and Semenza, G. (1970) Biochim. Biophys. Acta 196, 20.
32. Benson, R.L., Sactor, B. and Greenawalt, J.W. (1971) J. Cell. Biol. 48, 711.
33. Nishi, Y. and Takesue, Y. (1978) J. Cell. Biol. 79, 516.
34. Wilson, T.H. and Vincent, T.N. (1955) J. Biol. Chem. 216, 851.
35. Dahlqvist, A. (1964) Anal. Biochem. 7, 18.
36. Stevens, J.A. and Kidder, D.E. (1972) Brit. J. Nutr. 28, 129
37. Dahlqvist, A. and Thomson, D.L. (1964) Biochim. Biophys. Acta 92, 99.
38. Rubino, A., Zimbalatti, F. and Auricchio, S. (1964) Biochem. Biophys. Acta 92, 305.
39. Hijmass, J.C. and McCarthy, K.S. (1966) Proc. Soc. Expl. Biol. Med. 123, 633.
40. Siddons, R.C. (1969) Biochem. J. 112, 51.
41. Swaminathan, N. and Radhakrishnan, A.N. (1965) Indian J. Biochem. 2, 159.
42. Sivakami, S. and Radhakrishnan, A.N. (1975) Indian J. Exptl. Biol. 13, 238.
43. Auricchio, S. Rubino, A. and Murset, G. (1965) Pediatrics 35, 944.

44. Gray, G.M. and Ingelfinger, F.J., (1965) J. Clin. Invest. 44, 390.
45. Borgstrom, B. and Dahlqvist, A. (1958), Acta chem. Scand. 12, 1997.
46. Carnie, J.A. and Porteous, J.W. (1962) Biochem. J. 85, 620.
47. Auricchio, S., Dahlqvist, A. and Semenza, G. (1963) Biochim. Biophys. Acta 73, 582.
48. Semenza, G. and Auricchio, S. (1962) Biochim. Biophys. Acta 65, 172.
49. Alpers, D.H. and Tedesco, F.J. (1975) Biochim. Biophys. Acta 401, 28.
50. Dulaney, J.T. and Touster, O. (1970) Biochim. Biophys. Acta 196, 29.
51. Gitzelmann, R., Davidson, E.A. and Drinchak, J. (1964) Biochim. Biophys. Acta 85, 69.
52. Eggermont, E. and Hers, H.G. (1969) Eur. J. Biochem. 9, 488.
53. Maroux, S., Louvard, D. and Bar<sup>r</sup>/<sub>k</sub>atti, J. (1973) Biochim. Biophys. Acta 321, 283.
54. Sigrist, H., Ronner, P. and Semenza, G. (1975) Biochim. Biophys. Acta 406, 433.
55. Lee, L.M.Y., Salvatore, A.K., Flanagan, P.R. and Forstner, G.G. (1980) Biochem. J. 187, 437.
56. Sorensen, S.H., Noren, O., Sjostrom H. and Danielsen, E.M. (1982) Eur. J. Biochem. 216, 559.

57. Maestracci, D., Preiser, H., Hedges, T., Schmitz, T. and Crane, R.K. *Biochim. Biophys. Acta* 382, 147.
58. Dunnik, J.K., Marinett, G.V. and Greenland, P. (1972) *Biochim. Biophys. Acta* 266, 684.
59. Colbeau, A. and Maroux, S. (1978) *Biochim. Biophys. Acta* 511, 39.
60. Kolinska, J. and Semenza, G. (1967) *Biochim. Biophys. Acta* 146, 181.
61. Schlegel-Haueter, S., Hore, P., Kerry, K.R. and Semenza, G. (1972) *Biochim. Biophys. Acta* 258, 506.
62. Kolinska, J. and Kraml, J. (1972) *Biochim. Biophys. Acta* 284, 235.
63. Kelly, J. and Alpers, D.H. (1973) *Biochim. Biophys. Acta* 315, 113.
64. Swaminathan, N. and Radhakrishnan, A.N. (1970) *Indian J. Biochem.* 1, 24.
65. Seetharam, B. (1972) in thesis entitled 'Studies on mammalian amylases and disaccharidases, submitted to Bangalore University, Bangalore, India.
66. Sivakami, S. and Radhakrishnan, A.N. (1973) *Indian J. Biochem. Biophys.* 10, 283.
67. Sasajima, K., Kawachi, T., Sato, S. and Sujimura, T. (1975) *Biochim. Biophys. Acta* 403, 139.
68. Razin, S. (1972) *Biochim. Biophys. Acta* 265, 241.

69. Kessler, M., Acuto, O., Storelli, C., Murer, H., Murer, M. and Semenza, G. (1978) *Biochim. Biophys. Acta* 506, 136.
70. Helenius, A. and Simmons, K. (1975) *Biochim. Biophys. Acta* 415, 29.
71. Louvard, D., Maroux, S., Vannier, Ch. and Desnuelle, P. (1975) *Biochim. Biophys. Acta* 375, 236.
72. Frank G., Brunner, J., Hauser, H., Wacker, H., Semenza, G. and Zuber, H. (1978) *FEBS Lett.* 96, 183.
73. Brunner, J., Hauser, H., Brawn, H., Wilson, K.J. Wacker, H., O'Neill, B. and Semenza, G. (1979) *J. Biol. Chem.* 254, 1821.
74. Maroux, S. and Louvard, D. (1976) *Biochim. Biophys. Acta* 419, 789.
75. Capaldi, R.A. (1982) *Trends. Biochem. Sci.* 7, 292.
76. Rothman, J.E. and Lenard, J. (1977) *Science* 195, 743.
77. Lee, L.M.Y. and Forstner, G.G. (1984) *Can. J. Biochem. Cell. Biol.* 62, (Seen in title form only.)
78. Auricchio, S., Semenza, G. and Rubino, A. (1965) *Biochim. Biophys. Acta* 96, 498.
79. Dahlqvist, A. and Telenius, U. (1969) *Biochem. J.* 111, 139.
80. Swaminathan, N. and Radhakrishnan, A.N. (1970) *Indian J. Biochem.* 7, 19.
81. Galand, G. and Forstner, G.G. (1974) *Biochem. J.* 144, 281.

82. Galand, G. and Forstner, G.G. (1974) Biochem. J. 144, 293.
83. Critchley, D.R. Howell, K.E. and Eicholz, A. (1975) Biochim. Biophys. Acta 394, 361.
84. Green, J.R. and Hadorn, B. (1977) Biochim. Biophys. Acta 467, 86.
85. Doell, R.G. and Kretchmer, N. (1962) Biochim. Biophys. Acta 62, 353.
86. Alpers, D.H. (1969) J. Biol. Chem. 244, 1238.
87. Dahlqvist, A., Bull, B. and Thomson, D.L. (1965) Arch. Biochem. Biophys. 109, 159.
88. Hore, P. and Muser, M. (1968) Comp. Biochim. Physiol. 24, 717.
89. Swaminathan, N. and Radhakrishnan, A.N. (1967) Indian J. Biochem. 4, 64.
90. Hsia, D.Y.Y., Makler, M., Semenza, G. and Prader, A. (1966) Biochim. Biophys. Acta 113, 390.
91. Gray, A.M. and Santiago N.A. (1969) J. Clin. Invest. 48, 716.
92. Asp. N.G., Dahlqvist, A. and Koldovsky, O. Biochem. J. 114, 351.
93. Swaminathan, N. and Radhakrishnan, A.N. (1969) Indian J. Biochem. 6, 101.
94. Dahlqvist, A. (1960) Acta Chem. Scan. 14, 63.
95. Carnie, J.A. and Porteous, J.W. (1962) Biochem. J. 85, 620.



96. Seiji, M. (1953) J. Biochem. (Tokyo) 40, 519.
97. Dahlqvist, A. (1964) Biochem. J. 86, 18.
98. Cogoli, A., Mosimann, H., Vock, C., Von Balthazar, A.K. and Semenza, G. (1972) Eur. J. Biochem. 30, 7.
99. Cogoli, A., Eberle, A., Sigrist, H., Joss, C., Robinson E., Mosimann, H. and Semenza, G. (1973) Eur. J. Biochem. 33, 40.
100. Quaroni, A., Gershon-Quaroni, E. and Semenza, G. (1975) Eur. J. Biochem. 52, 481.
101. Braun, H., Cogoli, A. and Semenza, G. (1975) Eur. J. Biochem. 52, 475.
102. Nishi, Y. and Takesue, Y. (1978) J. Ultra. Struct. Res. 62, 1.
103. Semenza, G. and Balthazar, A.K. (1974) Eur. J. Biochem. 41, 149.
104. Gray, G.M., Lally, B.C. and Conklin, K.A. (1979) J. Biochem. 254, 6038.
105. Storelli, C., Vogeli H. and Semenza, G. (1972) FEBS Lett. 24, 287.
106. Yamashiro, K.M. and Gray, G.M. (1970) Gastroenterology 58, 1056.
107. Conklin, K.A. Yamashiro, K.M. and Gray, G.M. (1975) J. Biol. Chem. 250, 5735.
108. Asp, N.G. and Dahlqvist, A. (1973) FEBS Lett. 35, 303.

109. Skovbjerg, H., Sjostrom, H. and Noren, O. (1979) FEBS Lett. 108, 399.
110. McGeachin, R.L. and Gleason, J.R. and Adams, M.R. (1958) Arch. Biochem. Biophys. 75, 403.
111. McGeachin, R.L. and Ford, N.K. Jr. (1959) Amer. J. Physiol. 196, 972.
112. Dahlqvist, A. and Thomson, D.L. (1963), Biochem. J. 89, 272.
113. Flanagan, P.R. and Forstner, G.G. (1978) Biochem. J. 173, 553.
114. Flanagan, P.R. and Forstner, G.G. (1979) Biochem. J. 177, 487.
115. Sivakami, S. and Radhakrishnan, A.N. (1976) Biochem. J. 153, 321.
116. Sivakami, S. and Radhakrishnan, A.N. (1978) Indian J. Biochem. Biophys. 15, 354.
117. Seetharam, B., Swaminathan, N. and Radhakrishnan, A.N. (1970) Biochem. J. 117, 939.
118. Hiromi, K. (1970) Biochem. Biophys. Res. Comm. 40, 1.
119. Malathi, P. and Crane, R.K. (1969) Biochim. Biophys. Acta 173, 245.
120. Lorenz-Meyer, H. Blum, A.L., Haemmerli, H.P. and Semenza, G. (1972) Eur. J. Clin. invest. 2, 326.
121. Colombo, V., Lorenz-Meyer, H. and Semenza, G. (1973) Biochim. Biophys. Acta 327, 412.

122. Brikenmecer, E. and Alpers, D.H. (1974) Biochim. Biophys. Acta 350, 100.
123. Ramaswamy, S. (1974) in thesis entitled 'Studies on Lactase-phlorigin hydrolase complex of the small Intestine', submitted to the University of Madras, Madras, India.
124. Leese, H.J. and Semenza, G. (1973) J. Biol. Chem. 248, 8170.
125. Reithel, F.J. (1963) Adv. Prot. Chem. 18, 123-226.
126. Stadtman, E.R. (1966) Adv. Enzymol. 28, 41.
127. Williamson, A.R. (1969), Essays in Biochem. (Campbell, P.N. and Greville, G.D. Ed.) Vol.5 pp 139-176, Academic Press, London and New York.
128. Barker, D.L. and Jencks, W.R. (1969) Biochemistry 8, 3879.
129. Morino, Y. and Snell, E.E. (1967) J. Biol. Chem. 242, 5591.
130. Klapper, M.H. and Koltz, I.M. (1968) Biochemistry 7, 223.
131. Stancel, G.M. and Deal, W.C. (Jr.) (1968) Biochem. Biophys. Res. Comm. 31, 398.
132. Le John, H.B., McCrea, B.E., Suzuki, I., and Jackson, S. (1969) J. Biol. Chem. 244, 2484.
133. Wilk, S., Meister, A., and Haschemayer, R.H. (1969) Biochemistry 8, 3168.
134. Carlsen, R.B. and Pierce, J.G. (1972) J. Biol. Chem. 247, 23.

135. Marshall, M. and Cohen, P.P. (1972) J. Biol. Chem. 247, 1641.
136. Koltz, T.W. Dannall, D.W., Langermann, N.R. in Proteins Vol. 1 (Ed. H. Neurath and R. Hill) pp. 293-411, Ed., 3, Academic Press, New York, San Francisco, London.
137. Degani, Y. and Degani, C. Trends Biochem. Sci. 5, 337.
138. Keresztes-Nagy, S., Lazer, L., Klapper, M.H., and Koltz, I.M. (1965) Science 150, 357.
139. Finch, J.T. (1975) Proteins (Neurath, H. and Hill, R.T., Ed.), Vol. 1, Edn. 3, pp 413-497, Academic Press, New York, San Francisco, London.
140. Garcia de la Torre, J. and Bloomfield, V.A. Quart. Rev. Biophys. (1981) 14, 81-139.
141. Schachman, H.K. (1957) Methods Enzymol. 4, 32.
142. Van Holde, R.E. (1975) in Proteins (Neurath, H. and Hill, R.T., ed.), Vol.1, Edn.3, pp 225-291, Academic Press, New York, San Francisco, London.
143. Coalts, J.H. (1970) in Physical Principles and Techniques of Protein Chemistry (Leach, S.J., ed.) part, B, pp 1-98 Academic Press, New York and London.
144. Costing, L.J. Adv. Prot. Chem. 11, 430-554.
145. Kuntz, J.D. and Kauzmann, W. Adv. Prot. Chem. 28, 239-347.
146. Yang, J.T. (1961) Adv. Prot. Chem. 16, 323-400.
147. Bradbury, J.H. (1970) in Physical Principles and Techniques of Protein Chemistry (Leach, S.J., ed.) Part, B, pp 99-145, Academic Press, New York and London.

148. Creeth, J.M. and Pain, R.H. (1967) Prog. Biophys. Mol. Biol. 17, 219-287.
149. Cohn, E.J. and Edsall, J.T. (1941) Proteins, Amino acids and Peptides, pp 370-410, Reinhold, New York.
150. Svedberg, T. and Pedersen, K.O. (1940). The ultracentrifuge, Oxford University Press, London and New York.
151. Tanford, C. (1961) Physical Chemistry of Macro-molecules, pp 15-456, John Wiley & Sons, INC., New York, London, Sydney.
152. Van Holde, K.E. (1971) Physical Biochemistry, Prentice-Hall, Englewood Cliffs, N.J.
153. Haschemayer, R.H. and Haschemayer, A.E.V. (1973) Proteins, A Guide to study by Physical and Chemical Methods, 1st edn. pp 130-180, John Wiley and Sons, New York, London, Sydney and Toronto.
154. Perrin, F. (1936) J. Phys. Radium (Paris)[7] 7, 1.
155. Simha, R. (1940) J. Phys. Chem. 44, 25.
156. Simha, R. (1945) J. Chem. Phys. 13, 188.
157. Oncley, J.L. (1941) Ann. N.Y. Acad. Sci. 41, 121.
158. Scheraga, H.A. and Mandelkern, L. (1953) J. Am. Chem. Soc. 75, 179.
159. Holtzer, A. and Lowey, S. (1963) Biopolymers 1, 497.
160. Doty, P., Bradbury, J.H. and Holtzer, A.M. (1956) J. Am. Chem. Soc. 78, 947.

161. Kuhn, W. (1932) Z. Phys. Chem. A bt A 161, 1.
162. Shulman, S. (1953) J. Am. Chem. Soc. 75, 5846.
163. Debye and Brinkman (1947) Physica 13, 447.
164. Kirkwood, J.G. and Riseman, J. (1948) J. Chem. Phys. 16, 565.
165. Holtzer, A. and Lowey, S. (1959) J. Am. Chem. Soc. 81, 1370.
166. Stern, M.D. (1966) Biochemistry 5, 2558.
167. Yu, H. and Stockmayer, W.H. (1967) J. Chem. Phys. 47, 1369.
168. Teramoto, A., Yamashita, T. and Fujita, H. (1967) J. Chem. Phys. 46, 1919.
169. Zwanzig, R. (1966) J. Chem. Phys. 45, 1858.
170. Hearst, J.E. and Stockmayer, W.H. (1962) J. Chem. Phys. 37, 1425.
171. Hearst, J.E. (1963) J. Chem. Phys. 38, 1062.
172. Hearst, J.E. (1964) J. Chem. Phys. 40, 1506.
173. Hearst, J.E. and Tagami, Y. (1965) J. Chem Phys. 42, 4249.
174. Bloomfield, V.A., Dalton, W.O. and Van Holde, K.E. (1967) Biopolymers 5, 135.
175. Bloomfield, V.A., Dalton, W.O. and Van Holde, K.E. (1967) Biopolymers 5, 149.
176. Garcia de la Torre, J. and Bloomfield, V.A. (1977) Biopolymers 16, 1747.

177. Garcia de la Torre, J. and Bloomfield, V.A. (1977) Biopolymers 16, 1765.
178. Garcia de la Torre, J. and Bloomfield, V.A. (1977) Biopolymers 16, 1779.
179. Garcia de la Torre, J. and Bloomfield, V.A. (1978) Biopolymers 17, 1605.
- 180a. Oseen, C.W. (1927) Hydrodynamik, Akademisches Verlag, Leipzig.
- 180b. Burgers, J.M. (1938) Second report on viscosity and plasticity, Amsterdam Sci., Nordemann Publishing Co., Amsterdam, Chapt. 3
181. Yamakawa, H. (1970) J. Chem. Phys. 53, 436.
182. Yamakawa, H. (1972) J. Chem. Phys. 57, 1537.
183. Yamakawa, H., Yamaki, J. (1973) J. Chem. Phys. 58, 2049.
184. Wilson, R.W. and Bloomfield, V.A. (1979) Biopolymers 18, 1205.
185. Garcia Bernal, J.M. and Garcia de la Torre, J. (1981) Biopolymers 20, 129.
186. Teller, D.C., Swanson, E. and Christoph de Haen (1979) Methods Enzymol 61, 103.
187. Teller, D.C. (1976) Nature (London) 260, 729.
188. Chothia, C. (1975). J. Mol. Biol. 105, 1.
189. Green, N.M. (1969) Adv. Immunol. 11, 1.
190. Finch, J.T. and Klug, A. (1967) J. Mol. Biol. 24, 289.

191. Johanssen, W., Schutte, H., Mayer, F. and Mayer, H. (1979) J. Mol. Biol. 134, 707.
192. DeRosier, D.J., and Oliver, R.M. (1971) Cold Spring Harbor Symp. Quant. Biol. 36, 199.
193. Farrant, J.L. (1954) Biochim. Biophys. Acta 13, 569.
194. Hall, C.E. (1955) J. Biochem. Biophys. Cytol. 1, 1.
195. Brenner, S. and Horne, R.W. (1959) Biochim. Biophys. Acta 34, 103.
196. Oliver, R.M. (1973) Methods Enzymol. 27 part D 616.
197. Huxley, H.E. and Zubay, G. (1960) J. Mol. Biol. 2, 10.
198. Malech, H.L. and Alber, J.A. (1979) J. Ultra Res. 69, 191.
199. Lake, J.A., Pandergast, M., Katian, L. and Nomura, M.
- 200.a. Lake, J.A. (1979) Methods Enzymol. 61, 250-257.
201. Davis, B.J. (1964) Ann. N.Y. Acad. Sci. 121, 404.
202. Sammans, D.W. (1981) Electrophoresis 2, 135.
203. Weber, K. and Osborn, M. (1969) J. Biol. Chem. 244, 4406.
204. Lamelli, U.K. (1970) Nature (London) 227, 680.
205. Maddy, A.H. and Kelly, P.G. (1971) Biochim. Biophys. Acta 288, 2631.
206. Ray, T.K. and Marinetti, G.V. (1971) Biochim. Biophys. Acta 233, 787.



207. Weber, K. Pringle, J.R. and Osborn, M. (1972) *Methods Enzymol* 26, 3-27.
208. Archibald, W.J. (1947) *J. Phys. Colloid. Chem.* 51, 1204.
209. La Bar, F.E. (1966) *Biochemistry* 5, 2362.
210. Kawahara, K. (1969) *Biochemistry* 8, 2551.
211. Gibbons, R.A. (1972) in *Glycoproteins* (Gottschalk, A., ed.) part A, Vol.5, p.78, BBA Library, Elsevier Publishing Co., Amsterdam, London and New York.
212. Hartley, B.S. (1970) *Biochemical J.* 119, 805.
213. Neuhoff, V. (1973) in *Micromethods in Molecular Biology*, (Neuhoff, V., Ed.) pp.85-148, Springer-Verlag Berlin, Heidelberg, New York.
214. Woods, K.R. and Wang, K.T. (1967) *Biochim. Biophys. Acta* 133, 369.
- 214a. Gros, C. and Loboulise, B. (1969) *Eur. J. Biochem.* 7, 463-470.
215. Ambler, R.P. (1967) *Methods Enzymol.* 11, 156-168  
Dey and Rosmus, (1972) *J. Chromat.* 69, 129.
216. Seiler, N. (1970) *Methods of Biochem. Analysis* 18, 259.
217. Maddy, A.H. and Dunn, M.J. (1976) in *Biochemical Analysis of Membranes* (Maddy, A.H., Ed.), pp.177-196., London Chapman and Hall, A. Haltsted Press Book, John Wiley and Sons, Inc, New York.

218. Garewal, H.S. (1973) Anal. Biochem. 54, 319;  
Capaldi, R.A. (1982) Trends in Biochem. Sci. 1, 292.
219. Creeth, J.M. and Knight, C.G. (1965) Biochim Biophys. Acta, 102, 549.
220. Siegel, L.M. and Monty, K.J. (1966) Biochim Biophys. Acta 112, 346.
221. Tirrell, M. and Middleman, S. (1979) Biopolymers 18, 59-72.
222. Lilewellyn, P.J. and Smith, G.D. (1981) Arch. Biochem. Biophys. 207, 63.
223. Mann, K.G. and Fish, W.W. (1972) Methods Enzymol 26, 28-42.
224. Deutsch, D.G. (1976) Anal. Biochem. 71, 300.
225. Segrest, J.P., Jackson, R.L., Andrews, E.P., Marchesi, V.T. (1971), Biochem Biophys. Res. Comm. 44, 390.  
Mataci, S.S. and Lowey, A.G. (1978) Biochim Biophys. Acta. 576, 263.
226. Bernfeld, P. (1955) Methods Enzymol. 1, 149-158.
227. Dahlqvist, A. (1968) Analyt. Biochem, 22, 99.
228. Marshall, J.J. (1974) Adv. Carb. Chem. and Biochem. 30, 257-370.
229. Sivakami, S. (1976) in a thesis entitled Studies on Maltase-Glucoamylase Complex of the Rabbit small intestine, submitted to the University of Madras, Madras, India.
230. Dahlqvist, A. (1960) Acta. Chem. Scand. 14, 1797, 231.

231. Boyd, W.C. (1966) Fundamentals of Immunology, 4th edn. page Interscience Publishers.
232. Van Holde, K.E. and Miller, K.I. (1982) Quaterly. Rev. Biophys. 15, 1-129.
233. Edsall, J.T., and Wyman, J. (1958) in Biophysical Chemistry, Vol.1, pp.85-89, Academic Press, New York, San Fransisco and London.
234. Wood, W.I., Peterson, D.O. and Bloch, K. J. Biol. Chem. 253, 2650.
235. Hayes, H.B. and Wellner, D. (1969) J. Biol. Chem. 244, 6636.
236. Maticic, S.S. and Lowey, G.A. (1979) Biochim. Biophys Acta, 576, 263.